This is a draft copy intended only for the purposes of peer review. It is not intended for publication or dissemination.

Ecosystem-Based Fishery Management Strategy

Georges Bank Prototype Study

Summary Document

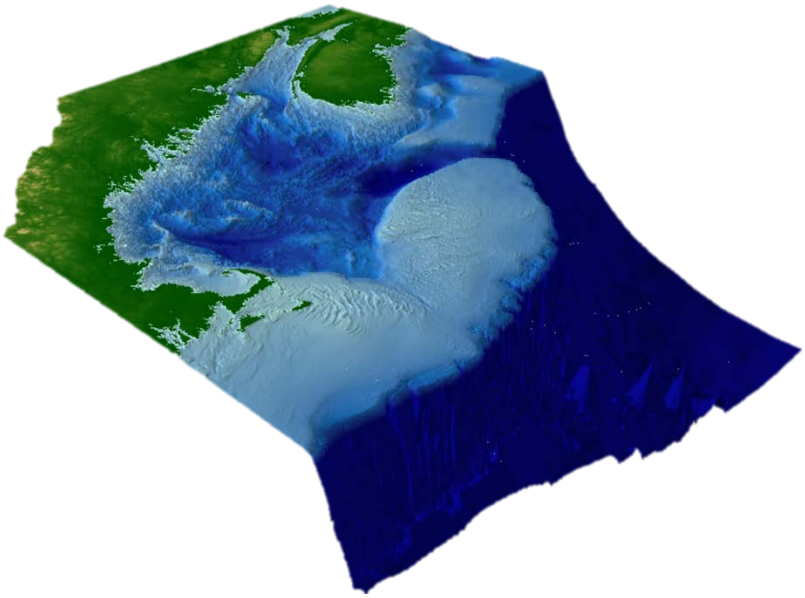

NEFSC Ecosystem Dynamics and Assessment Branch

April 30-May 2 2018

Woods Hole, MA

Section 1: *TOR 1*

Evaluate the approach used to identify Ecological Production Units on the Northeast Shelf of the United States and the strengths and weaknesses of using these Ecological Production Units as the spatial footprint for Ecosystem Based Fisheries Management in the region.

Ref: TOR 1

Delineation of Ecological Production Units on the Northeast U.S. Continental Shelf

Introduction

Identification of spatial management units is central to the development of strategies for Ecosystem-Based Fisheries Management (EBFM). Although many definitions of EBFM have been advanced, virtually all share at least three common elements: (1) the recognition that humans are an integral part of the ecosystem, (2) a focus on the inter-relationships among ecosystem components, the physical environment, and human communities and (3) a commitment to establishing spatial management units based on defined ecological boundaries. It will further be essential to consider the interplay between ecological production processes and human use patterns in defining appropriate spatial management units. Here, we delineate Ecological Production Units (EPUs) for marine Ecosystem-Based Fishery Management on the Northeast Continental Shelf of the United States. One of the fundamental ways in which EBFM differs from more conventional fishery management approaches is in the development of integrated management plans for defined ecological regions rather than for individual species/stocks: We emphasize that these spatial units are to be considered open and interconnected through oceanographic processes, movement and migration patterns of marine organisms, and wide-ranging human activities that can span multiple spatial management units.

Geographically-defined ecological units have previously been proposed for the Northeast Continental Shelf from Cape Hatteras to the Gulf of Maine and adjacent Scotian Shelf. The region in its entirety has been designated as a Large Marine Ecosystem (LME) on the basis of bathymetry, productivity, population structure, and fishery characteristics (Sherman and Alexander 1986). Longhurst (1998) identified three subdivisions of his Northwest Atlantic Shelves Province falling within the Northeast Shelf (NES) LME: *(1) Gulf of Maine and Bay of Fundy, (2) Shelf from Georges Bank to Long Island, and (3) Middle Atlantic Bight*. Subareas of the NES LME have also previously been defined for the Northeast Shelf for fishery assessment purposes. Clark and Brown (1977) considered a four unit subdivision of the NES LME within U.S. waters including *(1) Gulf of Maine (2) Georges Bank (3) Southern New England and (4)*

Middle Atlantic regions. To meet a broader set of management mandates, Higgens et al. (1985) delineated six Water Management Units within the Northeastern United States based on expert opinion: (1) *Coastal Gulf of Maine*, (2) *Gulf of Maine*, (3) *Georges Bank west to Block Channel*, (4) *Coastal Middle Atlantic, (5) Middle Atlantic Shelf* and (6) *Off-shelf* (See Figure 1.1) .

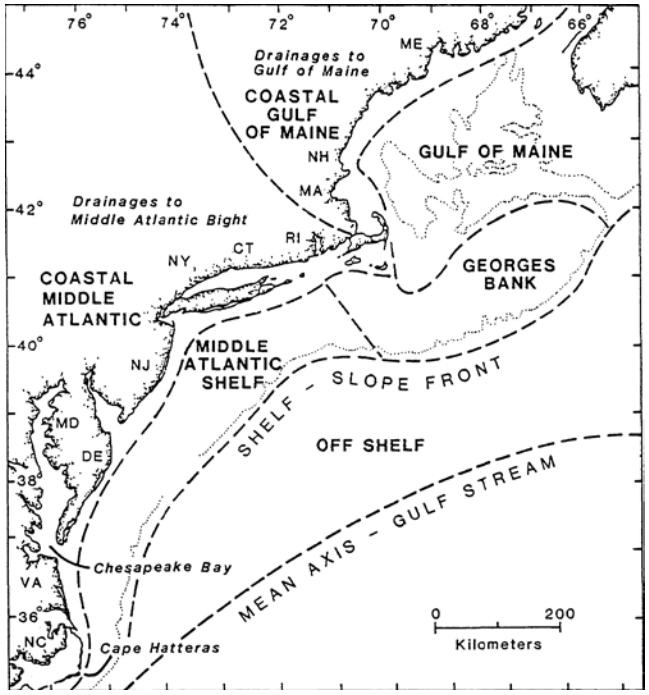

Figure 1.1 Proposed Water Management Units for the Northeast Continental Shelf (Higgens et al. 1985).

Methods

To define ecological production units, we assembled a set of physiographic, oceanographic and biotic variables on the Northeast U.S. Continental Shelf, and area of approximately 264,000 km^2 within the 200m isobath (Figure 1.1). A listing of the variables employed in the analysis is provided in Table 1.1. The physiographic and hydrographic variables selected have been extensively used in previous analyses of oceanic provinces and regions (e.g Roff and Taylor 2000). Primary production estimates have also been widely employed for this purpose in conjunction with physical variables (Longhurst 1998) to define ecological provinces throughout the world ocean. We did not include information on higher trophic levels or fishing patterns in our analysis. The biomass and production of higher trophic levels in this region has been sharply perturbed by fishing and other anthropogenic influences. Similarly, fishing patterns

are affected by regulatory change, market and economic factors and other external influences. Because of these malleable patterns of change, often unconnected with underlying productivity, we excluded factors directly related to fishing practices.

The physiographic variables considered in this analysis include bathymetry and surficial sediments (Table 1.1). The physical oceanographic and hydrographic measurements include sea surface temperature, annual temperature span, and temperature gradient water derived from satellite observations for the period 1998 to 2007. We used shipboard observations for surface and bottom water temperature and salinity in surveys conducted in spring and fall. Daily sea surface temperature (SST, ^{o}C) measurements at 4 km resolution were derived from nighttime scenes composited from the AVHRR sensor on NOAA's polar-orbiting satellites and from NASA's MODIS TERRA and MODIS AQUA sensors. We extracted information for the annual mean SST, temperature span, and temperature gradients from these sources. The latter metric is intended to provide information on frontal zone locations. The biotic measurements included satellite-derived estimates of chlorophyll *a* mean concentration, annual span, and CHL*a* gradients and related measures of primary production. Daily merged SeaWiFS/MODIS-Aqua chlorophyll *a* (CHL, mg m^{-3}) and SeaiWiFS photosynthetically available radiation (PAR, Einsteins m^{-2} d^{-1}) scenes at 1.25 km resolution were obtained from NASA Ocean Biology Processing Group. In all cases, we have standardized the data to common spatial units by taking annual means of each observation type within spatial units of 10' latitude by 10' longitude in an attempt to account for the disparate spatial and temporal scales at which these observations are taken. We note that shipboard sampling used to obtain direct hydrographic measurements is constrained by a minimum sampling depth of 27 m specified on the basis of prescribed safe operating procedures. As a result nearshore waters are not fully represented in our initial specifications of ecological production units. There are over 1000 spatial cells in the analyses presented.

The size of the spatial units employed further reflects a compromise between retaining spatial detail and minimizing the need for spatial interpolation of some data sets. For shipboard data sets characterized by relatively coarse spatial resolution, where necessary, we first constructed an interpolated map using an inverse distance weighting function. Although alternative interpolation schemes based on geostatistical approaches are possible, we considered

the inverse distance weighting function to be both tractable and robust for this application. We note that the data are archived at the original resolution scale and more detailed analyses to address specific requirements (e.g. evaluation of the placement of marine protected areas) can be readily undertaken at finer spatial scales.

Table 1. The variables used as input for the PCA and clustering analysis showing their original data type, source, units, and time period.

Variables	**Sampling Method**	**Units**
Bathymetry	Soundings/Hydroacoustics	Meters
Surficial Sediments	Benthic Grab	Krumbein Scale
Sea Surface Temperature	Satellite Imagery (4km grid)	^{0}C annual average
Surface Temperature	Shipboard Hydrography (point)	^{0}C (Spring and Fall)
Bottom Temperature	Shipboard Hydrography (point)	^{0}C (Spring and Fall)
Surface Salinity	Shipboard Hydrography (point)	psu (Spring and Fall)
Bottom Salinity	Shipboard Hydrography (point)	psu (Spring and Fall)
Stratification	Shipboard Hydrography (point)	Sigma-t units (Spring and Fall)
Chlorophyll-a	Satellite Imagery (1.25km Grid)	mg C/m^3 (annual average)
Chlorophyll-a gradient	Satellite Imagery (1.25km Grid)	dimensionless
Primary Production	Satellite Imagery (1.25 km)	gC/m^2 /year (cumulative)
Primary Production gradient	Satellite Imagery (1.25 km)	dimensionless

Ecological Production Units

We first employed a spatial principal components analysis (PCA; e.g. Pielou 1984; Legendre and Legendre 1998) to examine the multivariate structure of the data and to account any inter-correlations among the variables to be used in subsequent analysis. The variables included in the analysis exhibited generally skewed distributions and we therefore transformed each to natural logarithms prior to analysis. The PCA was performed on the correlation matrix of the transformed observations. We selected the eigenvectors associated with eigenvalues of the dispersion matrix with scores greater than 1.0 (the Kaiser-Guttman criterion; Legendre and Legendre 1998) for all subsequent analysis. These eigenvectors represent orthogonal linear combinations of the original variables used in the analysis.

To delineate ecological subunits, we used a disjoint cluster analysis based on Euclidean distances using the K-means procedure (Legendre and Legendre 1998) on the principal component scores The use of non-independent variables can strongly influence the results of classification analyses of this type (Pielou 1984), hence the interest in using the PCA results in the cluster analysis. The eigenvectors were represented as standard normal deviates. We used a Pseudo-F Statistic described by Milligan and Cooper (1985) to objectively define the number of clusters to use in the analysis. The general approach employed is similar to that of Host et al. (1996) for the development of regional ecosystem classifications for terrestrial systems.

Results

Principal Components Analysis

The first four eigenvalues all had magnitudes greater than one; these four eigenvalues accounted for 78.7% of the variance (Table 1.2). In all subsequent classification analyses, we used the first four principal component scores to characterize the joint physiographic, hydrographic and biotic structure of the data.

Table 1.2. Standardized eigenvalues for the first four principal components and the proportion of the variance accounted for by each.

PC	Eigenvalue	Prop. Var.	Cum. Prop.
1	6.707	0.363	0.365
2	4.600	0.256	0.628
3	1.600	0.090	0.717
4	1.251	0.069	0.787

We next examined the eigenvectors corresponding to the four selected eigenvalues to assist in interpretation of the relationship between the original variables and the reduced set of principal components (Table 1.3). The first principal component, accounting for 36.3% of the variance (Table 1.2), was dominated by depth, mean chlorophyll levels, and mean primary production (Table 1.3). The second principal component explained 25.6% of the variance (Table 1.2) and was strongly influenced by surface temperatures based on shipboard measurements and satellite observations (Table 1.3). The third principal component, accounting for 9% of the variance was strongly influenced by SST and chlorophyll gradients and the observed annual span range chlorophyll levels (Table 3). The gradient measures reflect the influence of frontal zones and mixing processes. The fourth principal component was strongly influenced by sediment grain size and SST span and gradient; it accounted for 7% of the variance (Table 1.2).

Table 1.3. Standardized eigenvectors of the first four eigenvalues.

Variable	PC 1	PC 2	PC 3	PC 4
Depth	0.355	-0.078	0.133	0.010
Grain size	0.093	-0.014	0.426	-0.509
Fall bottom salinity	0.333	0.102	0.157	0.231
Fall surface salinity	0.251	0.144	0.039	0.260
Spring bottom salinity	0.277	0.256	0.058	0.162
Spring surface salinity	0.124	0.295	-0.293	0.148
Fall bottom temperature	-0.281	0.195	-0.094	0.235
Fall surface temperature	-0.158	0.392	-0.133	-0.008
Spring bottom temperature	0.161	0.335	0.144	0.209
Spring surface temperature	-0.052	0.340	0.186	-0.086
SST mean	-0.132	0.416	0.006	-0.140
SST span	-0.105	0.266	0.003	-0.426
SST gradient	-0.205	0.031	0.480	0.381
CHLa mean	-0.325	-0.184	0.121	-0.013
CHLa span	0.145	0.181	0.431	-0.235
CHLa gradient	-0.279	-0.060	0.393	0.272
PDD mean	-0.364	0.045	0.080	-0.062
PDD Span	0.243	-0.269	0.107	-0.084

Cluster Analysis

Consideration of a range of dissimilarity scores corresponding to 4-8 cluster groups indicated that after seven cluster units were identified, no further major groupings could be identified that satisfied a minimum cell number constraint. Accordingly, all further considerations were based on seven cluster units. The clusters represent major ecological production units on the shelf including (1) Eastern Gulf of Maine-Scotian Shelf, (2) Western-Central Gulf of Maine (3) Inshore Gulf of Maine, (4) Georges Bank-Nantucket Shoals (5) Intermediate Mid-Atlantic Bight (6) Inshore Mid-Atlantic Bight and (7) Continental Slope (Cape Hatteras to Georges Bank) (see Figure 1.2).

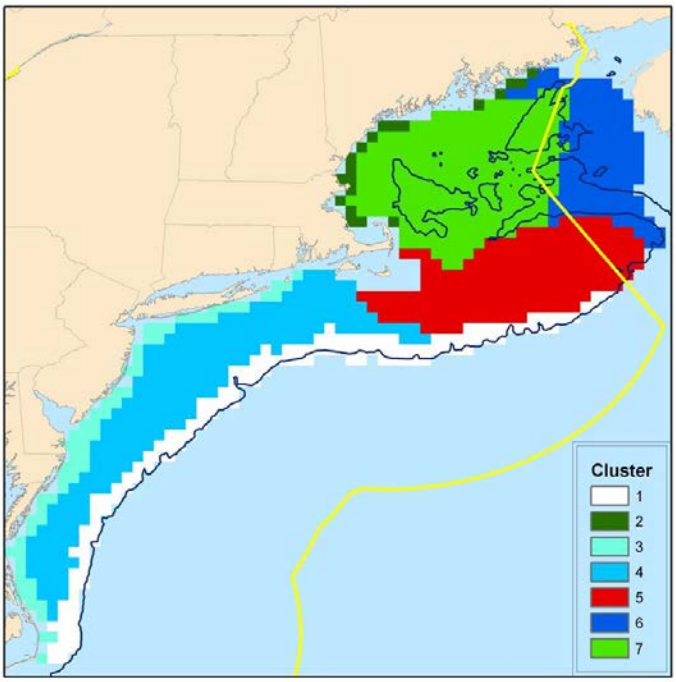

Figure 1.2. Results of initial cluster analysis defining seven ecological production units on the Northeast U.S. Continental Shelf. Specification of nearshore boundaries was limited by the extent of shipboard observations which were constrained by safe operating specifications.

We next considered options for interpolation of nearshore boundaries resulting from depth-related constraints on shipboard observations. For this, we relied on information from satellite imagery (Figure 1.3). For the missing nearshore areas in the Gulf of Maine and Mid-Atlantic Bight, the satellite information for chlorophyll concentration and sea surface temperature indicated a direct extension from adjacent observations. For the Nantucket Shoals regions south of Cape Cod, similarities in tidal mixing patterns reflected in chlorophyll and

temperature observations indicated an affinity with Georges Bank (Figure 1.3) and the boundaries were changed accordingly.

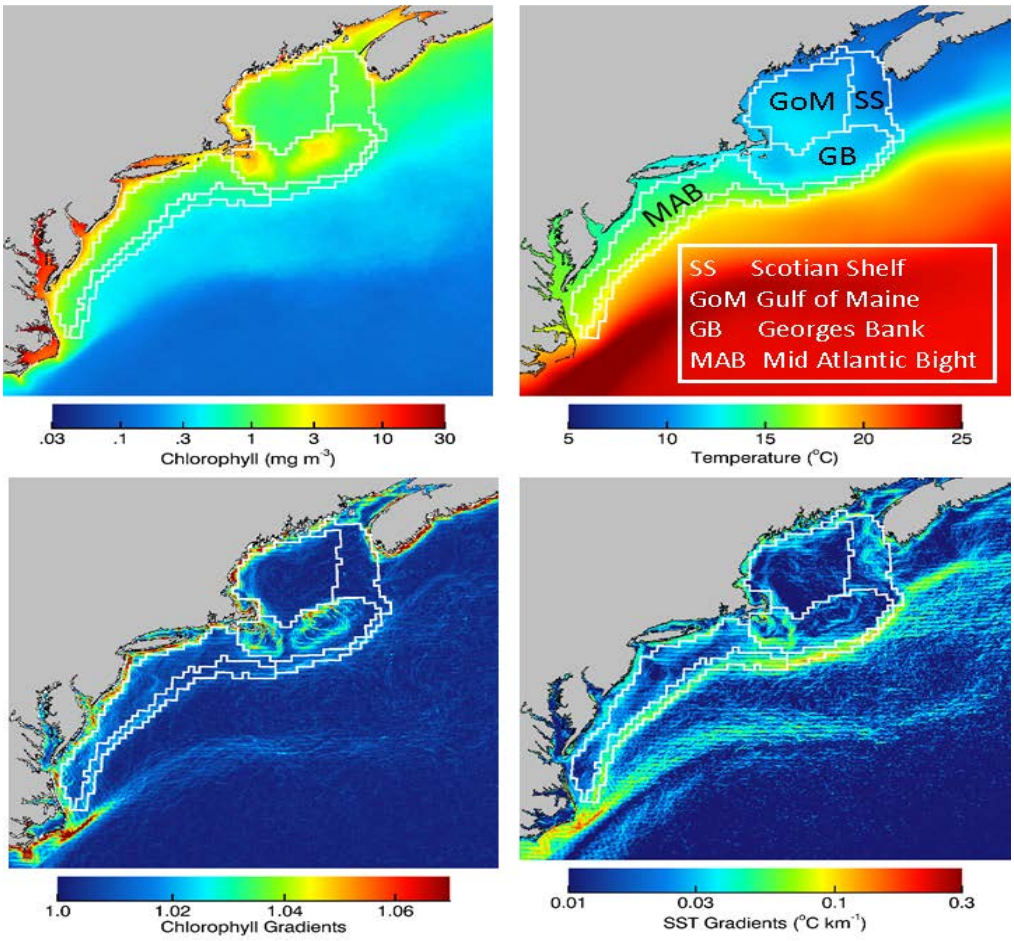

Figure 1.3. Proposed Ecological Production Units for the Northeast U.S. Continental Shelf after nearshore interpolation.

Finally, we next considered consolidation of ecological subareas so that nearshore regions are considered to be special zones nested within the adjacent shelf regions. Similar consideration led to nesting the continental slope regions within adjacent shelf regions in the Mid-Atlantic and Georges Bank regions (Figure 1.3). This leads to four major units: Mid-Atlantic Bight, Georges Bank, Western-Central Gulf of Maine, and Scotian Shelf-Eastern Gulf of Maine. These major

ecological production units can accommodate finer-scale structure and spatial management options (e.g closed areas etc.) nested within each unit.

Discussion

The objective identification of spatial management units is a critical pre-requisite for the implementation of ecosystem-based fishery management. EBFM is inherently a place-based processes. We assembled a set of physiographic, oceanographic and biotic (lower trophic level) variables to provide a basis for objective identification of ecological production units on the Northeast U.S. Continental Shelf. Our analysis indicates seven principal subregions on the Northeast Continental Shelf and Slope related to fundamental physical and production characteristics of each. We further consolidated these 7 subareas into four Ecological Production Units with nested sub-units within each. Our analysis shows a strong concordance with the Water Management Units on the Northeast U.S. Continental Shelf designated on the basis of expert opinion over 30 years ago (Figure 1.1; Higgens et al.1986).

The Gulf of Maine is a deep semi-enclosed inland sea with a cyclonic circulation pattern. Our analysis indicates a partitioning of the eastern Gulf of Maine-Scotian Shelf from the Central Gulf of Maine. The Eastern Gulf of Maine-Scotian Shelf differs from the rest of Gulf with respect to depth, substrate composition, temperature characteristics, stratification, and primary production. The Central Gulf of Maine region includes the several deep basin regions with the only major expanse of sand-silt-clay habitats in the region. Georges Bank is a shallow submarine plateau with a seasonally important anticyclonic circulation. It is characterized by high levels of chlorophyll concentration and primary production relative adjacent offshore areas on the shelf. It is further characterized by strong gradients in SST and primary production. The adjacent Nantucket Shoals region is separated from Georges Bank by the Great South Channel but shares many of the defining attributes of the bank (Figure 1.3). Shipboard hydrographic measurements were not available for Nantucket Shoals because of constraints related to safe operating depths for our research vessels and this area remained undefined in the PCA and cluster analyses. We elected to group the shoals region with Georges Bank because of its affinities related to production dynamics of the bank. We note however that it could be designated as a distinct subarea of the Georges Bank EPU. Alternatively, it could be placed as part of the nearshore subarea of the Mid-Atlantic Bight EPU. The Mid-Atlantic Bight is characterized by a gently

sloping continental shelf with an alongshore circulation regime. This region is distinctive in its dominant summer stratification regime. The Continental Slope subarea is distinguished by steep topographic gradients, low and a dominant role of shelf-slope front and Gulf Stream influences. Our analysis was limited by data availability to the upper reaches of the continental slope for many of the variables considered.

The EPU boundaries defined here are conceived as open and interconnected, reflecting dynamic water mass movements, seasonal and longer-term migration of organisms within the regions, and shifting fishing patterns. These considerations will play an important role in the practical implementation of this place-based management scheme. It will require that interchange among EPUs be addressed. We further anticipate that the production unit boundaries defined here will be subject to periodic updates and reanalysis as climate, human use patterns, and other factors change. Practical considerations dictate that re-evaluation on 5-10 year time scales would be reasonable.

Delineation of the Ecological Production Units is intended as a starting point for specification of spatial management units for Ecosystem-Based Fisheries Management on the Northeast U.S. Continental Shelf. The spatial footprint to be employed in management is of course ultimately the purview of managers. Stock boundaries have been developed for each managed species in New England and the Mid Atlantic. Of the species currently managed by NEFMC, nearly 70% are managed as single-unit stocks; approximately 25% comprise 2-stock complexes and the remainder are partitioned into three-stock complexes. There are nearly 30 distinct spatial footprints represented among these designated stock areas. Although these stock areas may appear to conform to a consistent methodology, a variety of different methods were in fact used to partition stocks depending on information available: genetic analyses, fishing patterns, management convenience, and survey information. A benefit of our approach is that it provides a consistent framework which can then be used as a unifying element for ecosystem based fishery management in this region while reducing the overall complexity of the spatial units now employed in management.

References

Clark, S.H. and B.E. Brown. 1977. Changes of biomass of finfishes and squids from the Gulf of Maine to Cape Hatteras, 1963-1974, as determined from research vessel survey data. *Bull. U.S. Bur. Fish.* 75:1-21.

Haliday, R.G. and A.T. Pinhorn. 1990. The delimitation of fishing areas in the Northwest Atlantic. J. Northw. Atl. Fish. Sci. 10:1-51.

Higgins, B.E., R. Rehfus, J.B. Pearce, R.J. Pawlowski, R.L. Lippson, T. Goodger, S. Mello, Roe, and D.W. Beach. 1985. Regional Action Plan. NMFS NEFSC TM F/NEC-37.

Host, G.E., P.L. Polzer, D.J. MLadenoff, M.A. White, and T.R. Crow. 1996. A quantitative approach to developing regional ecosystem classification. Ecol. Appl. 6:608-618.

Legendre, P. and L. Legendre. 1998. Numerical Ecology. 2nd Ed. Elsevier Press, Amsterdam.

Longhurst, A. 1998. Ecological Geography of the Sea. Academic Press, San Diego.

O'Reilly, J.E. and C. Zetlin. 1998. Seasonal, horizontal, and vertical distribution of phytoplankton chlorophyll *a* in the northeast U.S. Continental Shelf ecosystem. U.S. Dept. Commerce, NOAA Tech. Rep. NMFS 139, Fishery Bulletin. 120p.

Pielou, E. 1984. The Interpretation of Ecological Data : A Primer on Classification and Ordination. J. Wiley and Sons, New York.

Roff, J.C. and M.E. Taylor. 2000. National frameworks for marine conservation – hierarchical geophysical approach. Aquat. Cons.:Mar. Freshwater Ecosystems 10:209-223.

Sherman, K. and L.M. Alexander. 1986. Variability and Management of Large Marine Ecosystems. AAAS Selected Symposium 99, Westview Press, Boulder, CO.

Wigley, R.I., and R.B. Theroux. 1981. Macrobenthic fauna from the Middle Atlantic Bight region. Faunal composition and quantitive distribution. U. S. Dept. Int., Geol. Serv. Prof. Pap. 529 N, Woods Hole Oceanogr. Inst., Woods Hole, MA 02543, 198 p.

Section 2: *TOR 2*

Evaluate the methods for estimating ecosystem productivity for the Georges Bank Ecological Production Unit and advise on the suitability of the above methods for defining limits on ecosystem removals as part of a management procedure.

Ref: TOR 2

Ecological Production Potential on Georges Bank

Introduction

Patterns of energy flow and utilization shape the production potential of exploited ecosystems. The amount of carbon fixed at the base of the food web places constraints on overall production and, ultimately, on potential yield. Although the interplay of both top-down and bottom-up processes is a critical determinant of observed levels of production in marine systems, there is clear evidence of the importance of the latter for yields in large marine ecosystems (Chassot 2010). An understanding of these constraints provides essential insights into system structure and potential yield in exploited marine ecosystems.

Georges Bank has long been recognized as a highly productive fishery ecosystem. Riley (1941) documented key aspects nutrient dynamics and primary production on the Bank that underlie production at higher trophic levels. In turn, these characteristics fuel potentially high levels of fishery production. The topographic and hydrographic features of this shallow submarine plateau, dominated by strong tidal mixing forces and hydrodynamic features resulting in high levels of nutrient regeneration, result in correspondingly high primary production relative to the adjacent Gulf of Maine and the offshore components of the Mid-Atlantic Bight. Within the Georges Bank Ecological Production Unit, primary production is highest on the crest of the bank where the water column is isothermal and well-mixed throughout the year. It is also high in the shallow and tidally energetic Nantucket Shoals region.

This system has been exploited for several centuries by domestic fleets and was subject to a massive perturbation with the arrival distant water fleets during the period 1961-1976 (Fogarty and Murawski 1998). A pattern of sequential depletion of fishery resources and large-scale changes in the relative abundance of different species groups ensued. The rapid escalation in fishing effort by these fleets resulted in an initial increase in landings during an unsustainable fishing-up process as some previously lightly exploited resources were harvested and other abundant species were more heavily exploited. Standardized research vessel surveys indicated a decline of over 40% in overall fish abundance over the first five years of exploitation by foreign

fleets (Clark and Brown 1977). Following the implementation of the 200 mile limit establishing an Exclusive Economic Zone in 1976, foreign fleets were excluded from Georges Bank. Adjudication of a U.S.-Canada boundary dispute by the World Court ceded the northeastern third of the bank to Canada in 1984 and the region is now under joint management.

Clarke (1946) constructed the first characterization of energy flow to the higher trophic levels for this system in a highly simplified food web comprising diatoms, mesozooplankton, benthos, and fish. Energy budgets for this system have since been progressively expanded and refined to provide higher resolution of critical structural components of the system (Cohen et al. 1982; Sissenwine et al. 1984; Steele et al. 2007; Link et al. 2006; Link et al. 2008). These trophic transfer models invoke mass-balance constraints and return solutions conditioned on observed or inferred production, consumption, biomass, and, where relevant, harvest levels throughout the food web. They therefore provide *realized* representations of system structure and yield given a defined history of exploitation and environmental change.

Here we examine a separate but related issue – determining the production *potential* of Georges Bank conditioned on the input of primary production and specified levels of trophic transfer efficiency. Approaches to estimating the fishery production potential of marine systems based on simple food chain models were first described by Kestevan and Holt (1955). Subsequent developments by Graham and Edwards (1962), Schaefer (1965), Ricker (1969), Ryther (1969), Gulland (1970, 1971), Moiseev (1969, 1994), Ware (2000) and Stock et al. (2017) further expanded application of the approach. In the following, we seek to maintain the fundamental simplicity of these models while allowing expansion to a fuller food web structure and finer resolution of exploitation patterns throughout the food web. The resulting production potential model is intermediate in complexity to the earlier food chain models cited above and full network models (which now routinely consider dozens of functional group compartments).

Methods

Data Sources

We require information on net primary production for two major functional groups nano-picophytoplankon (<20 μ) and microphytoplankton (>20 μ). We must further specify pathways of energy flow in the system and associated ecological transfer efficiencies. For the former we

rely on satellite-derived estimates of surface chlorophyll concentration for each phytoplankton functional group coupled with empirical algorithms to estimate depth-integrated primary production. For the latter, we use estimates derived from previous network analyses of Georges Bank and adjacent systems. These issues are described in greater detail below.

Primary Production

Satellite-derived estimates of chlorophyll *a* concentration were determined using data from the Sea-viewing Wide Field-of-View Sensor (SeaWiFS) from 1998-2008 and from the Moderate Resolution Imaging Spectro-radiometer (MODIS) for the period 1999-2016. We computed monthly chlorophyll concentration and primary production by phytoplankton functional group on a pixel by pixel basis and summed over all pixels within defined ecoregions of the Northeast U.S. Continental Shelf including Georges Bank. Our analysis treats the satellite-derived data as a census with missing data for individual pixels due to seasonally varying cloud cover and other factors. Missing values are imputed from adjacent observed cells.

Estimates of depth integrated primary production were derived using a modification of the Vertically Generalized Productivity Model (VGPM) of Behrenfeld & Falkowski (1997). This modified model (designated VGPM2) replaces the original temperature-dependent description of photosynthetic efficiencies with the exponential Eppley function (Eppley 1972) as adopted by Morel (1991). The empirical estimate of primary production is given by:

$$PP = 0.66125 P^b_{opt} \left(\frac{I_o}{I_o + 4.1} \right) Chl \cdot Z_{\max} DL$$

where P^b_{opt} is the maximum carbon fixation rate within the water column (*mg C/mg Chl/hr)* as specified by the Epply (1972):

$$P^b_{opt} = 0.851 \cdot \left(1.066^T\right)$$

I_o is the daily integrated molar photon flux of sea surface photosynthetically active radiation (mol quanta $m^{-2}d^{-1}$), *Chl* is the chlorophyll concentration (mg m^{-3}), Z_{max} is the maximum depth, *DL* is photoperiod (hrs) for each day of the year and latitude, and *T* is sea surface temperature (^oC).

We partitioned total primary production into phytoplankton functional groups using chemotaxonomic methods developed specifically for the Northeast U.S. Continental Shelf (Pan *et al.* 2010). Diatom and dinoflagellate biomasses were then combined to represent the microplankton component and the remaining functional groups were combined in the nano-picoplankton group (Vidussi *et al.* 2001). Using a relationship based on more than 600 measurements of size fractionated chlorophyll and primary production in the NES LME (O'Reilly *et al.* 1987), we estimated the fraction of the total primary production associated with the microplankton functional group.

Transfer Efficiency

Clear thermodynamic constraints place limits on the transfer efficiency between successive levels in the food chains comprising a reticulated food web. Early laboratory experiments indicated that the expected transfer efficiency was on the order of 10% (Slobodkin 1961). With the accrual of additional information on marine food webs, Lalli and Parsons (1997) suggested that the transfer efficiency from microplankton to mesozooplankton is on the order of 20%, decreasing to 10-15% for higher trophic levels. We examined transfer efficiencies based on earlier food web models for Georges Bank Shelf supplemented by observations for other food webs models developed for the Northwest Atlantic continental shelf (Link et al. 2006; A. Bundy, DFO, personal communication; Sea Around US project). We used estimates for 14 systems ranging from the Mid-Atlantic Bight to the Grand Banks (Appendix Table A.1). For the grazing food web, we employed trophic level classifications based on the approach of Ulanowicz (1995).

These earlier estimates were based on network models that did not distinguish among phytoplankton functional groups and did not explicitly consider the microbial food web in detail. Accordingly, we used literature estimates of transfer efficiencies for these ecosystem nodes. For the microbial food web, we assumed that 50% of the nanoplankton is consumed by heterotrophic bacteria (Ware 2000). The gross growth efficiency of bacteria was taken to be 33% and the assimilation fraction to be 80% (Link et al. 2006). The transfer efficiency from bacteria to microzooplankton was taken to be 0.25 (Ware 2000).

Model Structure

Earlier estimates of fishery production potential were based on simple food chain models (Kestevan and Holt 1955; Graham and Edwards 1962; Schaefer 1965; Ricker 1969; Ryther 1969; Gulland 1970, 1971; Moiseev 1969, 1994). These models can be expressed:

$$EPP = NPP \cdot TE^{TL-1}$$

where *EPP* is the projected Ecosystem Production Potential; *NPP* is net primary production expressed in terms of biomass; *TE* is the transfer efficiency for the flow of energy or biomass between successive trophic levels; and *TL* is the mean trophic level at which catch is extracted. Ware (2000) modified this general approach to allow for direct consideration of the different pathways of energy flow involving two phytoplankton functional groups. Stock et al. (2017) considered additional elements including incorporation of detrital flux, zooplankton production, and temperature- dependent transfer efficiencies

Here, we extend these models to accommodate a simple food web architecture. We modify the earlier representation by Fogarty et al. (2014; 2016) to provide finer resolution of elements of the microbial food web and the benthic community. The general approach recognizes two pathways for transfer of primary production in the system: the classical grazing food web tracing the fate of production of microplankton, and production involving transfer through the microbial food web originating with the nano- picoplankton functional group (Figure 2.1). The former involves grazing by mesozooplankton and filtering of diatom production by suspension feeding invertebrates. The latter pathway entails utilization of nano-picoplankton by heterotrophic bacteria, principally in the form of both particulate and dissolved organic matter and resulting in the remineralization of inorganic nutrients. In this simplified representation, nanoflagellates consume bacteria which are in turn preyed on by microzooplankton. Mesozooplankton prey on both microzooplankton and microphytoplankton and serve as the nexus of the microbial food web and the grazing food web. The microbial pathway therefore involves two or more trophic transfer steps before reaching mesozooplankton as a bridge to higher trophic levels. Although both dissolved (DOM) and particulate organic matter (POM) derived from other sources in the food web and are utilized by bacteria, we assume that most of the POM and DOM utilized by bacteria are from phytoplankton sources (see also Ware 2000).

Bacteria associated with bottom sediments and organisms are also consumed by deposit-feeding benthos. The functional groups represented in the upper food web depicted in Figure 2.1 can be directly mapped to earlier food web models for Georges Bank (Cohen et al. 1978; Sissenwine 1984; Steele et al. 2008).

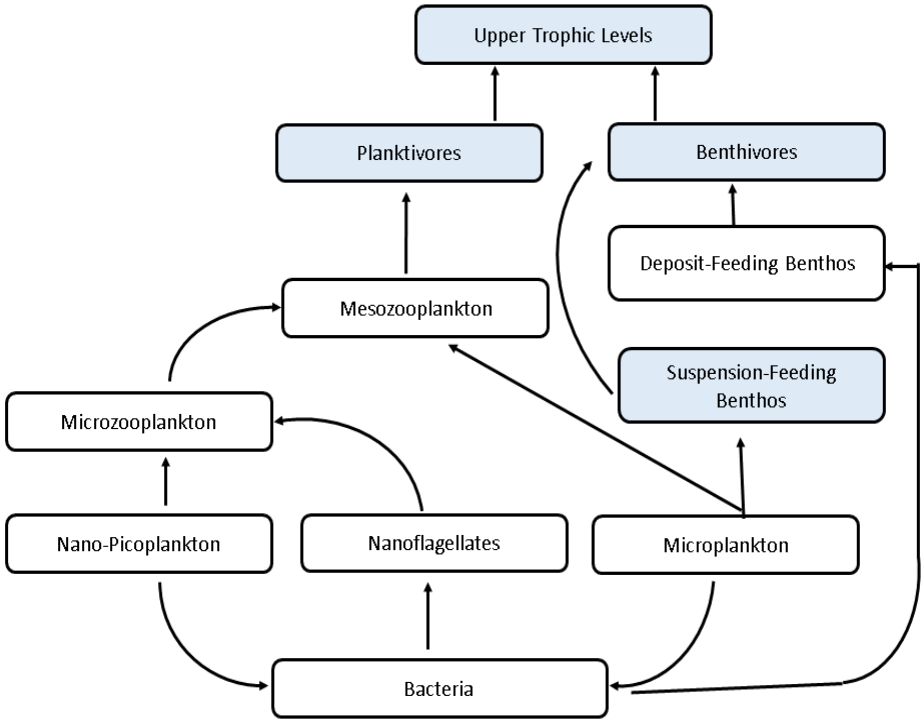

Figure 2.1. Model structure for ecosystem production potential on Georges Bank. The suspension feeding benthos, benthivore, planktivore, and upper trophic level nodes shaded in blue are subject to harvesting in this representation.

Production at a given node *i* is a function of the transfer efficiency from other nodes (*j*) to node *i*, the inputs from other locations and losses from the ith node:

$$\boldsymbol{P}_i = \boldsymbol{T}\boldsymbol{P}_j + \boldsymbol{A}_i - \boldsymbol{L}_i$$

where $\boldsymbol{P}_i$ is a vector of production values over all nodes. $\boldsymbol{T}$ is a matrix of ecological transfer efficiencies from node *j* to node *i*. $\boldsymbol{A}_i$ represents the addition of production to node *i* from other sources. $\boldsymbol{L}$ represents a loss term from node *i* (e.g. advective loss, removals due to harvest etc.).

Accounting for Uncertainty

To represent uncertainty in key input parameters to the production potential model, we specified empirically derived probability distributions for primary production, transfer efficiencies, and the split between transfer of energy from microplankton to benthos and mesozooplankton.

We used truncated normal probability distributions to represent uncertainty in predicted levels of microplankton and nano-picoplankton production from empirical models. We computed the mean phytoplankton production and its variance and assigned a coefficient of variation 30% to represent the uncertainty attributable to interannual phytoplankton production and to the application of the empirical production model relating chlorophyll to primary production.

For transfer efficiencies between microplankton and higher components of the food web we used Beta distributions at each level based on our compilation of regional estimates of transfer efficiencies as noted above. Transfer estimates are constrained between 0 and 1 and are application of the Beta distribution is appropriate. The probability density function is given by:

$$\frac{\Gamma(a_i + b_i)}{\Gamma(a_i)\Gamma(b_i)} TE_i^{\,a_i - 1}(1 - TE_i^{\,b_i - 1})$$

where Γ is the gamma function and a and b are parameters. We determined the parameters of the beta distribution using the method of moments:

$$\widehat{a}_i = \overline{TE}_i \left(\frac{\overline{TE}_i (1 - \overline{TE}_i)}{s_{TL_i}^2} - 1 \right)$$

and

$$\widehat{b}_i = (1 - \overline{TE}_i) \left(\frac{\overline{TE}_i (1 - \overline{TE}_i)}{s_{TL_i}^2} - 1 \right)$$

where $\overline{TE}_i$ is the mean transfer efficiency at each trophic level for the 14 systems and s_{TL}^2 is the estimated variance. We weighted the estimates inversely for each of the 14 systems according to its distance from Georges Bank.

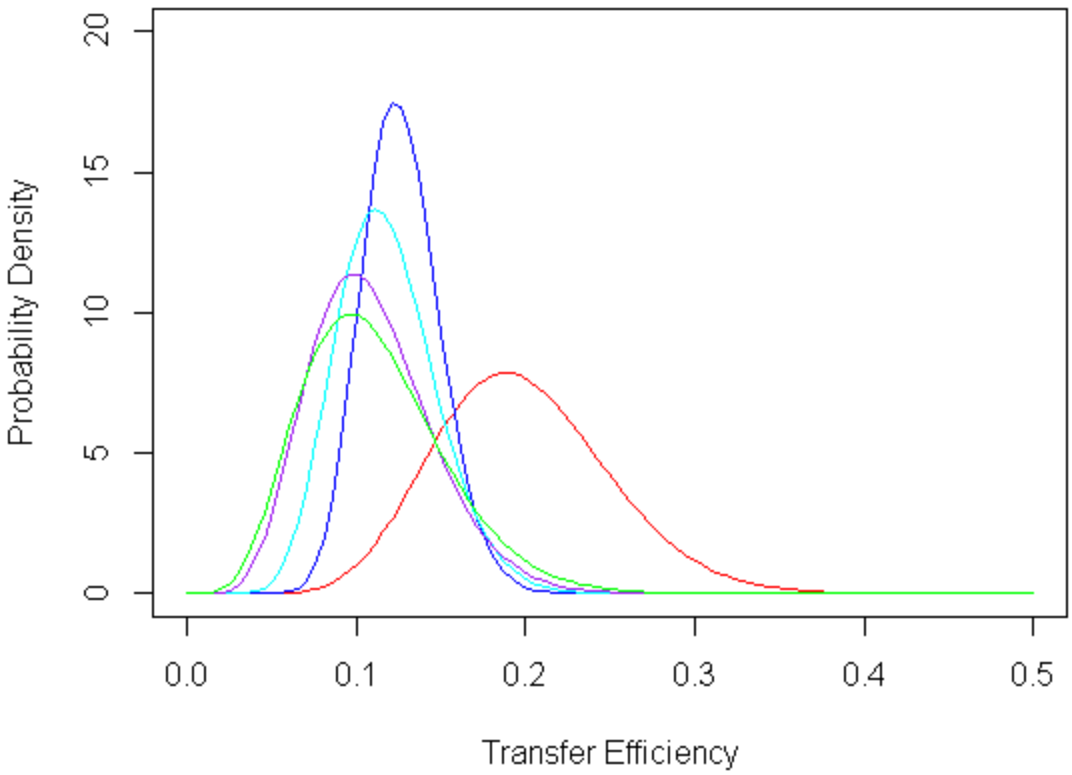

Figure 2.2. Beta probability density functions for trophic levels II (red), III (dark blue), IV (cyan), V (purple) and VI (green) based on14 food web models for continental shelf systems ranging from the Mid-Atlantic Bight to the Grand Banks.

Energetic pathways involving the benthos differed substantially in different food web models we examined. In recognition of the limitations of using these models to characterize uncertainty in energetic pathways involving the benthos, we used uniform probability distributions bounded by the upper and lower quartiles of the range of observed splits between the benthos and mesozooplankton in our analyses.

Most of the existing models for the region that we examined did not partition phytoplankton production by size class and therefore did not allow treatment of the microbial food web as specified in our model. In those cases, we used literature values for ecotrophic efficiencies (proportion of production consumed within the microbial food web and the gross growth efficiency of bacteria and microzooplankton (Straile 1997; Ware 2000).

Fishery Production Potential

The model represented in Figure 2.1 permits estimation of the total ecosystem production potential, but the production available for fishing is only a fraction of this total production. This fraction will be a function of the production potential at the nodes being harvested, and the harvesting rate imposed on those nodes. If we discriminate between losses of production due to fishing (C_i) (including both discarded and landed components) and all other sources of removals attributable to natural predators (L'_i). The basic model can be re-written as

$$P_i = TP_j + A_i - L'_i - C_i$$

For the purposes of this analysis, we assume that inputs and losses from sources other than fishing are in balance at each node. Then, harvest extracted from node *i* can be expressed as

$$C_i = E_i P_i$$

where E_i is the fractional exploitation rate applied to the production at node *i*. The model was implemented in JAGS and employed a Gibbs Markov Chain Monte Carlo sampler. A total of 10,000 iterations were used for each run to characterize uncertainty.

Ecosystem Reference Points

Earlier estimates of fishery production potential typically assumed that 50-70 per cent of production at a defined mean trophic level could be sustainably extracted as catch (e.g Graham and Edwards 1962; Ryther 1969; Schaefer 1965 Ricker 1969; but see Moiseev 1994). These proposed extraction rates were predicated on prevailing single-species recommendations based on the (implicit) assumption that fishing mortality rates could equal natural mortality for the stock (Pauly & Christensen 1995a). It is now recognized that these earlier target levels for single-species management were too high and led to risk-prone decisions (Pauly & Christensen 1995a). Standard reference points have not been fully established to guide overall extraction policies for marine ecosystems. Iverson (1990) proposed that exploitation rates (encompassing human and natural predators) should not exceed the *f*-ratio (the ratio of new primary production to total primary production) in marine systems. This suggestion is based on the underlying recognition that new production (primarily by larger phytoplankton species) is more readily

available to fuel production at the higher trophic levels of principal economic interest while the production derived from the nano-picoplankton is largely, but not exclusively, consumed within the microbial food web. Ware (2000) indicated that new production can be expected to range from 0.2 to 0.45. Direct estimates of the *f*-ratio based on isotopic analysis are not available for Georges Bank. Based on nutrient budget calculations however, Steele et al. (2007) reported an estimate of approximately 30%. In this analysis, we considered the ratio of microplankton production to total primary production as a first-order approximation and basis for testing a limit reference point. Moiseev (1994) proposed that ecosystem-level exploitation rates not exceed 20% of available production. In the following demonstration, we employed Moiseev's recommendation to set a target reference point.

Results

Satellite derived estimates of nano-picoplankton and microplankton production are shown in Figure 2.3. Production levels are highest on the crest of the bank and the adjacent Nantucket Shoals region where strong tidal forces and shallow water depths permit mixing of nutrients throughout the water column. Estimates of total net primary production averaged 321 gC/m^2/yr during 1998-2016. The earliest ^{14}C-derived estimate for Georges Bank for Georges Bank of 373gC/m^2/yr (Cohen et al. 1982) was subsequently lowered to 332 gC/m^2/yr with the accrual of additional information (Sissenwine et al. 1984).

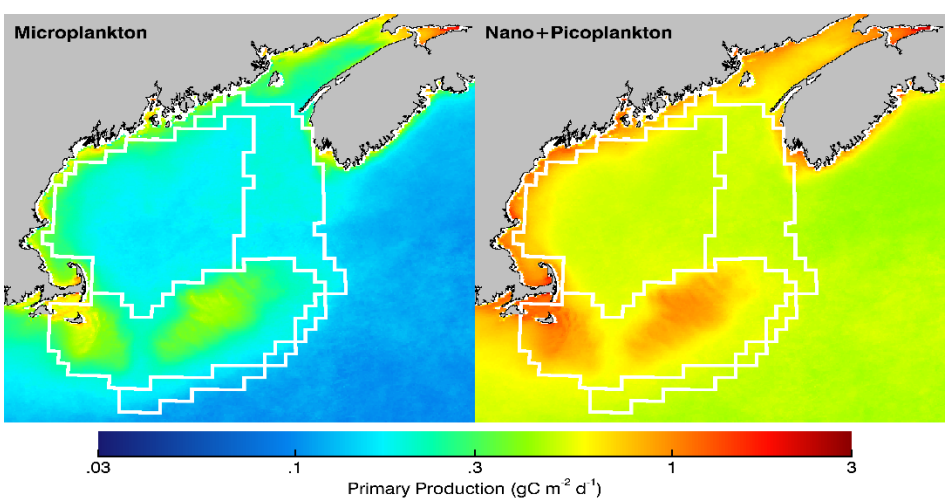

Figure 2.3 Spatial pattern of microplankton and nano-picoplankton production on the Georges Bank ecological production unit and adjacent areas.

An examination of climatological monthly mean phytoplankton production shows a distinct peak during the summer months particularly for the nano-picoplankton component (Figure 2.4). An earlier sub-peak in late spring reflects the importance of the spring bloom. Although the shallow central crest of the bank is well mixed throughout the annual cycle, stratification on the southern flank and other areas surrounding the crest ultimately impedes nutrient regeneration in these regions. There is also evidence that silicate may be limiting for diatom production on the bank (Townsend et al. 2008).

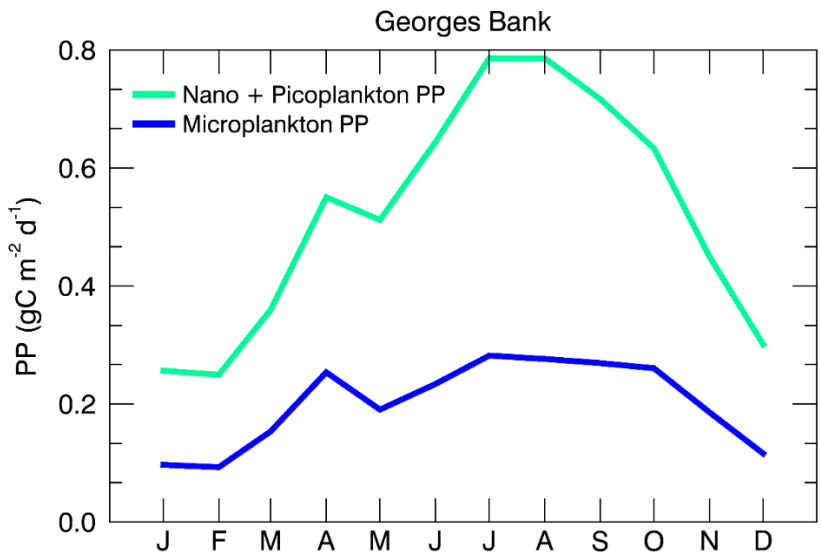

Figure 2.4 Seasonal climatology of primary production by nano-picoplankton and microplankton on Georges Bank.

To obtain annual production estimates, we integrate under the seasonal production curve for each year. Our estimates indicate a steady increase in nano-picoplankton production at a rate of 3.0 gC/m^2/ yr and an increase in microplankton production of 1.6 gC/ m^2/ yr over the period of instrumental record (Figure 2.5).

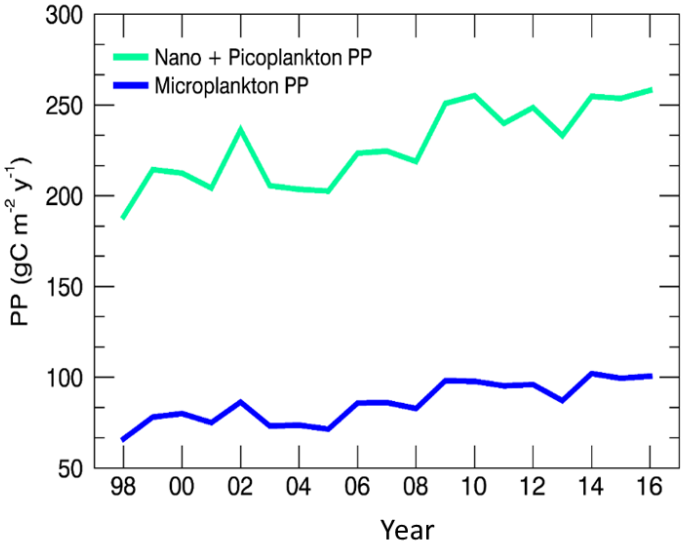

Figure 2.5. Trends in estimated primary production (cG/m^2/yr) for nano-picoplankton and microplankton components on Georges Bank.

The proportion of microplankton production as a fraction of total phytoplankton primary production also exhibits a secular trend, suggesting some increase in food directly available to the grazing food web (Figure 2.6).

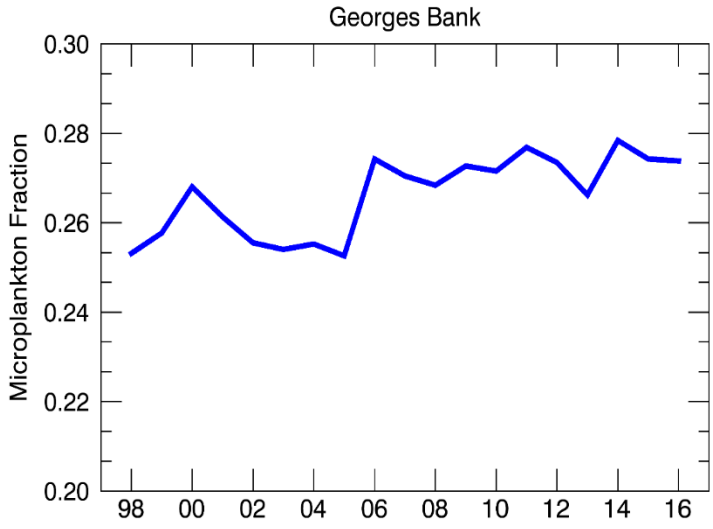

Figure 2.6. Trends in the estimated proportion of microplankton primary production (cG/m^2/yr) on Georges Bank.

To examine the implications of these secular trends, we determined production potential for four time periods spanning the range of observation: 1998-2002, 2003-2007, 2008-2012, and 2013-2016. We begin by examining the estimated ecosystem production potential for the unexploited case conditioned on observed levels of primary production and the trophic transfer probabilities adopted.

The estimated ecosystem production potential in the absence of exploitation provides one approach to evaluating the ecosystem carrying capacity of the system. In Figure 2.7 we provide estimates of the production by functional group for the 4 time periods in the analysis. The increase in primary production over the time period results as expected in increases in production for each of the potentially harvestable functional groups. However, the magnitude of the temporal increase becomes increasingly attenuated at successively higher trophic levels (Figure 2.7). The effect of applying a 20% exploitation rate on each functional group as per Moiseev (1994) is depicted in Figure 2.8.

The total median live weight) for the system under an exploitation rate of 0.2 ranges from 400- 460 kt over the four temporal stanzas. The median harvested production for combined benthivore, planktivore, and upper trophic level predators ranged from 192-217 kt over each of the four temporal stanzas. The median potential yield for suspension feeding bivalves ranged from 128-155 kt live weight over these time periods. Note that these estimates represent production integrated over all size classes. The harvested component of the suspension feeding bivalve functional group is composed of bivalves. Landings of these species are typically reported as meat weight rather than live weight (including shell). For the three dominant harvested bivalve species on Georges Bank, the mean conversion coefficient from live weight to meat weight is 0.145. These estimates for each harvested compartment do include production by species not currently subject to exploitation. Therefore a broader-based harvesting strategy including latent resource species could provide one avenue to increased utilization of available production.

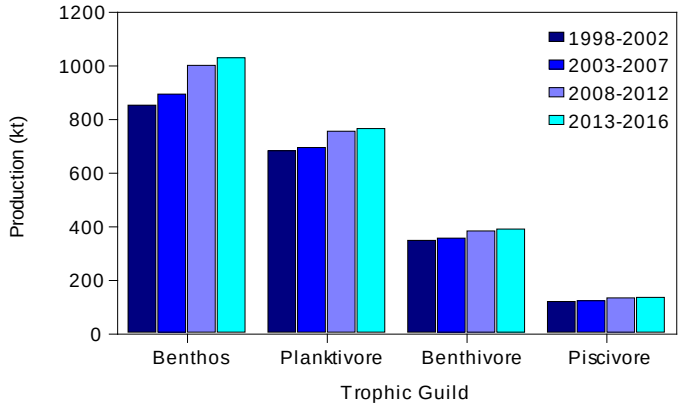

Figure 2.7 Estimated median ecosystem production potential in the absence of exploitation by functional group on Georges Bank for four time periods.

Table 2.1. Estimated Production (kt) by functional group and total secondary production for 4 time periods with no exploitation.

Time Period	Estimate	Benthos	Benthivore	Piscivore	Planktivore	Total
1998-2002	Median	853.90	349.41	121.56	684.04	60234.71
	Mean	938.20	369.90	126.85	702.14	59249.4
	25th Percentile	597.95	226.66	95.88	553.50	50814.37
	75th Percentile	1198.68	489.41	152.70	828.88	68608.15
2003-2007	Median	895.14	357.84	124.30	696.06	61286.71
	Mean	973.25	378.44	129.81	717.47	60383.7
	25th Percentile	610.01	235.11	98.11	566.91	51880.58
	75th Percentile	1247.56	495.49	155.92	844.33	69906.98
2008-2012	Median	1002.22	384.91	134.95	756.72	66059.08
	Mean	1098.71	410.06	140.52	779.09	64437.54
	25th Percentile	702.38	255.33	106.70	620.13	56243.17
	75th Percentile	1403.68	539.85	168.06	916.42	73962.95
2013-2016	Median	1030.36	391.75	136.99	766.60	66979.17
	Mean	1126.15	417.79	142.25	786.65	65250.62
	25th Percentile	722.65	259.08	107.81	625.46	57190.55
	75th Percentile	1446.25	549.52	170.89	928.80	75035.5

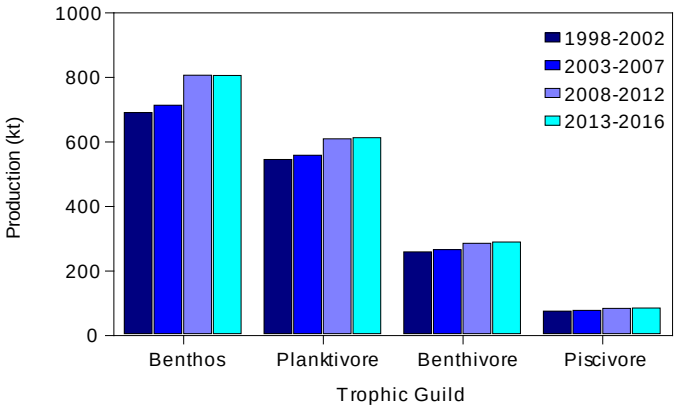

Figure 2.8. Estimated median ecosystem production potential by functional group on Georges Bank for four time periods at an exploitation rate of 0.2

Table 2.2. Estimated Production (kt) by functional group and total secondary production for 4 time periods with an exploitation rate of 0.2 for each functional group.

Time Period	Estimate	Benthos	Benthivore	Piscivore	Planktivore	Total
1998-2002	Median	691.13	259.41	75.72	545.57	59481.42
	Mean	756.02	277.41	79.08	559.73	58706.13
	25th Percentile	476.26	166.88	59.04	441.50	50299.69
	75th Percentile	970.96	368.95	95.60	661.54	68198.51
2003-2007	Median	714.04	266.22	78.07	558.81	61037.41
	Mean	781.65	284.74	81.22	574.81	59920.61
	25th Percentile	492.72	171.97	60.53	455.29	51632.31
	75th Percentile	993.84	377.25	97.68	676.79	69498.57

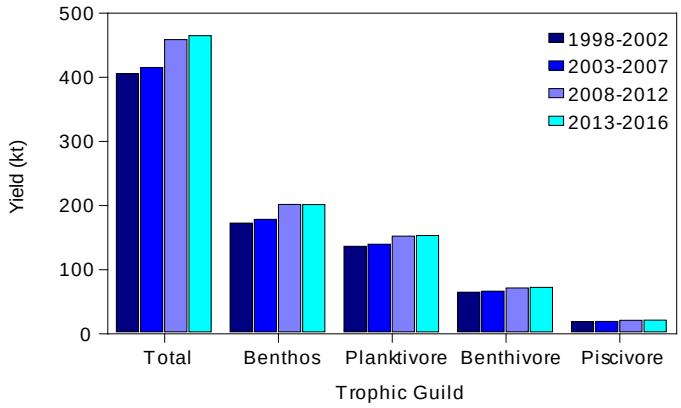

Figure 2.9 Estimated median harvested production potential by functional group on Georges Bank for four time periods at an exploitation rate of 0.2.

Table 2.3. Estimated Yield (kt) by functional group and total secondary production for 4 time periods with an exploitation rate of 0.2 applied to each functional group.

Time Period	Estimate	Total	Benthos	Benthivore	Piscivore	Planktivore
1998-2002	Median	405.38	172.78	64.85	18.93	136.39
	Mean	418.06	189.01	69.35	19.77	139.93
	25th Percentile	324.66	119.07	41.72	14.76	110.37
	75th Percentile	497.60	242.74	92.24	23.90	165.38
2003-2007	Median	415.30	178.51	66.55	19.52	139.70
	Mean	430.60	195.41	71.19	20.30	143.70
	SD	133.63	97.69	35.81	6.98	42.33
	25th Percentile	336.14	123.18	42.99	15.13	113.82
	75th Percentile	509.21	248.46	94.31	24.42	169.20
2008-2012	Median	458.67	201.68	71.52	21.13	152.39
	Mean	473.92	219.46	76.57	21.91	155.98
	25th Percentile	368.70	140.11	46.45	16.61	124.61
	75th Percentile	564.60	281.06	102.04	26.30	182.92
2013-2016	Median	465.02	201.55	72.44	21.33	153.27
	Mean	477.41	220.85	77.02	22.12	157.43
	25th Percentile	374.20	140.94	47.23	16.78	124.93
	75th Percentile	565.90	283.77	101.68	26.63	184.98

Discussion

Attempts to define the fishery production potential of marine systems based on energetic considerations have an extensive history (Kestevan & Holt 1955; Graham & Edwards 1962; Schaefer 1965; Moiseev 1969; Ricker 1969; Ryther 1969; Gulland 1970, 1971; Moiseev 1994). Bottom-up control of fish production has now been demonstrated in many regions of the world ocean (Ware 2000) supporting the general approach of tracing pathways involved in the translation of primary production to fishery yields. These earlier estimates of fishery production potential based on energetic principles employed estimates of primary production integrated over all phytoplankton size classes, inferred ecological transfer efficiencies from laboratory experiments and other observations, and observed or assumed levels of the mean trophic level of the catch. The general strategy was laid out by Kestevan and Holt (1955). Graham and Edwards (1962) provided the first estimate of potential global fish yield using this method. Ryther (1969) was the first to apply a partitioning of fishery production potential among different oceanic domains including coastal, offshore, upwelling, and open ocean systems. Ryther (1969) further applied different estimates of food chain length in these different system types to reflect fundamental differences in ecosystem structure and patterns of energy flow.

These methods, essentially collapsing food webs into food chains, have been largely superseded by applications of full network models using the Ecopath modeling framework (Christensen and Pauly 1992) and its dynamic extension, EcoSim. Ware (2000) and Stock et al. (2016) however have developed extensions to these earlier approaches, including additional components but retaining a connection to the fundamental simplicity of the production potential approach.

Recent network models for Georges Bank provide a useful point of comparison with the estimates of Ecological Production Potential provided here. Link et al. (2006) developed Ecopath models for major subregions of the Northeast U.S. Continental Shelf including Georges Bank. Estimates of fishery production for Georges Bank provided by Link et al. (2008) and translated to fish yield are approximately 90,000 mt when adjusted to the same spatial footprint used in our analysis. Collie et al. (2009) provided fishery production estimates using the end-to end food web model of Steele et al. (2008). Again converting to fish yield and employing our spatial footprint for Georges Bank, yields an estimate of approximately 130,000 mt. Both the

Link et al. (2008) and the Collie et al. (2009) analyses integrate estimates of biomass or production at each node in their respective food web and represent 'realized' production given a history of change and anthropogenic impact in the system. They further are contingent on the species and nodal structure included in the analysis.

Perhaps not surprisingly, our production potential estimates for fish are somewhat higher (on the order of 200,000 mt). They represent an attempt to provide first order estimates of potential yield given the energy inputs at the base of the food web -- estimates of what could be rather than what has been, given probabilistic estimates of transfer efficiencies. We have attempted to adjust our estimates of the suspension feeding benthos and the planktivore functional groups to exclude components for which prospects of fishery exploitation is highly unlikely (at least at present). However, all of our functional groups subject to harvesting do implicitly include consideration of latent resources that could in principle support fisheries, again contributing to the higher overall estimate of potential yield. Although the ecosystem risks of exploiting currently latent resources would need to be carefully evaluated, diversification of the exploitable resource base holds the potential to reduce pressure on the system overall if carefully implemented (Fogarty and Murawski 1997).

We note that the apparent secular trend in primary production on Georges Bank, if continued, suggests the potential for increased yields in the future. Trends in research vessel surveys over the last several decades on Georges Bank have been increasing (Bell et al. 2014) although the degree to which this may reflect increasing production in general is presently unknown. Trenkel (2017) recently proposed a management procedure in which adjustments to multispecies annual catch limits could be calibrated to changes in primary production. As shown in our analysis, the implications for changes in potential yield within the range of observed changes in primary production can be readily explored.

References

Behrenfeld, M.J. and P.G. Falkowski. 1997. Photosynthetic Rates Derived from Satellite- based Chlorophyll Concentration. Limnol. Oceanogr. 42(1):1-20.

Chassot, E., S. Bonhommeau, N.K. Dulvy, F. Melin, R. Watson, D. Gascuel, and O. Le Pape. 2010. Global marine primary production constrains fisheries catches. Ecol. Lett. 13:495-505.

Christensen V, Walters CJ, Pauly D. 2005. Ecopath with Ecosim: A user's guide. Fisheries Centre, University of British Columbia, Vancouver, B.C. (Canada)

Clark, S.H. and Brown, B.E. 1977. Changes in biomass of finfishes and squids from the Gulf of Maine to Cape Hatteras, 1963-74, as determined from research vessel survey data. Fishery Bulletin 75:1-21.

Clarke, G.L. 1946. Dynamics of production in a marine area. Ecol. Monogr. 16:321-337.

Cohen, E.B., M.D. Grosslein, and M.P. Sissenwine. 1982. Energy budget of Georges Bank. Can. Spec. Publ. Fish. Aquat. Sci. 59:95-107.

Collie, J.S., D.J. Gifford, and J.H. Steele. 2009. End-to-end foodweb control of fish production on Georges Bank ICES J. Mar. Sci. 66:2223-2232.

Eppley, R. W. 1972. Temperature and phytoplankton growth in the sea. Fish. Bull. 70: 1063-1085.

Fogarty, M. J., and S. A. Murawski. 1998. Large-scale disturbance and the structure of marine systems: Fishery impacts on Georges Bank. Ecological Applications 8(S1):S6-S22.
Fogarty, M.J., Rosenberg, A.A., Cooper, A.B., Dickey-Collas, M., Fulton, E.A., Gutiérrez, N.L., Hyde, K.J.W., Kleisner, K.M., Kristiansen, T., Longo, C., Minte- Vera, C.V., Minto, C., Mosqueira, I., Osio, G.C., Ovando, D., Selig, E.R., Thorson, J.T., Ye, Y., 2016. Fishery production potential of large marine ecosystems: A prototype analysis. Environmental Development 17, Supplement 1, 211-219.

Graham, H.W. and R.L. Edwards. 1962. The world biomass of marine fishes. (In) E. Heen and R. Kreuzer, Eds. Fish in Nutrition. Fishing News Books. London. pp 3-8.

Gulland, J.A. 1970. The Fish Resources of the Ocean. Fishing News Books. West Byfleet.
Johnson, N.L., S. Kotz, and N. Balakrisnnan. 1995. Continuous Univariate Distributions. 2nd Ed. J. Wiley and Sons, NY.

Iverson, R.L. 1990. Control of marine fish production. Limn. Oceanogr. 35:1593-1604.

Kestevan, G.K. and S.J. Holt. 1955. A note on the fisheries resources of the Northwest Atlantic. FAO Fish. Pap. 7:1-11.

Lalli, C.M. and T.R. Parsons. 1997. Biological Oceanography: An Introduction. 2nd Ed. Butterworth-Heinemann, Oxford.

Link, J.S., Griswold, C.A. Methratta, E.M. & Gunnard, J. (eds). 2006. Documentation for the Energy Modeling and Analysis eXercise (EMAX). Northeast Fisheries Science Center Reference Document, 06-15. 166 pp.

Link, J. J. O'Reilly, M. Fogarty, D. Dow , J. Vitaliano, C. Legault, W. Overholtz, J.Green, D. Palka, V.Guida, and J. Brodziak. 2008. Energy flow on Georges Bank revisited: the Energy Modeling and Analysis Exercise in historical context. J. Northwest Atl. Fish. Sci. 39:83-101.

Morel, A. 1991. Light and marine photosynthesis: a spectral model with geochemical and climatological implications. Progress in Ocean.

O'Reilly, JE and C. Zetlin. 1998. Seasonal, Horizontal, and Vertical Distribution of Phytoplankton Chlorophyll a in the Northeast U.S. Continental Shelf Ecosystem. NOAA Tech. Rep. NMFS 139; 120 p.

Pan, X., A. Mannino, M. E. Russ, S. B. Hooker and L. W. Harding Jr . 2010. Remote sensing of phytoplankton pigment distribution in the United States northeast coast. Remote Sensing Envir. 114: 2403-2416.

Pan, X., A. Mannino, H. G. Marshall, K. C. Filippino and M. R. Mulholland. 2011. Remote sensing of phytoplankton community composition along the northeast coast of the United States. Remote Sensing of Environment 115: 3731-3747.

Pauly, D. 1996. One hundred million tons of fish, and fisheries research. Fish. Res. 25:25-38.

Pauly D, Christensen V (1995) Primary production required to sustain global fisheries. Nature 374:255-257

Ricker, W.E. 1970. Food from the Sea. (in) Resources and Man. U.S. National Academy of Sciences. W.H. Freeman, San Francisco.

Ryther, J. 1969. Photosynthesis and fish production from the sea. Science 166:72-76.

Schaefer, M.B. 1965. The potential harvest of the sea. Trans. Am. Fish.Soc. 94: 123-128.

Sherman, K. and L. Alexander. 1986. Variability and management of large marine ecosystems. United States, Westview Press, Inc.,Boulder, CO.

Sissenwine, M. P., E. B. Cohen, and M. D. Grosslein. 1984. Structure of the Georges Bank ecosystem. Rapports et Proces-Verbaux des Reunions du Conseil International pour l'Exploration de la Mer 183:243-254.

Steele,J., J. Bisagni, J. Collie, M. Fogarty, D. Gifford, J. Link, M. Sieracki, B. Sullivan and A. Beet. 2007. Constructing end-to-end budgets for the Georges Bank ecosystem. Prog. Oceanogr. 74:423-448

Stock, C.A. and 9 others. 2016. Reconciling fisheries catch and ocean productivity. Proc. Nat. Acad. Sci.DOI/10.1073/pnas.16102381114.

Trenkle, V.M. 2018. How to provide scientific advice or ecosystem-based management. Fish. Fisher. DOI:10.111/faf.1263

Vidussi, F., H. Claustre, B. B. Manca, A. Luchetta and J.-C. Marty. 2001. Phytoplankton pigment distribution in relation to upper thermocline circulation in the eastern Mediterranean Sea during winter. Journal of Geophysical Research 106(C9): 19939-19956.

Ware, D.M. 2000. Aquatic ecosystems: properties and models. In P.J.Harrison and T.R. Parsons (Eds). Fisheries Oceanography: An Integrative Approach to Fisheries and Ecology and Management. Blackwell Sci., Oxford.

Appendix

Table A.1 Estimated transfer efficiencies, region, and sources. EMAX (J. Link, NEFSC Pers. Comm.), SAUP (Sea Around US Project).

Transfer Efficiency					Region	Source
II	III	IV	V	VI		
0.23	0.12	0.09	0.09	0.09	Mid-Atlantic Bight	EMAX
0.23	0.13	0.10	0.13	0.13	Southern New England	EMAX
0.17	0.11	0.11	0.11	0.10	Georges Bank	EMAX
0.17	0.17	0.17	0.16	0.17	Gulf of Maine	EMAX
0.23	0.12	0.12	0.06	0.07	Bay of Fundy-Western SS	A. Bundy (pers. comm)
0.11	0.14	0.06	0.04	0.04	Western Scotian Shelf	SAUP
0.15	0.07	0.05	0.03	0.02	Eastern Scotian Shelf	SAUP
0.13	0.13	0.10	0.09	0.10	Eastern Scotian Shelf	A. Bundy (pers. comm)
0.12	0.16	0.11	0.09	0.04	Eastern Scotian Shelf	SAUP
0.12	0.16	0.12	0.07	0.05	Grand_Banks	SAUP
0.11	0.14	0.15	0.08	0.05	Grand_Banks_1900s	SAUP
0.14	0.13	0.13	0.10	0.07	Grand_Banks_1980s	SAUP
0.19	0.16	0.11	0.06	0.04	Grand_Banks_1990s	SAUP
0.34	0.14	0.16	0.11	0.05	Newfoundland Shelf	A. Bundy (pers. comm)

Section 3: *TOR 3*

Evaluate the approach and rationale for specifying Fishery Functional Groups as proposed management units

Ref: TOR 3

Functional Group Management

"…functional groups are not just an empirical convenience but the basic operational units to describe how ecosystems work. But this approach has not got into the practice of EBFM."
(John Steele pers. comm. Sept. 13, 2013)

Introduction

Confronting the challenge of complexity is central to any attempt to implement operational Ecosystem-Based Fisheries Management (EBFM; Fogarty 2014). The problem is particularly acute in effectively managing mixed-species fisheries comprising assemblages of interacting species. The complexity of the system, related to both biological and technical interactions among managed species, and our inability to exert exact compositional control of catches and fishing mortality in mixed-species fisheries lie at the heart of the difficulties in managing these systems. Tradeoffs in managing species connected by technological and ecological interactions remain unresolved in conventional single-species approaches. Yield targets derived from a single-species perspective in which each is treated in isolation generally cannot be simultaneously met in mixed species fisheries (e.g. Walters et al. 2005; MacKinson et al. 2009). Single species management strategies in this setting can actively work at cross purposes when applied to assemblages of interacting species (Fogarty 2014). One possible avenue for addressing these intertwined issues is to focus management actions at higher levels of social-ecological organization in an attempt to capitalize on emergent properties at the system level while sidestepping known problems in effective management of species linked by technological and biological interactions.

Here, we explore Fishery Functional Group Management as one possible avenue to simplifying management in a way that reflects the role that species play in fishery ecosystems as human prey and as predators, prey, and competitors in the 'natural' food web. Fishery Functional Groups are framed by the intersection of fishery structure and practice with the role played by species within an ecosystem. We define a Fishery Functional Group (FFG) as comprising species that are caught together by specified fleet sectors and that play similar roles in the ecosystem with respect to energy transfer. Because these species are caught together, *inter alia* they share similar habitat use patterns and also size structures related to specific selectivity

characteristics of the fishing gears employed. The concept accordingly encapsulates information on the catch characteristics and targeting practices of different fleet sectors and fundamental ecological characteristics of assemblages of exploited species within these operational fisheries or *metiers.* We further note that functional groups defined in this way will also comprise species of differing vulnerabilities to harvesting due to fundamental difference in life history characteristics. It will therefore be necessary to address the issue of differential risk to species within the functional group(s).

Previous analyses of the Northeast US mixed species trawl fishery have consistently concluded that clear limits to the targeting capability of fishers exist. Murawski (1996) related these constraints to patterns of species co-occurrence (see also Murawski and Finn 1988). These patterns of co-occurrence were found to vary in space and time, offering some opportunities to enhanced targeting. A succession of economic analyses have clearly demonstrated, however, constraints on separability of species catches in the Northeast mixed species trawl fishery (Squires 1987; Scheld and Anderson 2016). Scheld and Walden (in review) do indicate that appropriate incentive structures to avoid bycatch of depleted species can be devised and implemented; however, clear limits on separability remain in this joint production system. Other studies conclude that reduction of by-catch in the mixed species fishery is difficult to achieve without reducing overall catches (Fare et al. 2006).

Seemingly intractable difficulties have arisen in attempts to manage groundfish resources in mixed-species fisheries in the Northeastern United States (Appollonio and Dykstra 2008). These problems were anticipated nearly half a century ago by McHugh (1959) who recommended a strategy management '*en masse'* of aggregate species groups rather than single-species management. Edwards (1975) similarly advocated the concept of Total Biomass Management in explicit recognition of the fundamental difficulties arising from the confluence of technical and biological interaction in mixed species fisheries.

Defining Fishery Functional Groups

As an illustration of how fleet structure has been defined in previous work, we review the characterization of operational fisheries provided by Lucey and Fogarty (2013). Analyses of this type can provide objective specification of fishery-based assemblages to start the process of

defining fishery functional groups. Similarly, feeding guilds have been defined for the Georges Bank ecosystem. To define trophic guilds of fish and squid on Georges Bank, Garrison and Link (2000) analyzed diet composition data obtained during standardized NEFSC research vessel surveys. Ontogenetic shifts in diet composition were shown to be important for several species which were then assigned to more than one trophic guild depending on their size.

Finally, the unavoidable occurrence of species of differing life histories in mixed species fisheries requires consideration of options to identify and afford protection to vulnerable species. We further consider differences in species vulnerability to exploitation in relation to life history characteristics.

Operational Fisheries

Lucey and Fogarty (2013) defined operational fisheries for fleets operating out of New England ports on the basis of species catch compositions in space and time. Analyses were conducted separately for six gear types (otter trawl; dredges, pots; longlines, gillnets, and seines. Each gear category was further divided by vessel size. Small vessels were designated as those with a gross registered tonnage less than or equal to 150 tons, while large vessels were designated as those with a gross registered tonnage of greater than 150 tons. Murawski et al. (1983) had earlier delineated nine major operational fisheries for the otter trawl fleet of New England. In the following, we will review the demersal fisheries important on Georges Bank.

Lucey and Fogarty (2013) identified 10 operational otter trawl fisheries on the northeast shelf using k-means cluster analysis. Of these, two had a widespread presence on Georges Bank. These fisheries differed principally with respect to the relative mix of groundfish species comprising the catch and their spatial location on the bank. Fishery 1 of the otter trawl gear category as defined by Lucey and Fogarty (2013) was dominated by haddock with strong contributions from Atlantic cod, winter flounder, and smaller contributions from 7 other species (Table 3.1). Otter trawl fishery 5 reflects a seasonal pattern of resource use on Georges Bank. From April to June, haddock , Atlantic cod, and winter flounder are the primary species landed while from July to September, skate, yellowtail flounder, summer flounder, and winter flounder dominate the landings.

Table 3.1 Major otter trawl fisheries on the Northeast U.S. Continental Shelf defined by Lucey and Fogarty (2013) with dominant species composition. Otter trawl fisheries 1, and 5 have a major spatial

presence on Georges Bank. Black boxes represent a large contribution (>20%), grey boxes represent a medium contribution (~5-20%), light grey boxes represent a low contribution (~1-5%).

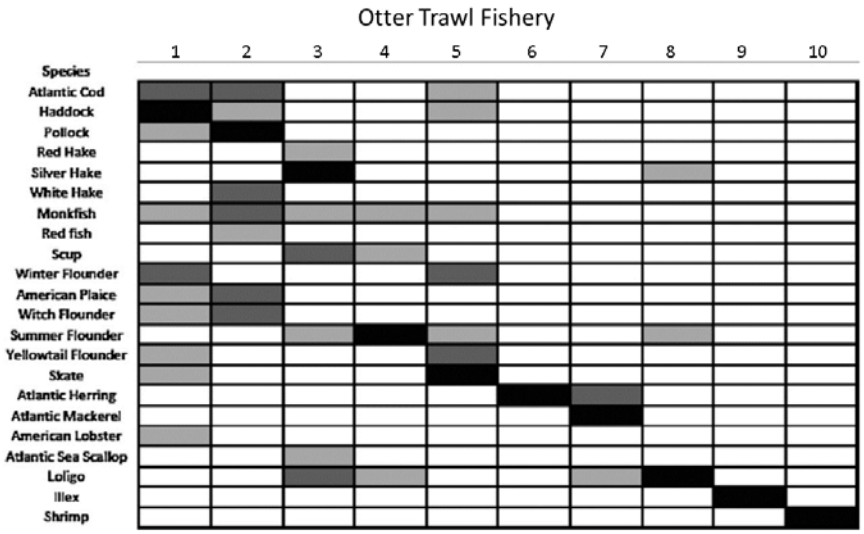

An additional three otter trawl fisheries have a more spatially restricted presence on the bank. Trawl fishery 3 is located on the southern flank of the bank and focuses on silver and red hake, scup, and longfin squid. Trawl fishery 6 targets Atlantic herring on the herring spawning grounds on the northern edge of the bank in autumn. Fishery 8 operates on the shelf break region of Georges Bank.

The demersal fixed gear fisheries employing longlines and gillnets on Georges Bank occupy a much smaller spatial footprint than the otter trawl fisheries. The longline fisheries on Georges Bank are concentrated in southwest portion of the bank and on the northern edge. Lucey and Fogarty (2013) identified two longline fisheries operating on Georges Bank and the adjacent Gulf of Maine. The longline fishery in the southwest portion of the bank and the adjacent Gulf of Maine (longline fishery 1) concentrates on cod and haddock. Longline fishery 2 on the northern edge and in the Gulf of Maine harvested cod, haddock, cusk, and spiny dogfish. Two gillnet métiers operate in southwestern Georges Bank and the Gulf of Maine. Gillnet fishery 1 was dominated by cod, pollock, monkfish, and spiny dogfish. Gillnet fishery 2, in contrast, concentrates on monkfish and skates.

Trophic Structure

The Georges Bank food web is recognized as complex and highly interconnected (Figure 3.1). Link (2002) provided a detailed evaluation of the Georges Bank food web based on multidecadal sampling program documenting diet composition carried out in conjunction with standardized bottom trawl surveys on the Northeast U.S. Continental Shelf (Link and Almedia 2000). Link (2002) reported that this food web was characterized by higher levels of linkage density and connectivity than many other reported marine foodwebs. The system is further characterized by relatively high levels of omnivory).

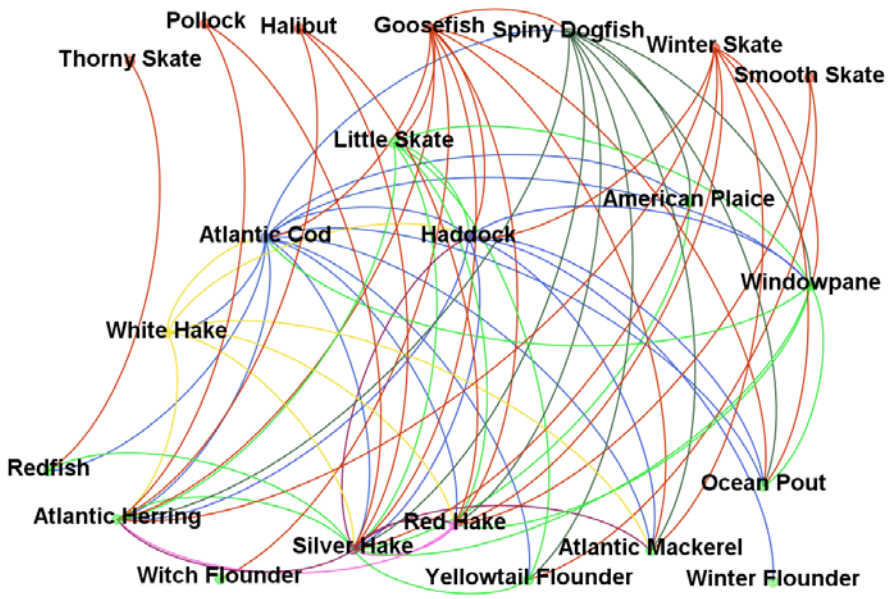

Figure 3.1 NEFMC managed species connected by predator-prey interactions based on Northeast Fisheries Science Center diet composition studies (see Smith and Link 2010 for a summary of methods and results). Connections between predators (red node) and their prey (green nodes) are shown for species pairs in which any predation interactions were recorded.

Garrison (2000) defined feeding guilds for the Georges Bank system based on hierarchical agglomerative cluster analysis of diet composition estimates for 29 predator species obtained during standardized research vessel surveys (Link and Almedia 2000). Species were partitioned into size classes to capture ontogenetic shifts in diet. Feeding assemblages were examined separately for spring and fall survey observations. In both spring and autumn, five major feeding groups were identified with further levels of substructure defined within most (but not all) of the major groupings (Figures 3.2)

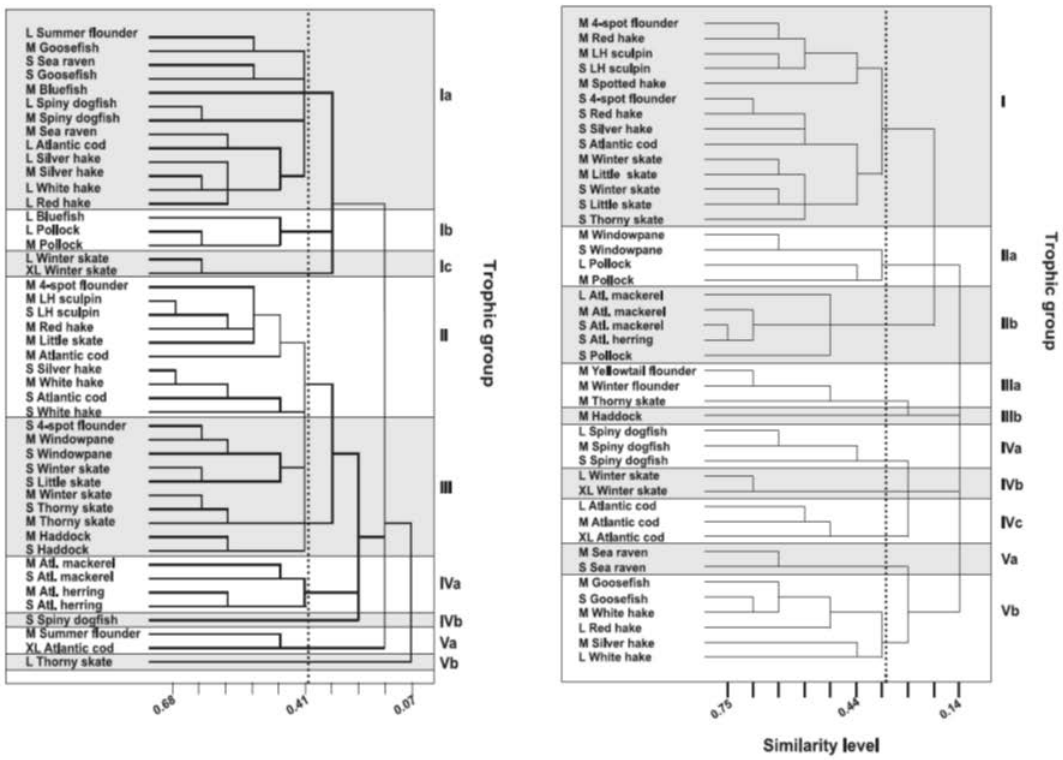

Figure 3.2. Dendrograms of species diet similarities based on diet composition studies during NEFSC standardized research vessel surveys in spring (left panel) and autumn (right panel) (Garrison 2000).

We consolidated the spring and autumn feeding groups of Garrison (2000) into the following feeding assemblages:

1) Benthivores (predators of species in the benthos category)
2) Mesoplanktivores (predators of mesozooplankton, principally copepods)
3) Macroplanktivores (predators of macrozooplankton, principally amphipods but including decapod shrimp)
4) Macrozoo-Piscivores (predators of macrozooplankton and fish) and
5) Piscivores (predators of fish species)

Previous designations of feeding guilds on Georges Bank have employed a somewhat simpler classification of benthivores, planktivores, and piscivores (e.g. Cohen et al. 1982; Sissenwine et al. 1984; Steele et al. 2008).

Joint consideration of trophic guild membership and species representation in the catch in different fishing gears for NEFMC-managed fish species (NEFMC EBFM Plan Development Team)[1] is provided in Appendix Table A3.1. In this case, the fishery membership designation indicates presence or absence in reported landings of a species in a particular gear type on Georges Bank.

Life History Characteristics and Vulnerability

Differential vulnerability of species to overexploitation in mixed-species fisheries can emerge as a result of differences in life history characteristics. Species characterized by slow growth, late maturation, and low fecundity are particularly vulnerable to over-exploitation. The interplay between behavioral attributes affecting catchability and vulnerable life history traits can exacerbate the risk to individual species. We compiled information (where available) on the intrinsic rate of increase, mean trophic level, individual growth rate (von Bertalanfy *k*) , mean age-at-maturation, longevity, maximum size, and fecundity.

We obtained estimates of the intrinsic rate of increase for NEFMC-managed fish populations from Gamble and Link (2009) and Applegate et al. (1998). Estimates of individual growth, longevity, mean age at maturation, and maximum size (length) were obtained from the Fishbase repository (http://www.fishbase.org). When more than one estimate was available for a species, we took the mean. When information was provided separately by sex, we used the estimates for females. Appendix Table A3.2 provides the compilation of estimates for fish species managed by the New England Fishery Management Council.

Nonmetric multidimensional scaling (Legendre and Legendre (1998) was used to provide a reduced dimension analysis of the life history data. We found that focusing on attributes related to reproduction allowed the greatest species separation in two dimensional canonical space. Two major groupings emerged including one dominated by the skate species and another by a broad

[1] The NEFMC EBFM PDT has assembled a broader compilation including species not directly managed by NEFMC including consideration of species caught in recreational fisheries

mixture of teleost species (Figure 3.3). Spiny dogfish, halibut, and redfish were widely separated from the two principal groupings in this analysis, suggesting that special considerations would apply for these species. In the simulation studies to be described in Section 4 of this report, we applied enhanced protection for elasmobranchs.

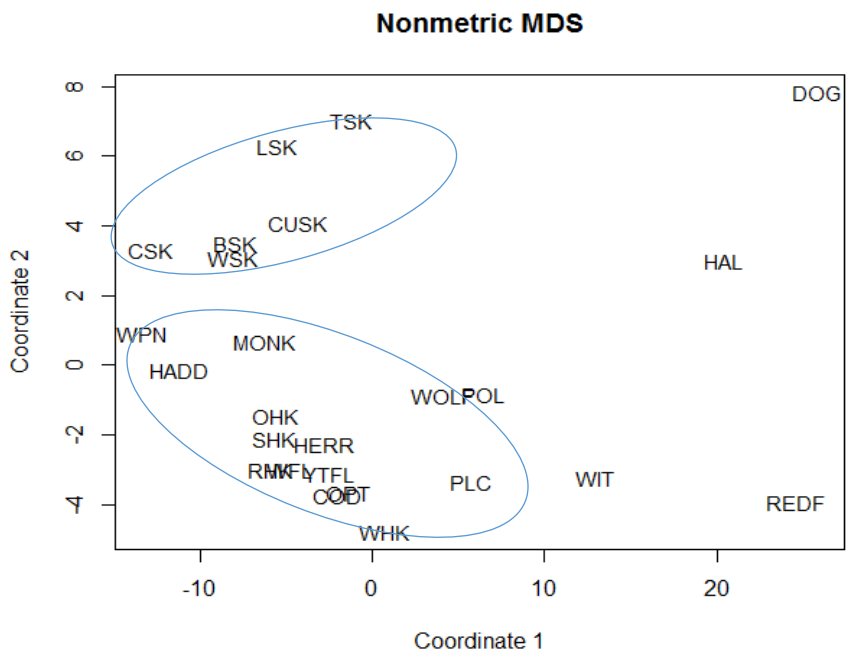

Figure 3.3. Results of nonmetric multidimensional scaling based on life history characteristics or species managed by the New England Fishery Management Council. Species abreviations: DOG Dogfish; TSK Thorny Skate; LSK Little Skate; CSK Clearnose Skate; BSK Barndoor Skate; WSK Winter Skate; CUS K Cusk; WPN Windowpane Fl; HADD Haddock; MONK Monkfish; OHK Offshore Hake; SHK Silver Hake; HERR Herring; WOLF Wolffish; POL Pollock; YTFL Yellowtail Flounder; COD Cod; RHK Red Hake; WHK White Hake; WIT Witch Flounder; HAL Halibut.

Discussion

The special challenges that emerge in the management of mixed species fisheries inevitably entails consideration of their operating characteristics with respect to gear types employed and the magnitude and distribution of fishing effort in space and time. This has led to the recognition of the potential for fleet-based management to provide a viable approach to navigating the complications of managing fisheries characterized by strong technical interactions (e.g. Ratz et al. (2007). Simulation studies of management performance in mixed species

fisheries require explicit consideration of fleet characteristics both to capture the relevant technical interactions related to gear performance and the potential for interactions among fleet components (e.g. Mackinson et al. 2009; 2017; Thorp et al. 2015, 2016, 2017; Gaichas et al. 2016). The fundamental connections between the mechanics of the fish-catching process, yields, and management outcomes are explicitly addressed in this approach.

The concept of fishery functional groups builds on the principle of identifying operational fisheries defined by commonality in catch composition in order to effectively focus management efforts. It further is intended to bring in additional ecological and biological dimensions to maintain ecosystem structure (balance of trophic guilds). Ralston and Polovina (1982) provided an early example of management strategies aimed at higher levels of ecological organization. They identified distinct species assemblages in the Hawaiian deep sea handline fishery. Cluster analysis of commercial fish capture records revealed three major groups defined by depth of occurrence, apparently reflecting habitat preferences of the component species. Ralston and Polovina then applied simple surplus production models to each species individually, the aggregate catch of each cluster group and to the total over the three groups. Aggregation at the cluster group and total catch levels significantly improved the model fits relative to the individual species analysis. Models incorporating all three cluster groups indicated that interactions among groups was negligible.

Tyler et al. (1982) advanced the concept of Assemblage Production Units (APUs) as focal points for management. They identified APUs based on a cluster analysis of research vessel survey catches off the west coast of the United States. The assemblages were largely delineated by depth. Tyler et al. (1982) advocated management at the assemblage-level and outlined an adaptive management strategy to test the efficacy of the overall approach.

Link (2018) provides an overview of the potential advantages of implementing system-level optimum yield strategies. At least two instances of implementation of this concept can be identified. The International Commission for Northwest Atlantic Fisheries (ICNAF) implemented system-level catch quotas on the Northeast U.S. Continental Shelf starting in 1973. The ICNAF ‘Two-Tier” management system for this region entailed the specification an upper-level constraint on total fishery removals and a strategy for allocating catches by species among stakeholders (in this case comprising nation states participating in the fishery; (Hennemuth and

Rockwell 1987). The ICNAF management regime was supplanted by the declaration of extended jurisdiction in 1976 and the implementation of national management under the Magnuson-Stevens Fishery Management and Conservation Act of 1976. A similar system-level constraint has been in place for Bering Sea-Aleutian Islands fishery since 1984 (Witherell et al. 2000; David Witherell NPFMC personal communication). System-wide *target* reference points can then be established to accommodate precautionary buffers to account for uncertainty.

The original system-level cap for the northeastern US was established based on the results of an aggregate-species production model analysis (Brown et al. 1976). The system-level limit for the BSAI was originally established on a precautionary basis based on examination of proposed allocations developed using single-species assessments. Mueter and Megrey (2006) subsequently re-evaluated the system-wide limit using an aggregate production model approach. In both the northeastern US and Alaska, the overall cap was approximately 25-30% lower than the sum of the individual species MSY levels. In the northeastern US, the allowable catch for individual species was set using a linear programming approach incorporating penalties for by-catch. In the BSAI, catch allocations for individual species are determined by negotiation among stakeholders with the constraint that the upper cap is not exceeded; if agreement cannot be reached, the council makes the determination (D. Witherell, NPFMC personal communication).

Gaichas et al. (2012) simulated the effect of employing different aggregation strategies for defining functional groups. Attempting to take the maximum total yield from entire assemblage resulted in the collapse of approximately 40% of the species in each of two different systems (Georges Bank and Gulf of Alaska). However, reducing exploitation to the level resulting in 90% of the maximum total catch provided a very sharp reduction of the number of species being driven to collapse. The remaining species still in trouble are predictably those with 'slow' life histories and these will require additional forms of protection. Worm et al. (2009) show very similar results for Georges Bank using a length-structured multispecies operating model. These analyses reveal the dynamic tension between maintaining biodiversity and extraction of yield and point to the utility of adopting a precautionary harvest level (see also Brander 2010).

These examples suggest that implementation of management strategies at higher levels of ecological organization is indeed feasible. In Section 4 of this report, we provide simulation tests of setting catch ceilings or caps at the system and functional group levels.

References

Andrew Applegate, Steven Cadrin, John Hoenig, Chris Moore, Steven Murawski, and Ellen Pikitch. 1998. Evaluation of Existing Overfishing Definitions And Recommendations for New Overfishing Definitions To Comply with the Sustainable Fisheries Act. NEFMC, Newburyport MA.

Appolonio, S. and J.J. Dykstra. 2008. "An enormous, immensely complicated intervention": groundfish, the New England Fishery Management Council and the world fisheries crisis. E Book Time LLC, Montgomery 246pp.

Bell, R.J., M.J. Fogarty, and J.S. Collie. Stability in marine fish communities. Mar. Ecol. Prog. Ser. In press.

Brander, K. 2010. Reconciling biodiversity conservation and marine capture fisheries production. Curr. Opin. Env., Sustain. 2:416-421.

Brown, B. E., J. A. Brennan, M. D. Grosslein, E. G. Heyerdahl, and R. C. Hennemuth. 1976. The effect of fishing on the marine finfish biomass in the Northwest Atlantic from the Gulf of Maine to Cape Hatteras. Int. Comm. Northwest Atl. Fish. Res. Bull. 12:49-68.

Brown J.H. 1995. Macroecology. Univ. Chicago Press, Chicago. 269 pp.

Butterworth, D.S. 2007. Why a management procedure approach? Some positives and negatives. ICES J. Mar. Sci. 64:613-617.

Butterworth, D.S. and R.B. Thompson. 1995. Possible effects of different levels of krill fishing on predators – some initial modeling attempts. CCAMLR Sci. 2:79-97.

Butterworth, D.S., K. Cochrane, and J. DeOliveira. 1997. Management procedures: A better way to manage fisheries? Am. Fish. Soc. Symp. 20:83:90.

Cohen, E.B., M.D. Grosslein, and M.P. Sissenwine. 1982. Energy budget of Georges Bank. Can. Spec. Publ. Fish. Aquat. Sci. 59:95-107.

Chassot, E., S. Bonhommeau, N.K. Dulvy, F. Melin, R. Watson, D. Gascuel, and O. Le Pape. 2010. Global marine primary production constrains fisheries catches. Ecol. Lett. 13:495-505.

Collie, J.S. and A. K. DeLong. 1999. Multispecies interactions in the Georges Bank Fish Community. Ecosystem Approaches for Fisheries Management. Univ. Alaska Sea Grant, AK-SG-99-01, Fairbanks. pp. 187-210.

Collie, J.S. and H. Gislason. 2001. Biological reference points for fish stocks in a multispecies context. Can. J. Fish. Aquat. Sci. 58:2167-2176.

Färe, Rolf, Shawna Grosskopf, and CA Knox Lovell. 1994. *Production Frontiers*. Cambridge University Press.

Färe, Rolf, Shawna Grosskopf, and Carl A Pasurka. 2007. "Environmental Production Functions and Environmental Directional Distance Functions." *Energy* 32 (7): 1055–66.

Fogarty, M.J. 2014. The art of ecosystem-based fishery management. Can. J. Fish. Aquat. Sci. 71:479-490.

Fogarty, M. J. and S. A. Murawski. 1998. Large-scale disturbance and the structure of marine systems: fishery impacts on Georges Bank. Ecol. Appl. 8:6-22.

Fogarty, M.J., R.Gamble, K. Hyde S. Lucey, C. Keith, 2011. Spatial Considerations for Ecosystem-Based Fishery Management on the Northeast U.S. Continental Shelf. In (D. Packer, Ed.) Proceedings of the Mid-Atlantic Management Council's Habitat-Ecosystem Workshop, NOAA Tech. Mem. NMFS-F/SPO-115 pp 31-33.

Gaichas, S.K., R. Gamble, M. Fogarty, H. Benoit, T. Essington, C. Fu, M Koen-Alonso, J. Link. 2012. Assembly Rules for Aggregate-Species Production Models: Simulations in Support of Management Strategy Evaluation. Mar. Ecol. Prog. Ser. 459: 275–292.
Garcia, S.M. and A.T. Charles. 2008. Fishery systems and linkages: implications for science and governance. Ocean. Coast. Man. 51:505-527.

Hollowed, A.B., N. Bax, R. Beamish, J. Collie, M. Fogarty, P. Livingston, J. Pope, and J.C. Rice. 2000. Are multispecies models an improvement on single-species models for measuring fishing impacts on marine ecosystems? ICES J. Mar. Sci. 57: 707-719.

Legendre, P. and L. Legendre. 1998. Numerical Ecology. 2nd Ed. Elsevier Press, Amsterdam.

Lucey, S. and M.J. Fogarty. 2013. Operational fisheries in New England: Linking current fishing patterns to proposed ecological production units Fish. Res. 141 3-12

Mackinson, S., B. Deas, D. Beveridge, and J. Casey. 2009. Mixed-species or ecosystem conundrum: Multispecies considerations inform thinking on long-term management of North Sea demersal stocks. Can. J. Fish. Aquat. Sci. 66:1107-1129.

Mackinson, S., M. Platts, C. Garcia, and C. Lynam. 2018. Evaluating the fishery and ecological consequences of the proposed North Sea multi-annual plan. PLOS ONE https://doi.org/10.1371/journal.pone.0190015.

McHugh, J.L. 1959. Can we manage our coastal fisheries? Trans. Am. Fish. Soc. 88:.105-110.

McHugh, J.L. 1988. Can we manage our coastal fisheries - II? Mar. Fish. Rev. 50:41-45.

Mueter, F.J., and B.A. Megrey. 2006. Using multi-species surplus production models to estimate ecosystem-level maximum sustainable yields. Fish. Res. 81:189-201.

Murawski, S.A.A.M. Lange, M.P. Sissenwine, and R.K. Mayo.1983. Definition and analysis of multispecies otter[trawl fisheries off the northeast coast of the United States. J. Con. Int. Explor. Mer 41:13-27.

Ralston, S. and J.J. Polovina. 1982. A multispecies analysis of the commercial deep-sea handline fishery in Hawaii. Fish. Bull. U.S. 80:435-448.

Ratz, H-J, E. Berthke, H. Dorner, D. Beare, and K. Groger. 2007. Sustainable management of mixed demersal fisheries in the North Sea though fleet-based management – a proposal from a biological perspective. ICES J. Mar. Sci. 64:652-660.

Scheld, Andrew M., and Christopher M. Anderson. 2016. "Selective Fishing and Shifting Production in Multispecies Fisheries." *Canadian Journal of Fisheries and Aquatic Sciences*, no. 999: 1–8.

Sheld, A. and J. Walden. Do catch shares lead to selectivity improvements in multispecies fisheries? An analysis of bottom trawlers in the Gulf of Maine and Georges Bank. In review.

Sissenwine, M. P., E. B. Cohen, and M. D. Grosslein. 1984. Structure of the Georges Bank ecosystem. Rapports et Proces-Verbaux des Reunions du Conseil International pour l'Exploration de la Mer 183:243-254,

Squires, Dale. 1987. "Public Regulation and the Structure of Production in Multiproduct Industries: An Application to the New England Otter Trawl Industry." *The Rand Journal of Economics*, 232–47.

Steele,J., J. Bisagni, J. Collie, M. Fogarty, D. Gifford, J. Link, M. Sieracki, B. Sullivan and A. Beet. 2007. Constructing end-to-end budgets for the Georges Bank ecosystem. Prog. Oceanogr. 74:423-448

Thorpe, R.B. 2016. Assessing fishery and ecological consequences of alternate management options or multispecies fisheries. ICES J. Mar. Sci. 73:1503-1512.

Thorpe , R.B., S. Jennings, and P.J. Dolder. 2017. Risks and benefits of catching pretty good yield in multispecies fisheries. ICES J. Mar. Sci. doe:10.1093/icesjms/fsx062.

Tyler, A.V., W.L. Gabriel, and W.J. Overholtz. 1982. Adaptive management based on structure of fish assemblages of northern continental shelves. Can. Spe. Publ. Fish. Aquat. Sci. 59:149-156.

Walters C.J., V. Christensen, S.J. Martell, and J.F.Kitchell. 2005. Possible ecosystem impacts of applying MSY policies from single-species assessment. ICES J Mar Sci 62:558-568.

Ware, D.M. 2000. Aquatic ecosystems: properties and models. In P.J.Harrison and T.R. Parsons (Eds). Fisheries Oceanography: An Integrative Approach to Fisheries and Ecology and Management. Blackwell Sci., Oxford.

Ware, D.M. and R.E. Thompson. 2005. Bottom-up ecosystem trophic dynamics determine fish production in the Northeast Pacific. Science 308:1280-1284.

Wetherill, D., C. Pautzke, and D. Fluharty. 2000. An ecosystem-based approach for Alaska groundfihs fisheries. ICES J. Mar. Sci. 57:771-777.

Worm B, R. Hilborn, J.K. Baum, T.A. Branch, J.S. Collie, C. Costello, M.J. Fogarty, E.A. Fulton, J.A. Hutchings, S. Jennings, O.P. Jensen, H.K. Lotze, P.A. Mace, T.R. McClanahan, C. Minto, S.R. Palumbi, A.M. Parma, D. Ricard, A.A. Rosenberg, R. Watson , and D. Zeller D. 2009. Rebuilding global fisheries. Science 325:578-585.

Appendix

Table A3.1. Designation of trophic guilds for species managed by the New England Fisheries Management Council. When ontogenetic changes in dietary guild membership were identified (Garrison 2000), the size range (cm) follows the species name. Fleets that capture each species are also indicated. NEFMC EBFM PDT personal communication.

	Species	Trophic Guild	Demersal Trawl	Mid-water Trawl	Sink gillnets	Drift gillnets	Bottom longline	Drift longline	Pot	Seine
1.	Witch Flounder	Benthivore	X							
2.	American Plaice, > 20	Benthivore	X							
3.	Rosette Skate	Benthivore	X							
4.	Yellowtail Flounder	Benthivore	X							X
5.	Haddock	Benthivore	X		X					X
6.	Winter Flounder	Benthivore	X							X
7.	Ocean Pout	Benthivore								
8.	American plaice, < 20	Macroplanktivore								

Species	Trophic Guild	Demersal Trawl	Mid-water Trawl	Sink gillnets	Drift gillnets	Bottom longline	Drift longline	Pot	Seine
9. Red hake < 40	Macroplanktivore	X							
10. White hake, 20 – 40	Macroplanktivore	X							
11. White hake, < 20	Macroplanktivore	X							
12. Cusk	Macrozoo-piscivore					X			
13. Blackbelly Rosefish	Macrozoo-piscivore								
14. Little Skate	Macrozoo-piscivore	X		X					X
15. Smooth Skate	Macrozoo-piscivore								
16. Pollock	Macrozoo-piscivore	X		X					
17. Clearnose Skate	Macrozoo-piscivore	X							
18. Windowpane	Macrozoo-piscivore	X							
19. Red Hake, < 40	Macrozoo-piscivore	X							X
20. Offshore hake, < 40	Macrozoo-piscivore								
21. Silver hake, < 40	Macrozoo-piscivore								
22.									
23. Atlantic Herring	Mesoplanktivore		X						X
24. Spiny Dogfish < 60 cm	Piscivore	X		X		X			
25. Thorny Skate	Piscivore								
26. Barndoor Skate	Piscivore								
27. Atlantic Cod	Piscivore	X		X		X			X
28. Fourspot Flounder	Piscivore								
29. Atlantic Halibut	Piscivore	X				X			
30. Winter Skate	Piscivore	X		X					

Species	Trophic Guild	Demersal Trawl	Mid-water Trawl	Sink gillnets	Drift gillnets	Bottom longline	Drift longline	Pot	Seine
31. Goosefish	**Piscivore**	X		X					X
32. Offshore Hake, > 40	**Piscivore**	X							
33. Silver Hake, > 40	**Piscivore**	X				X			X
34. Spiny Dogfish > 60 cm	**Piscivore**	X		X		X			
35. White Hake, > 40	**Piscivore**	X		X		X			
36. Acadian Redfish	**Planktivore-Piscivore**	X		X					

Table A3.2. Life history metrics and mean trophic level (TL) for species managed by the New England Fishery Management Council. Life history metrics include the intrinsic rate of increase (r), the vonBertalannfy growth coefficient (k), mean age at maturity (AgeMat, yr), longevity, and the maximum size attained (MaxSize, cm).

Species	TL	r	k	AgeMat	Longevity	MaxSize
Barndoor Skate	3.5	0.2	0.14	6.5	11	150
Clearnose Skate	4	0.2	0.15	5.5	7	94
Cod	3.79	0.66	0.115	1.8	17.5	148
Cusk	4	-		8	14	110
Goosefish	4.45	0.3	0.1	4.7	13	126
Haddock	3.67	0.51	0.29	3	9	73.8
Halibut	3.8	0.212	0.02	12	35	190
Herring	3.38	0.62	0.32	2.95	16.5	35
Little Skate	3.6	0.2	0.19	9.5	12.5	53
Ocean pout	3.11	0.12	0.095	2	18	97.8
Offshore Hake	3.42	0.9	0.174	3	14	70
Plaice	3.86	0.31	0.17	3.7	24	61
Pollock	3.72	0.88	0.14	6	24	111
Redfish	3.2	0.17	0.145	7	40	45.7
Red Hake	3.69	0.88	0.19	1.6	14	60.2
Silver Hake	3.42	0.9	0.42	2.5	14	65.4
Spiny Dogfish	3.39	0.11	0.116	17	38.6	100
Thorny Skate	4	0.2	0.12	11	16	89.5
White Hake	3.89	0.45	0.165	1.5	20	136
Windowpane	3.89	0.50	0.255	3.5	7	41
Winter Flounder	3.36	0.66	0.34	1.9	15	45.5
Winter Skate	4	0.25	0.1414	6.5	11	114.1
Witch	3.61	0.23	0.15	5.25	30	39.3
Wolffish	3.3	-	0.04	5.5	22	98
Yellowtail Flndr	3.86	0.79	0.34	2.1	17	50

Section 4: *TORs 4-9*

4) *Comment on the applicability and utility of the strawman management objectives and associated performance metrics which were used to guide the development of operating models.*

5) *Evaluate the utility of the proposed management reference points as part of a management control rule for ecosystem-based fishery management. These include: an overall catch cap at the Ecological Production Unit level conditioned on environmental conditions, ceilings on catch for each Fishery Functional Group (defining overfishing) conditioned on aggregate properties, and biomass floors at the single species level (defining overfished conditions).*

6) *Review harvest control rules embodying the proposed floors and ceilings approach using the ceiling reference points in ToR 5 to cap removals at the Ecological Production Unit and Functional Group levels, while ensuring that no species biomass falls below the single species floor reference points.*

7) *Review the structure and application of operating models for Georges Bank.*

8) *Review ecosystem assessment models and required data sources, as applied to the simulated data from the operating models in ToR 7.*

9) *Review simulation tests and performance of the proposed management procedure incorporating the floors and ceilings approach, given the set of EBFM goals and objectives.*

Ref: TOR 4-8

A Prototype Management Procedure for Multispecies Fisheries on Georges Bank

Introduction

The issue of cost and complexity in conventional fishery assessment and management has been a motivating factor in developing simpler Management Procedures (MPs) as protocols (e.g Butterworth et al. 1997; Butterworth 2007). Management Procedures entail the specification of a potentially simple set of rules for translating information from empirical observations and/or assessment models into a management action. Ideally there is binding agreement beforehand on factors such as the model choice, associated data, and the actions to be taken if a management threshold is crossed. MPs typically remain in place for multiyear (3-5 year) time frames and can be explicitly structured to enhance prospects for stability in the fishery by modulating the amount of change from one time step to the next, providing a more manageable time horizon for business, scientific, and administrative planning. The performance of alternative MPs is rigorously evaluated by simulation with respect to factors such as yield and/or profitability, uncertainty, and risk before any consideration of actual implementation. Examples of the specification and simulation testing of multispecies or ecosystem-level management procedures are provided by De Oliveria et al. (1997), Mackinson et al. (2009; 2018), Howell and Bogstad (2010), Thorpe et al. (2015, 2016, 2017) and Gaichas et al. (2016). Because multispecies and ecosystem management procedures necessarily encompass a broader range of considerations relative to single-species approaches, a strategy for deliberately coping with complexity will be required.

In the following, we evaluate potential avenues to implementing system-level management for the fish species on Georges Bank with particular emphasis on the mixed-species groundfish resources. We build on the concept of Fishery Functional Groups (see Section 3) to define focal points for management. For illustrative purposes, we focus on three major fleet sectors with distinct catch characteristics (Lucey and Fogarty 2013): (1) demersal trawl, (2) fixed gear [gillnets and longlines], and (3) pelagic trawls. Species that are caught together share common habitats and size compositions. We further identify three major trophic guilds critical to

energy flow and utilization in this system (a) benthivores, (b) planktivores, and (c) piscivores. These three trophic guild can be represented within one or more fleet sectors.

The prevalence of technical interactions in these mixed species fisheries places inherent limitations on the degree of control of fishing mortality possible. Although many factors, including estimation error, market conditions, and regulatory constraints applied to depleted stocks can affect levels of implementation error in current management, it is clear that by-catch issues are an important contributor. A focus on setting Annual Catch Limits applied independently to individual stocks further results in a disconnect with the underlying dynamics of the fishery based on the magnitude and spatial distribution of fishing effort by different fleet sectors. Our approach sets exploitation reference points at the Fishery Functional Group (FFG) level (and by extension, the system level). We identify target exploitation rates that, when applied to a biomass estimate for an FFG, can be translated into a catch level for a specified time period (fishing year). We evaluate the effects of exploitation at the FFG level and at the individual species level. If the total biomass of a functional group drops below a specified threshold level, remedial action is taken to reduce exploitation on the FFG. Consideration of functional group-level status alone of course cannot eliminate the possibility of impact on the individual species comprising the FFG. Accordingly, we also examine a set of control rules in which remedial action is taken if any one species drops below a threshold level.

Methods

Simulation Tests

To illustrate how fishery functional groups could be used in management, we develop an example based on characteristics of the Georges Bank fishery ecosystem. We focus on a ten species subsystem of the whole: Atlantic cod, haddock, silver hake, winter flounder, yellowtail flounder, monkfish, spiny dogfish , winter skate, Atlantic herring, and Atlantic mackerel (see Table 4.1 for scientific names and trophic guild assignments). The first 9 species are under direct NEFMC management control or are jointly managed with the Mid-Atlantic Fishery Management Council (spiny dogfish and monkfish). Mackerel are managed exclusively by MAFMC but are included here because of their importance as a forage species on Georges Bank. The first 9 species accounted for approximately 90% of the landings of fish species on Georges

Bank for which NEFMC has complete or shared management authority during the period 1977-2014. These species are known to interact through predation (Figure 4.1)

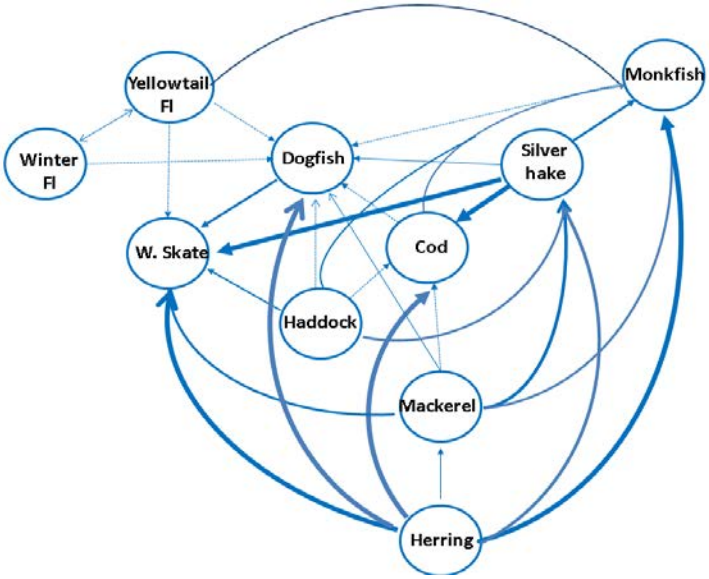

Figure 4.1 Species included in the prototype Georges Bank analyses. Arrows trace pathways from prey to predators; the width of the lines indicate the relative average importance of a prey species to a predator based on an extensive compilation of food habits data obtained during standardized NEFSC research-vessel surveys.

Table 4.1Species common names, scientific names, and trophic guild membership.

Common Name	**Species**	**Aggregate Group Name**
Spiny dogfish	*Squalus acanthias*	Elasmobranchs
Winter skate	*Leucoraja ocellata*	Elasmobranchs
Atlantic herring	*Clupea harengus*	Planktivores
Atlantic cod	*Gadus morhua*	Piscivores
Haddock	*Melanogrammus aeglefinus*	Benthivores
Yellowtail flounder	*Limanda ferruginea*	Benthivores
Winter flounder	*Pseudopleuronectes americanus*	Benthivores
Atlantic mackerel	*Scomber scombrus*	Planktivores
Silver hake	*Merluccius bilinearis*	Piscivores
Monkfish	*Lophius americanus*	Piscivores

Our objectives are to maintain overall system resilience and to optimize yield and revenues subject to conservation constraints. Here, overfishing is defined at the functional group level but "overfished" criteria apply at the functional group and species levels. This management procedure is intended to simplify management by requiring accounting against fewer catch limits, and using an integrated assessment of interacting species to determine stock status. Input data required include the total catch from the ecosystem and each aggregate species group, current and reference biomass levels for each species, and information on economic revenues.

In the following we describe the development of two operating models designed to test features of the prototype management procedure for multispecies fisheries on Georges Bank. These include a multispecies-multifleet length-structured simulation model (*Hydra;* Gaichas et al. 2017) and a multispecies production model (*Kraken*) based on an earlier model developed by Gamble and Link (2009).

Hydra Operating Model

Hydra is implemented in ADMB (Fournier *et al.*, 2012) with a modular design to accommodate expansion of model components, multiple functional forms for growth and recruitment, and options for incorporation of environmental effects on growth, recruitment. Fishery selectivity patterns and size-specific fishing mortality from effort-driven multispecies fleets are represented. We have elected to use a size-based model because fishing processes and predation are size-based rather than age-based. Size composition information, in contrast to age composition, is available for all species on Georges Bank taken during standardized research vessel surveys. Currently *Hydra* is implemented for three fleets: demersal trawl, fixed gear (longline and gillnet), and pelagic trawl but is designed to accommodate expansion.

Multiple forms for growth and recruitment are implemented in the operating model to represent different states of nature. In Hydra, the growth function is used to determine the time spent in each length category for each species. The Georges Bank ecosystem supports a highly interconnected food web, reflecting opportunistic feeding patterns and broad diet compositions or many fish species (Link 2002). Because of the general lack of high specificity in the diets of most fish predators in this system, and the availability of a broad spectrum of alternative prey, mechanistic feedback between prey consumption and predator growth in Hydra is not currently

implemented. The implementation in Hydra dictates that sufficient food is always available from the pool of species directly modeled and an 'other' prey category. If evidence supports prey limitation or changes in food quality, it is possible to include prey abundance, availability, and quality in the growth, condition, and reproduction modules to reflect the changes in predator growth and condition. In the following we briefly describe the structure in Hydra for each module depicted in Figure 4.2 and more detailed descriptions are provided in the Appendix.

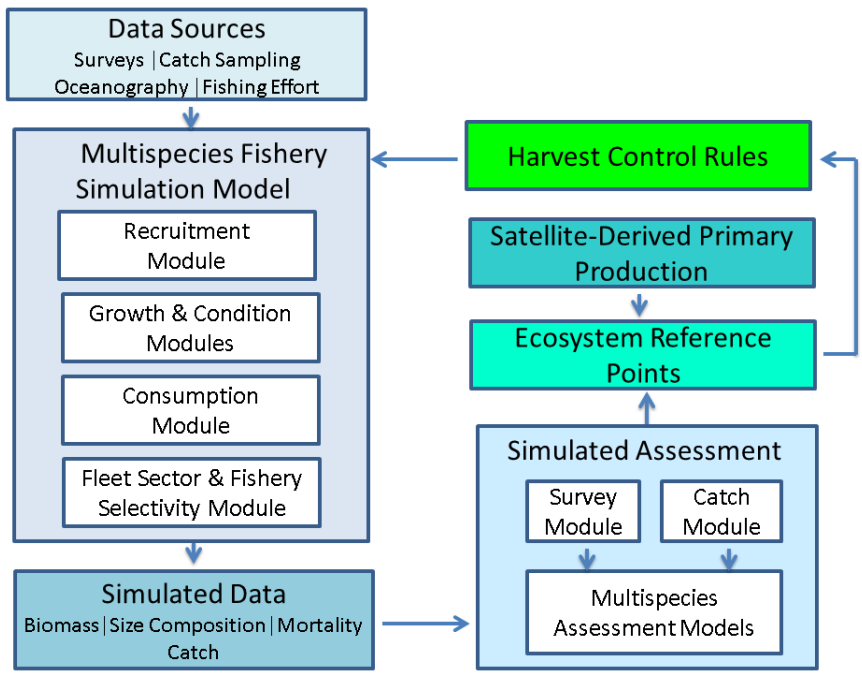

Figure 4.2. Modular design and implementation sequence in *Hydra*.

Basic Model Structure

Hydra traces the population trajectories of a multispecies assemblage as a function of size, growth, recruitment, and survival. The number of individuals N in size class j at time t+1 represent the survivors from that cohort from the previous time step (t) that have not grown into a larger size class, plus the number of individuals growing into size class j from smaller size classes during the time interval. We only consider transitions among immediately adjacent size classes. The model for each species i can be written:

$$N_{i,j,t+1} = \phi_{i,j\to j,t} S_{i,j,t} N_{i,j,t} + R_{i,1,t} \qquad \mathrm{j} = 1$$
$$N_{i,j,t+1} = \sum_{j'=j-1}^{j} \phi_{i,j'\to j,t}\, S_{i,j',t} N_{i,j',t} \qquad \mathrm{j} = 2, \ldots, J$$

Such that

$$\begin{cases} \phi_{i,j\to j,t} + \phi_{i,j\to j+1,t} = 1 & j = 1, \dots, J-1 \\ \phi_{i,j\to j,t} = 1 & j = J \end{cases}$$

The proportion surviving from size class *j*-1 to size class *j* for a species at time t is denoted $S_{j',t,}$. $\phi_{j'\to j}$ is the probability of moving from size class *j*-1 to size class *j* within a specified time step, *w*here *J* is the number of size classes (5 in the current implementation). Size classes used for each species are provided in Table S.1. The transition probabilities are determined from species-specific growth functions (see Growth and Time-in-Stage below). The time steps in Hydra are determined by the transition times of the fastest growing species. $R_{i,1,t}$ is the number of recruits of species i, in time t, and $S_{i,j,t}$ is the proportion of individuals of species i, size class j, surviving from the time t to t+1.

Key elements of the model structure can be depicted as a multispecies life-cycle diagram (Figure 4.3). Circles represent size classes; colored circles represent size classes subject to harvesting. For simplicity, we depict only two fishing fleets. Arrows connecting size classes represent the probability of surviving and growing between adjacent size groups in each time step. Closed loops indicate the probability of surviving and staying within a given size class in each time step. Arcs connect mature size classes to the first (recruit) size class. Broken lines trace patterns of size-specific predation

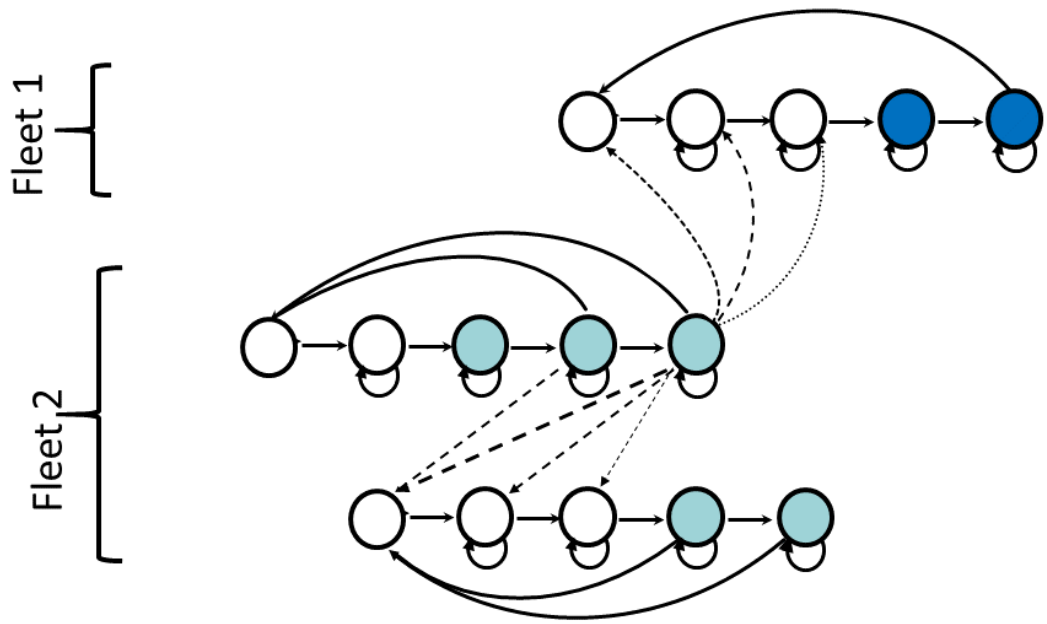

Figure 4.3. Multispecies-multistage life cycle diagram for species employed in Hydra. For simplicity, only three species and two fleets are shown.

Recruitment Module

The recruitment model form is:

$$\mathrm{R}_t = \alpha f(S_{t-1}, \underline{\theta}) e^{\varepsilon_t}$$

where e^{ε_t} are independent and identically distributed lognormal random variables such that $\varepsilon_t \sim N(0, \sigma^2)$, and $\underline{\theta} = (\alpha, \beta, \delta)$ is a vector of model parameters. R_t, recruitment (millions) and has been scaled to represent age 0 individuals. S_t, spawning stock is defined in metric tons. The functional form, $f\left(S_{t-1}, \underline{\theta}\right)$, is a segmented linear representation of the stock-recruitment relationship. In principle, the approach can accommodate multiple break-points in the relationship, allowing a piece-wise approximation to a broad spectrum of functional forms. Pielou (1977; pp. 35-38) introduces the use of segmented linear functions for a general class of

population models. In the following, we restrict these options to a single break-point. The well-known hockey stick model (Barrowman & Myers, 2000) is a special case of this form.

The functional form, $f(S_{t-1}, \underline{\theta})$, of the spawner-recruit relationship is given by:

$$f(S_{t-1}, \underline{\theta}) = S_{t-1} \qquad \text{if } S_{t-1} \leq \delta$$

$$= S_{t-1} + \frac{\beta}{\alpha}(S_{t-1} - \delta) \qquad \text{if } S_{t-1} > \delta$$

where α is the slope at origin (recruits/spawning biomass), δ is the change-point (the value of spawning stock biomass at which the slope changes. β is the change in slope at the change-point. When $\beta = -\alpha$, the above equation simplifies to the hockey stick model and resembles a simple piecewise linear approximation to the Beverton Holt model. When $\beta < -\alpha$, the slope after the change point decreases, allowing representation of over-compensatory processes.

We begin by fitting segmented linear models to estimates of stock and recruitment derived from multispecies sequential population analyses for cod, haddock, silver hake, monkfish, and winter skate (Curti 2012). Three of the ten species in our simulated system, herring, mackerel, and spiny dogfish undertake extensive seasonal migrations on the Northeast Continental Shelf and are resident on Georges Bank for only part of the year. We used coastwide estimates derived from a multispecies virtual population analysis for herring and mackerel (Tyrell et al. (2008). We then adjusted the biomass levels of these species to reflect their intra-annual mean abundance on the bank based on NEFSC seasonal surveys. A similar approach was used for spiny dogfish based on single-species population analyses (K. Sosebee, pers. comm.). Two species included our assemblage, winter and yellowtail founder, were not included in recent multispecies analyses. We used recent recruitment and spawning biomass estimates based on the most recent accepted NEFSC stock assessments for these species as employed by Perretti et al. (2016).

The initial piece-wise model fits were used as a point of departure to assemble an ensemble of plausible recruitment models for the 10 species system. We determine *a priori* which species would take the form of a hockey stick model and which species would take on an over-compensatory form based on the importance of intraspecific predation indicated in NEFSC diet composition data. Cannibalistic species (cod, silver hake, monkfish, and spiny dogfish)

were tested for evidence of overcompensation; all other species were fit using the hockey-stick model. To account for uncertainty in the data and to tackle the issue of “missing” data for lower levels of spawning stock biomass we adopt a sampling regime to select variants of these fitted models using the initial fits as starting points. The sampling regime adopts a similar approach to that of Thorpe et al (2015) in that an operating model is used in the selection process and that empirical data is used to set bounds for model output to satisfy. Accordingly, the final models in the filtered ensemble do not represent fits to the observations in any conventional sense. We employed three tests: (1) all species must persist in the absence of fishing, (2) the modeled biomass of all species must fall within the range of empirically-derived estimates and (3) the modeled catch must fall within the range of empirically observed levels for Georges Bank. The filtered ensemble comprised a total of 124 plausible recruitment models out of an initial pool of 1024 models. In Figure 4.4, we show a selection of the plausible recruitment models in the filtered ensemble (not all plausible models are shown in the interests of clarity). Parameter estimates for the segmented models are provided in Table A.1. For a full account of the analyses employed see the Appendix).

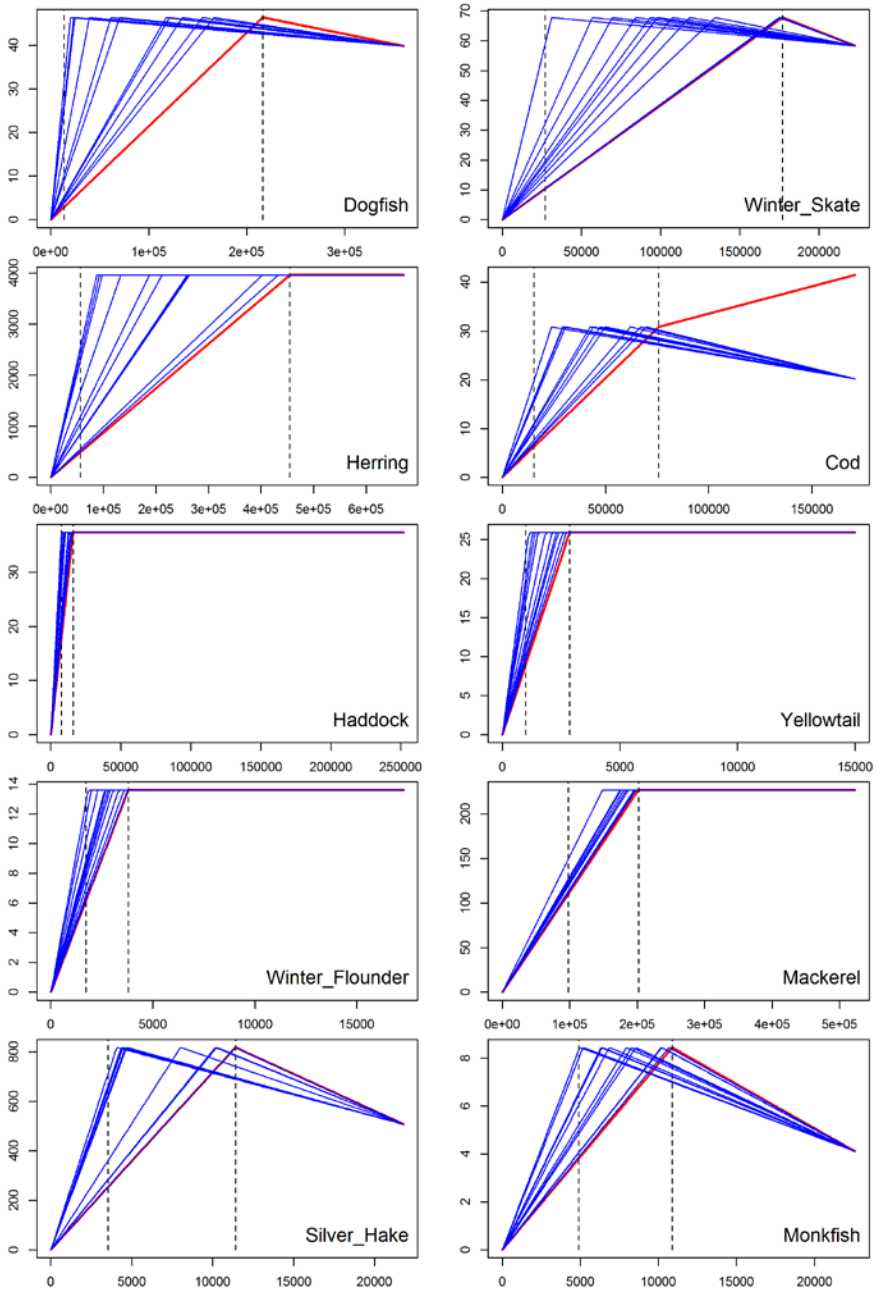

Figure 4.4. Representatives of plausible recruitment models in the filtered ensemble (blue lines). The red lines represent the initial model configuration.

Growth and Time-in-Stage

We considered two possible representations of growth, the classical von Bertalanffy growth model and a simple power function. The growth function is used in the determination of

size and weight-at-age (when coupled with a length-weight relationship). It is also used to determine the time-in-stage and transition probabilities. The Bertalanffy growth model is:

$$l_{i,t} = L_{i,\infty}\left(1 - e^{-k_i(t-t_0)}\right)$$

and the time required to grow through a specified length interval defined by upper ($l_{u,i}$)and lower ($l_{l,i}$) boundaries is:

$$\Delta t_i = \frac{1}{k_i}\log_e\left[\frac{L_{\infty,i} - l_{\ell,i}}{L_{\infty,i} - l_{u,i}}\right]$$

The power function model takes the form:

$$l_{i,t} = \psi_i a_i^{\kappa_i}$$

where $l_{i,t}$ is the length of species *i*, at time t; ψ_i and κ_i are model parameters and the time required to grow though the designated length interval is:

$$\Delta t_i = \left[\frac{l_{u,i}}{\psi_i}\right]^{1/\kappa_i} - \left[\frac{l_{l,i}}{\psi_i}\right]^{1/\kappa_i}$$

The models applied to each species are shown in Figure A.1 and parameters are provided in Table A.2.

Food Consumption

Predation processes represented in *Hydra* are partitioned into three principal elements: size selectivity, prey suitability, and food intake. The size preference function, $\vartheta_{n,j}$, is the preference for a prey item of size n by a predator of size j:

$$\vartheta_{n,j} = \frac{1}{(w_n/w_j)\sigma_j\sqrt{2\pi}} exp\left(-\frac{1}{2{\sigma_j}^2}\left(ln(w_n/w_j) - \Psi_j\right)^2\right)$$

where Ψ_j is the 'preferred' predator/prey weight ratio on a logarithmic scale, and σ_j^2 is the variance in predator size preference. The suitability, $\rho_{i,j,m,n}$, of prey species m of size n to predator species i of size j is:

$$\rho_{i,j,m,n} = \vartheta_{n,j}\lambda_{m,i}$$

where $\lambda_{m,i}$ is the vulnerability of prey species *m* to predator species *i*. The parameters $\lambda_{m,i}$ are set to either 0 or 1 depending on whether predator *i* is known to prey on species *m.*

We next require an estimate of the food intake. Direct consumption estimates have been made for a number of species on the Northeast Continental Shelf. The yearly food intake function is:

$$I_{i,j,t} = 365 * 24\left[\alpha_i e^{\beta_i \mathrm{T}_t}\right]\bar{C}_{i,j,t}$$

where the term in brackets gives the temperature-dependent hourly consumption rate with stomach evacuation parameters α_i and β_i and $\bar{C}_{i,j,t}$ is the mean stomach content weight (g) over a diel cycle, T_t is observed temperature at time t.

The predation mortality rate, $M2_{m,n,t}$, on a particular prey species m is a function of predator consumption, prey suitability, and the available prey biomass to its predators. Predation mortality is given by:

$$M2_{m,n,t} = \sum_i \sum_j I_{i,j,t}\, N_{i,j,t} \frac{\rho_{i,j,m,n}}{\sum_a \sum_b \rho_{i,j,a,b}\bar{W}_{a,b}N_{a,b,t} + \Omega}$$

where $\bar{W}_{a,b}$ is the mean weight of prey a in size class b, Ω is “other” food not explicitly included in the model.

Fleet Module

Exploitation rates in *Hydra* are driven by explicit representation of fishing effort. For our simulations, we constructed a 53 year time series of domestic fishing effort based on historical patterns for the three major gear types. We extracted archived effort data for Georges Bank and

developed estimates of standardized fishing effort data for our three broad gear categories, accounting for vessel size and specific gear type within categories in a General Linear Model. Details of the estimation procedure are provided in the Appendix.

Representation of mixed species fisheries require specification of species-specific selectivity patterns by different gears and fleets, catchability characteristics reflecting both morphology and behavior. The size-specific selectivity for a specified gear type g in *Hydra i*s given by:

$$s_{i,j,g} = \left[1 + e^{-(c_{i,g} + d_{i,g} L_{i,j})}\right]^{-1}$$

where $c_{i,g}$ and $d_{i,g}$ are model parameters and $L_{i,j}$ is the midpoint of the jth size class interval. Estimates of model parameters by species and gear type are provided in Appendix Table and plots for all species are provided in Figure 5.x.

We can specify the fishing mortality generated by each fleet as:

$$F_{i,j,g,t} = s_{i,j,g} q_{i,j,g} E_{g,t} \left[1 - p(D_{i,j,g,t}) p\left(Surv_{i,j,g,t} \middle| D_{i,j,g,t}\right)\right]$$

where $s_{i,j,g}$ and $q_{i,j,g}$ are time independent fishing selectivity and catchability coefficients for fishing fleet with gear g, species *i*, and size class *j*; $E_{g,t}$ is the effort by fleet with gear g in time t. It is assumed that each fleet has a unique gear type; $p(D_{i,j,g,t})$ is the probability species i, size class j, is discarded by fleet with gear g in time t, and $p\left(Surv_{i,j,g,t} \middle| D_{i,j,g,t}\right)$ is the probability of survival of discarded individuals.

Given estimates of the instantaneous rate of predation mortality (M2) derived above, fishing mortality (F), and other mortality (M1), We can specify the total mortality rate as:

$$Z_{i,j,g,t} = M1_{i,j,t} + M2_{i,j,t} + F_{i,j,g,t}$$

where $M1_{i,j,t}$ is the natural mortality due to factors not explained in the model; for the purposes of these simulations, we have set M1 to 0.1. The yield from species i at time t is then:

$$Y_{i,t} = \sum_{j}\sum_{g} \frac{s_{i,j,g}F_{i,j,g,t}}{M1_{i,j,t} + M2_{i,j,t} + s_{i,j,g}F_{i,j,g,t}} \left[1 - e^{-\left(M1_{i,j,t}+M2_{i,j,t}+s_{i,j,g}F_{i,j,g,t}\right)}\right] N_{i,j,t} w_{i,j}$$

Where is the mean weight of a individual of species *i* and length *j*.

Harvest Control Rules y

The harvest control rules examined here determine overfishing at the species complex level but overfished status at the functional group or individual species levels (Figure 4.5; Table 4.2). We explored 6 principal scenarios with 8 levels of exploitation nested within each (Table 4.2) to define options for harvest control rules but here we will present information on a subset of outcomes. The harvest control rules involve different options for floors and ceilings. Ceiling levels are defined at the system level based on exploitation rates of 0.05-0.4 in increments of 0.05. In the present set of simulations, we have applied these exploitation rates directly to the species functional group with each subject to this same sequence of exploitation levels. We translate these exploitation rates into standardized fishing effort by dividing by the mean catchability coefficient for the species in the complex. It should be noted that these exploitation rates defined at the species complex level will be manifest as different rates on the individual species level because of different gear selectivity factors. The resulting catch for the complex as a whole and the individual species catch within each species complex is determined by the product of these species-level partial recruitment factors and the total biomass of the species

complex.

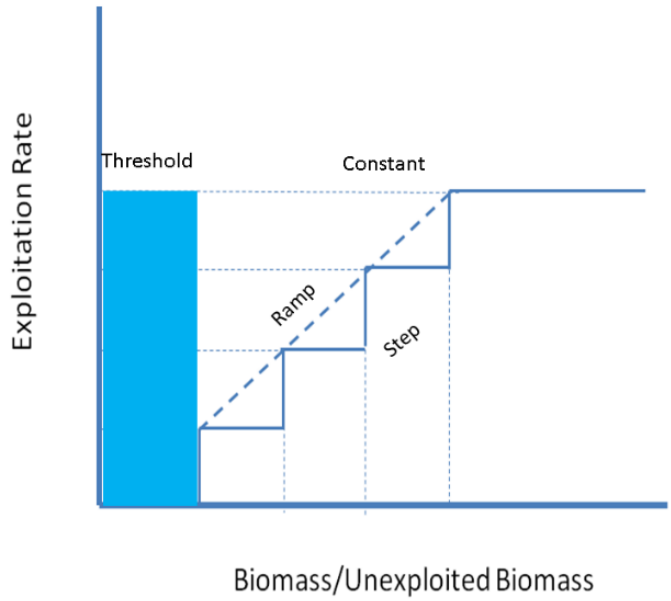

Figure 4.5. Structure of the ecosystem-based harvest control rules tested. Overfishing is determined at the species complex level. Overfished status is determined at the species complex or individual species levels (see details in Table 4.2).

Table 4.2. Scenarios Tested in simulation studies of the prototype management procedure

Scenario 1 Threshold exploitation (no ramp down) at Ex=0.05-0.4 in increments of 0.05 and Floor=0.2 of unfished biomass applied at the species complex level
Scenario 2 Threshold exploitation (no ramp down) at Ex= 0.05-0.4 in increments of 0.05 and Floor=0.2 of unfished biomass applied at the individual species level
Scenario 3 Threshold exploitation (no ramp down) at Ex= 0.05-0.4 in increments of 0.05 and Floor=0.2 of unfished biomass for each species except winter skate and dogfish (Floor=0.3 of unfished biomass) applied at the individual species level
Scenario 4 Ramp-down exploitation using 'steps' at Ex= 0.05-0.4 in increments of 0.05 and starting at B/Bo = 0.4 applied at the species complex level
Scenario 5 Ramp-down exploitation using 'steps' at Ex=0.05-0.4 in increments of 0.05 and starting at B/Bo = 0.4 applied at the individual species level
Scenario 6 Ramp-down exploitation using 'steps' at Ex= 0.05-0.4 in increments of 0.05 and starting at B/Bo = 0.5 applied at the individual species level for winter skate and dogfish

Performance metrics

We provide an overview of performance metrics covering two time periods for each of the six scenarios. The performance metrics selected are revenue, functional group status, species status, landings, biomass, stability of landings, the proportion of large fish in the population, and the proportion of large fish in the landings. Species status is a function of how many species fell below 20% of unfished biomass. For each year we count the number of times this event occurs over all 100 runs. Comparable calculations are made to assess Functional Group status. The metric employed is the complement of the proportion overfished. For the remaining six performance metrics, we take the median in each year for each species over the 100 iterations.

To encapsulate the information for eight performance metrics at six levels of exploitation we depict the results as radar plots. The radar plots take the form of octagons with each performance metric occupying one of the axes

Simulated Stock Assessment

From the simulated series of biomass, length composition, survival rates, and catch generated by Hydra we generated 'observational' data incorporating measurement error. We simulated the survey process by taking the population outputs from Hydra and adding observation error to reflect factors such as uncertainty in survey catchability coefficients and variation in the area swept by the net on a given haul. We then used the generated survey data as inputs to multispecies stock assessment models. In recognition of uncertainties in the quality of real world catch data, we also employ index-based multispecies assessments as an alternative that do not utilize fishery-dependent observations. Our intention is to complement the structural models described below. In these simulations, we conduct assessments every three years (time periods).

$$B_{i,t+1} = (r_i - \alpha_{ii} B_{i,t}^{\gamma-1} + \sum_{j \neq i} \alpha_{ij} B_{j,t_i}) B_{i,t} - C_{i,t}$$

We evaluated simple, broadly applicable multispecies assessment models tailored to empirical data availability for the 10 species included in Hydra for possible inclusion in simulated assessments. Currently a broad spectrum of single-species stock assessment models, ranging from sophisticated age and size structured models to survey-based index values are used

to support fisheries management for groundfish resources. Data limitations preclude the use of age-structured models for all of these species. We centered our investigation on a size-based delay-difference models with simple demographic structures comprising pre-recruit and recruited individuals. In principle, the delay-difference models can accommodate an expanded stage structure with several life-history stanzas.

The basic form of the multispecies delay-difference model incorporates two life history stanzas (recruits and post-recruits). In this version, predation occurs on pre-recruits (although this can be readily relaxed to encompass predation on post-recruits). This constraint is generally consistent with observations on the size of prey. For the recruitment function we employ a generalized Lotka-Volterra model. For the case of a Type I functional feeding response the model is:

$$B_{i,t+1} = \left[(r_i - \alpha_{ii} B_{i,t+1-k_i}^{\gamma-1} + \sum_{j \neq i} \alpha_{ij} B_{j,t+1-k_i}) B_{i,t+1-k_i} \right] + \rho_i B_{i,t} - C_{i,t}$$

where $B_{i,t}$ is the biomass for species i at time t, r_i is the growth rate for species i, $C_{i,t}$ is the removals by fisheries on species i at time t, and α_{ij} is the interaction coefficient between species i and j (including intraspecific interaction terms α_{ij}). The shape parameter γ equals 2 for quadratic model. The subscript k_i denotes the age at recruitment for species i. The assessment model structure is implement to allow Type II and Type III functional feeding responses as alternatives to the Type I structure. For comparison, we also tested a simplified production model – a generalized Lotka-Volterra model in which distinctions between pre-recruits and post-recruits and multiple time delays are not considered.

In our prototype analysis we have a system of 10 simultaneous equations. Because of the cross-dependencies in the model structure related to species interactions, we employed Full Information Maximum Likelihood (FIML) estimation, a robust non-linear estimation method to addresses the issue of simultaneous equation bias. We attach multiplicative observation error to the *Hydra* model outputs as:

and

$$e^{\upsilon_t - \sigma^2/2}$$

$$\upsilon_t = \rho\upsilon_{t-1} = (1-\rho^2)^{1/2}\varphi_t$$

where ρ is a first order autocorrelation coefficient, σ^2 is the variance of the observation error and $\varphi_t \sim N(0, \sigma^2)$.

To assess assessment model performance, we adopted a Modelling Efficiency (MEF) metric (Stowe et al. 2009), which measures how well the model predicts relative the average of the observations. The MEF is given by:

$$MEF = \frac{\left(\sum_{i=1}^{n}\left(O_i - \overline{O}\right)^2 - \sum_{i=1}^{n}\left(P_i - \overline{O}\right)^2\right)}{\sum_{i=1}^{n}\left(O_i - \overline{O}\right)^2}$$

where O_i is the ith observation, *O bar* is the average over all observations, and P_i is the ith predicted value. Alternatively, the MEF can be expressed as $(1\text{-}RMSE^2)/s^2$ where RMSE is the root mean square error and s^2 is the sample variance of the observations. Values of MEF close to 1 indicate close correspondence between prediction and observation; a value of zero indicates that the prediction is no better than taking the mean of the observations as a forecast. Negative values indicate that the average of the observations provides a better forecast.

Kraken Operating Model and Portfolio Analysis

Jin et al. (2016) employed portfolio theory to assess historical performance in the Northeast Large Marine Ecosystem, in terms of minimizing the variance around the attainment of a revenue target. In an extension, this model can be coupled to the multispecies models such as Hydra and Kraken in order to provide measures of stability and returns for Georges Bank within a simulated world. As a worked example, of this approach, we have coupled the portfolio analysis with the Kraken surplus production function (Figure 4.6).

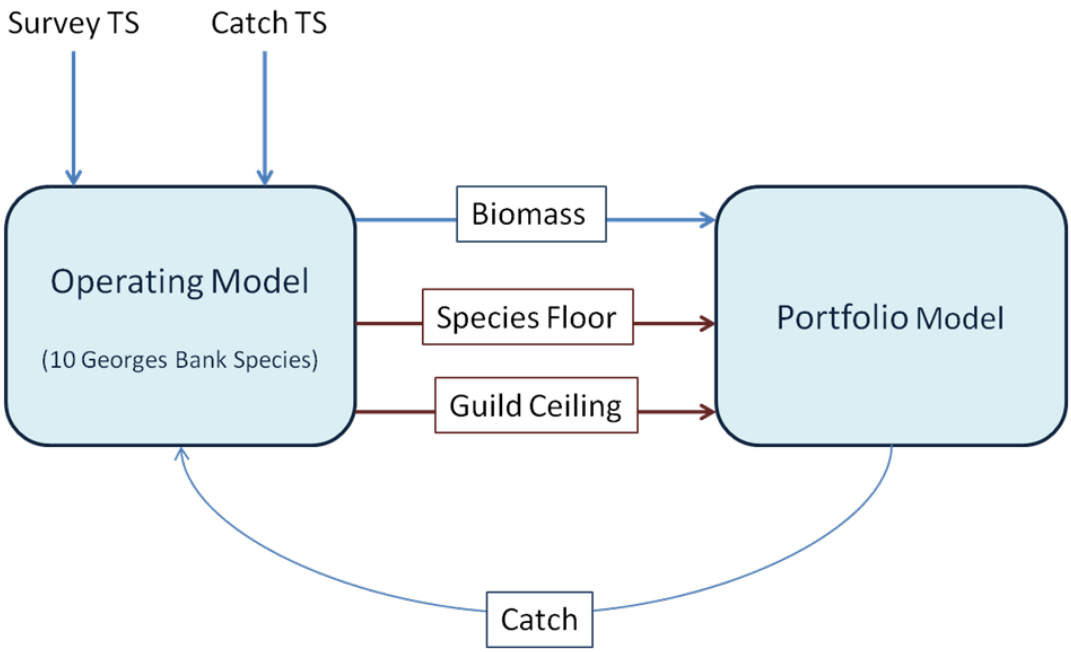

Figure 4.6. Flow diagram of the coupled Kraken surplus production model with the portfolio analysis optimization.

The surplus production function is a multispecies logistic model derived from the Lotka-Volterra family of models:

$$B_{i,t+1} = r_i B_{i,t} - B_{i,t} \sum_{1}^{j} \alpha_{ij} B_{j,t} - C_{i,t}$$

where $B_{i,t}$ is the biomass for species i at time t, r_i is the growth rate for species i, $C_{i,t}$ is the removals by fisheries (determined by the portfolio analysis optimization, as described below) on species i at time t, and α_{ij} is the interaction coefficient between species i and j (including the density dependent interaction of a species on itself).

The Kraken surplus production function acts as an operating model; simulating biomasses for 10 species loosely modeled on Georges Bank equivalents. Tuning runs were done to determine parameters for each species (r_i α_{ij} , $B_{i,t=0}$). At each annual time step, these

biomasses are then passed to the portfolio analysis for optimization. This optimization relies on two constraints which are generated by Kraken:

Constraint 1: The Guild Ceiling which is calculated as 0.18 * the sum of the biomasses for each species within a guild within the relevant time period– this is the maximum removal allowed for that guild.

Constraint 2: The Species Floor which is calculated as 0.2 * the unfished biomass for each species. For each species, subtracting the floor from the current biomass determines the maximum removal allowed at each time step.

In each time period, the choice of optimal harvest strategies, based on the historical time series of revenue and biomass generated from Kraken and in terms of a balanced portfolio, can then be passed back to the operational model to generate a simulated harvest trajectory. The biomass is then updated to reflect the simulated catch and the process can be iterated for the requisite number of time steps.

For the 10 species (indexed by *i*) in the Georges Bank example, this optimization is represented more formally as:

$$min_{\mathbf{w_t}} \mathbf{w}_t' \mathbf{\Sigma}_t \mathbf{w}_{t\,,}\ s.t.\ \mathbf{w}_t{}'\boldsymbol{\mu}_t \ \geq\ R_t,\ \ w_{i,t} \leq \frac{B_{i,t}}{\Omega_{i,t}}\ \forall\ i,\ w_{i,t}\Omega_{i,t} \leq\ \boldsymbol{G}_t.$$

For each time period t, a vector optimal weights $\mathbf{w_t}$ are chosen to minimize the variance-covariance of the system $\mathbf{\Sigma}_t$, subject to constraints on the revenue generated and biological sustainability of the system. The revenue target, R_t is set equal to the revenue realized in the previous period *t-1*, and $\boldsymbol{\mu}_t$ is a vector of average revenue generated at the species level. Maximum species-level weights are calculated by dividing the aforementioned 20% of unfished biomass $B_{i,t}$ by the average catch $\Omega_{i,t}$. Guild level maximum catch, $\boldsymbol{G}_{,t}$, is 18% of summed Guild-level biomass. The variance-covariance is estimated as:

$$\Sigma_{i,j,t} = \frac{\sum_{k=1}^{t} \lambda^{t-k+1}(r_{i,k}-\mu_{i,t})(r_{j,k}-\mu_{j,t})}{\sum_{k=1}^{t} \lambda^{t-k+1}},$$

with

$$\mu_{i,t} = \frac{\sum_{k=1}^{t} \lambda^{t-k+1} r_{i,k}}{\sum_{k=1}^{t} \lambda^{t-k+1}}$$

for decay factor λ= 0.549, such that 5% of an observation remains after 5 years[2]. Finally, the average catch is given by:

$$\Omega_{i,t} = \frac{\sum_{k=1}^{t} \lambda^{t-k+1} p_{i,k} y_{i,k}}{\sum_{k=1}^{t} \lambda^{t-k+1} p_{i,k}},$$

where p represents the fish price; and *y* is the catch quantity.

Results

Hydra

Comparison of the performance characteristics of the harvest control rules examined here reveal stark contrasts in the threshold and ramp-down options. Overall performance and resilience was considerably enhanced by adopting a strategy in which reducing exploitation rates prior to declines in biomass approaching the overfished condition was reached. Early intervention strategies preserved resilience as measured by maintenance of species diversity (measured as the proportion of species not overfished) and the representation of large fish in the population(s). Further, while the threshold strategy in which remedial action is not taken until biomass drops below 20% of the unfished state (30% for elasmobranchs) showed sharp diminution of landings and revenues, under the ramp-down strategy, higher levels of yield and economic returns were maintained at higher exploitation levels.

[2] Jin et al. (2016) find that the optimal portfolios are generally robust to the choice of decay factor.

In the following, we show the status of the system for years 21-30 and 41-50 of the simulations. For each time period, we use the average of each metric over the decadal period as its representative value. We then use these to obtain global maxima and minima over all scenarios for each metric. These global maxima and minima represent the range of values for each metric in each time period. All radar plots are produced relative to these maxima and minima and are therefore directly comparable. Observations for each metric and exploitation level near the outer vertices of each plot indicate good status. Contraction of the observations toward the center of the radar plot indicates increasingly poor performance.

For the intermediate time period (years 21-30) in the simulations, increasing exploitation rates result in degradation of performance in all dimensions for each of the fixed rate (threshold) strategies (Figure 4.7). The performance of each of the scenarios under the threshold strategy (Figure 4.7a-c) reveal only subtle differences with the greatest distinction residing in somewhat better outcomes for the large fish landings index under the functional group scenario. For the case in which remedial action is taken once functional group biomass as whole drops below 20% of unfished biomass (Figure 4.7a), landings prohibitions are enacted for all species in that functional group. Figure 4.7b depicts the situation in which remedial measures are enacted if any species within an assemblage drops below its designated floor. The effects of an increase in the threshold to 40% of unfished biomass for elasmobranchs is depicted in Figure 4.7c). There is no appreciable difference when increasing the elasmobranch threshold to 40% relative to the 30% level in these results.

For the harvesting strategies employing a ramped exploitation rate strategy (Figure 4.7d-f)) during the intermediate time period, the main feature that emerges is the additional resilience in each of the metrics to increasing exploitation rate, including better performance in the landings and revenue categories relative to the corresponding fixed rate strategies. The conservatism in the additional protection afforded to elasmobranchs (Figure 4.7f) is manifest in reduced revenues at low exploitation rates. Among the six scenarios depicted in Figure 4.7, it is evident that the metric depicting stability in landings reveals moderate performance outcomes in general. The apparent increase in stability of landings at higher exploitation rates under the functional group strategy is an exception. Overall, the stability outcomes suggest that further

consideration should be given to evaluating the consequences of putting constraints on the amount that exploitation rates and yield can change between successive time steps.

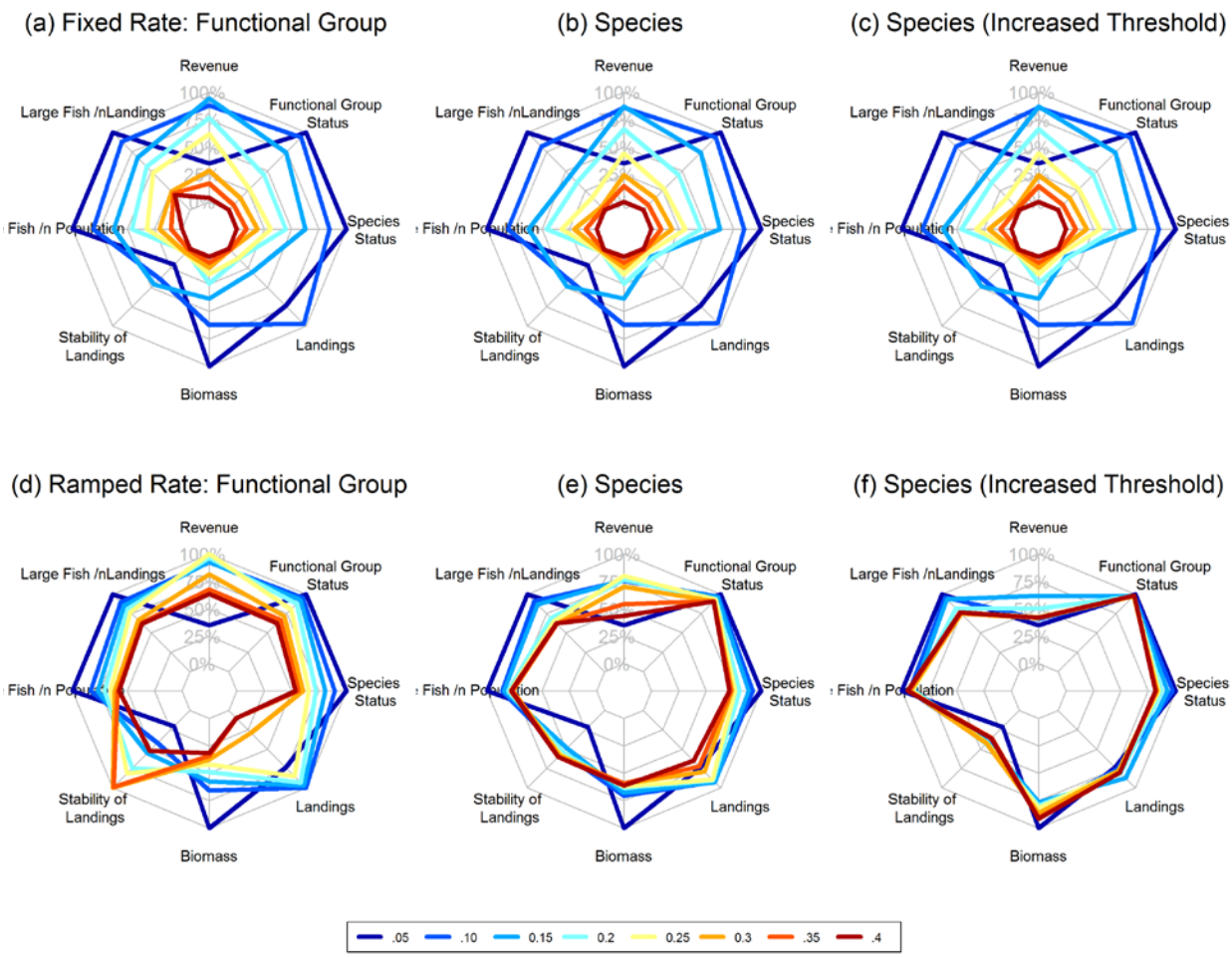

Figure 4.7. Radar plots depicting the performance of the 6 major scenarios for 8 performance metrics for years 21-30 in the simulations. Performance metrics are each evaluated at eight levels of exploitation (represented by colored lines).

Results during the final decade of the simulation show relatively minor difference with those of the intermediate time period (Figure 4.8). While it is clear that the pattern observed

during years 21-30 had not fully equilibrated relative to the final decade, the differences are relatively minor.

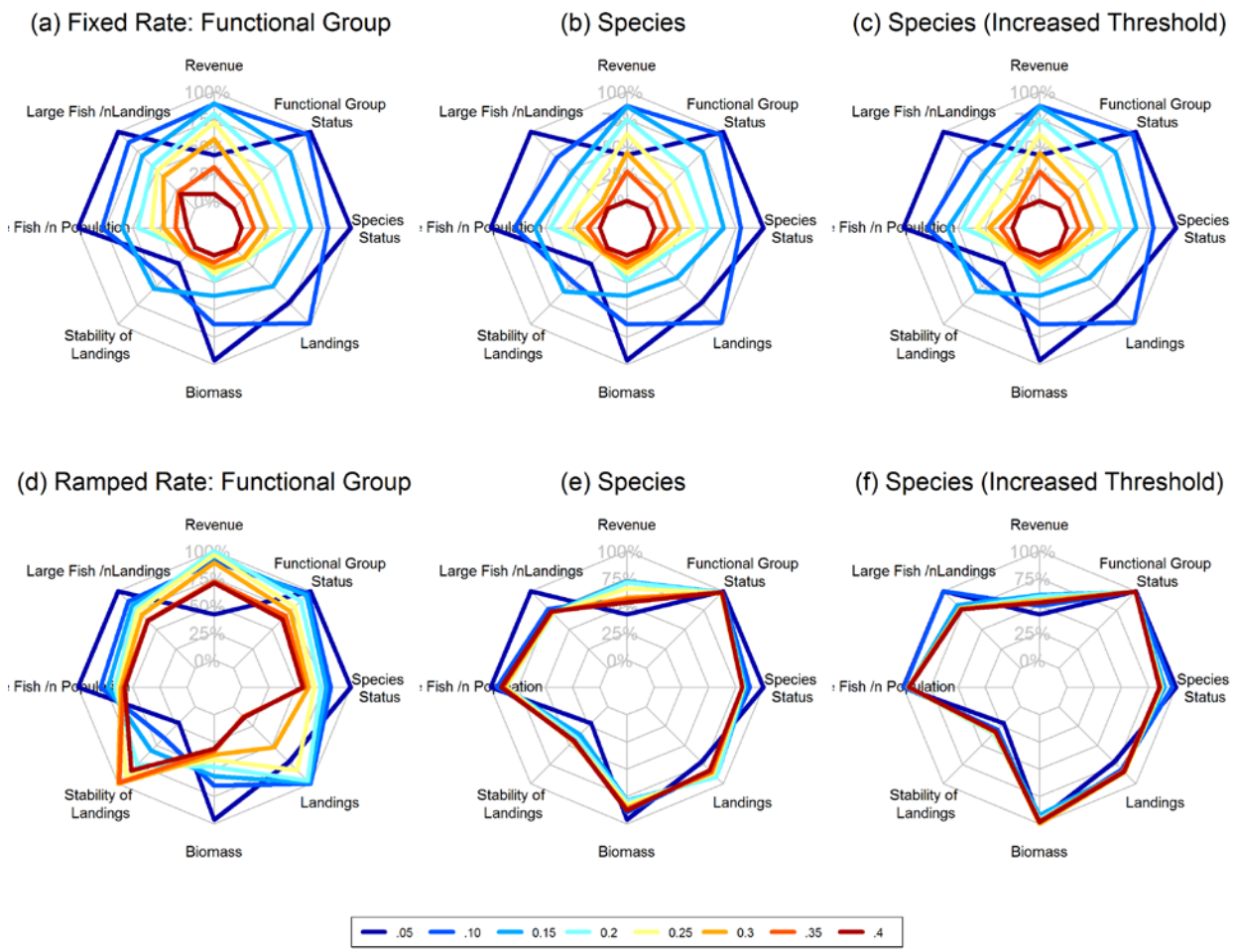

Figure 4.8. Radar plots depicting the performance of the 6 major scenarios for 8 performance metrics for years 41-50 in the simulations. Performance metrics are each evaluated at eight levels of exploitation (represented by colored lines).

To dissect some of the underlying factors leading to the observed patterns, below we provide comparisons between two of the six scenarios examined in these analyses which offer the greatest contrast in levels of precautionary action. We examine the results at the functional

group and individual species levels and focus on the biomass, yield, and proportion overfished performance metrics. Comparable results are available for each of the six scenarios examined and each of the performance metrics but are not shown here. The fixed rate (threshold) strategy in which action is taken only when biomass at the functional group level falls below 20% of the unfished state is the least conservative option examined. The ramp down strategy implemented with enhanced protection for the most vulnerable species (elasmobranches) affords the greatest overall protection. We will show results integrated over fleet sectors to portray the overall status of the biomass, catch, and proportion overfished metrics. These can be further partitioned by fleet for closer examination of results if desired.

Results for the fixed rate strategy implemented at the functional group level are shown in Figure 4.9. Biomass for each of the four functional groups declines monotonically with increasing exploitation rates. Landings for the piscivores rises to a peak and then begins to decline at the highest level of exploitation examined. In contrast, the landings of planktivores and benthivores are highest at low to moderate exploitation rates, then dropping precipitously in particular for the planktivores. Elasmobranch landings remain relatively stable at low levels with increasing exploitation rates. The most striking result for the proportion overfished metric is the sensivity of the planktivore and benthivore groups (as can be anticipated by the shape of the landings functions). At the guild level, the differences in resilience to exploitation and overall biomass levels of spiny dogfish and winter skate dominate the result for the overfished status determination. The elasmobranch functional group does not reach overfished status within the range of exploitation rates examined. Winter skate biomass markedly exceeds that of spiny dogfish and it does not drop to low levels in these simulations.

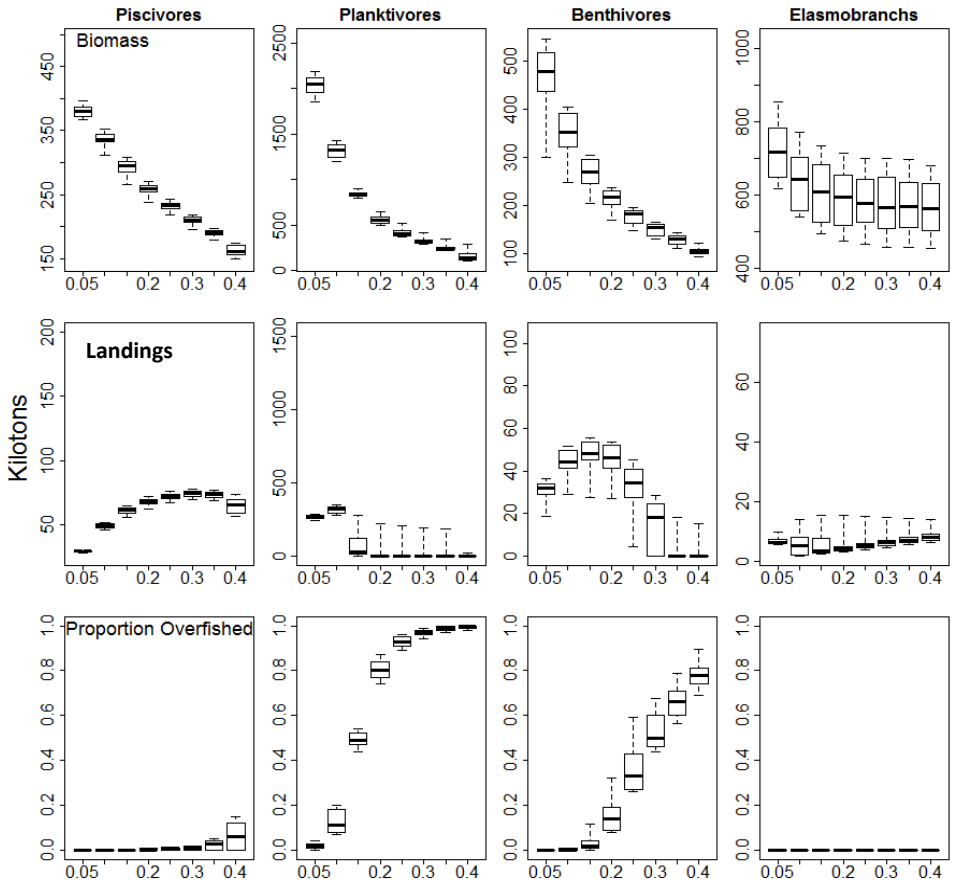

Figure 4.9. Biomass, landings, and proportion overfished as a function of exploitation rates ranging from 0.05-0.4 in increments of 0.05 (rows) for each of the four functional groups (columns) under the fixed rate (threshold) scenario implemented at the functional group level.

Examination of the biomass trajectories by species as a function of exploitation rate indicates the expected declines for all except winter skate (Figure 4.10) which remains relatively constant. Clear differences in the observed rate of decay do emerge for the remaining species.

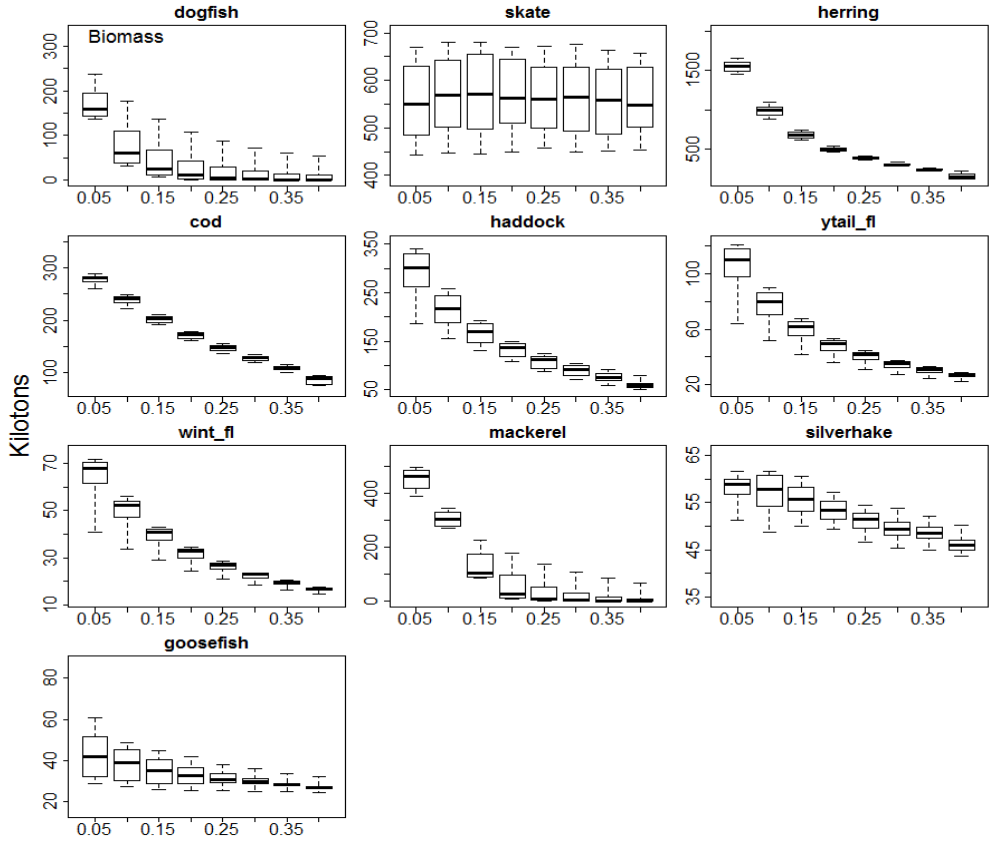

Figure 4.10. Biomass as a function of exploitation rates for the fixed rate (threshold) scenario implemented at the functional group level and for exploitation rates ranging from 0.05-0.4 in increments of 0.05.

Catch levels in response exploitation rates reveal sharp thresholds for some species (herring, yellowtail flounder winter flounder and mackerel) in which precipitous drops in yield suddenly occur (Figure 4.11). Again, winter skate exhibits a much different pattern where yield increases monotonically as exploitation increases within the ranges considered.

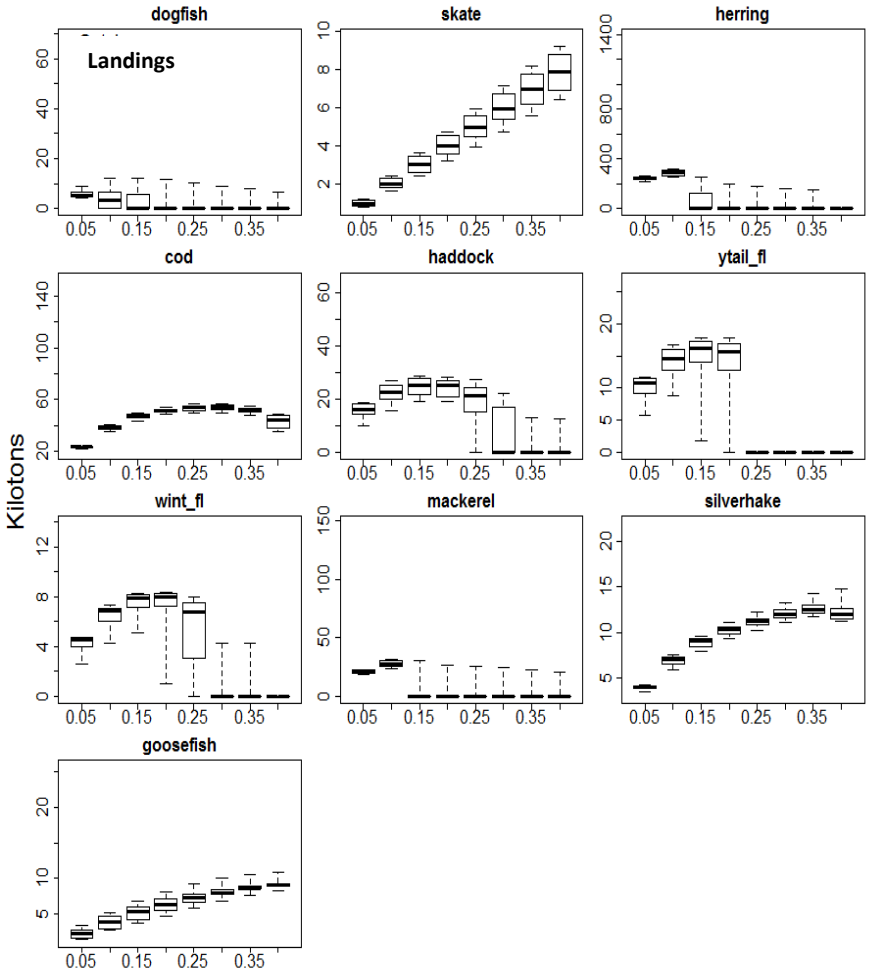

Figure 4.11. Catch as a function of exploitation rates for the fixed rate (threshold) scenario implemented at the functional group level and for exploitation rates ranging from 0.05-0.4 in increments of 0.05.

For the most conservative strategy considered (ramped exploitation with enhanced protection for elasmobranches), greater overall stability is observed for biomass and yield levels (Figure 4.12) relative to the threshold exploitation strategy implemented at the functional group level, albeit with higher levels of variability of biomass in particular. The proportion overfished is sharply reduced overall, although the planktivore group again exhibits higher vulnerability relative to the other functional groups even under this conservative strategy.

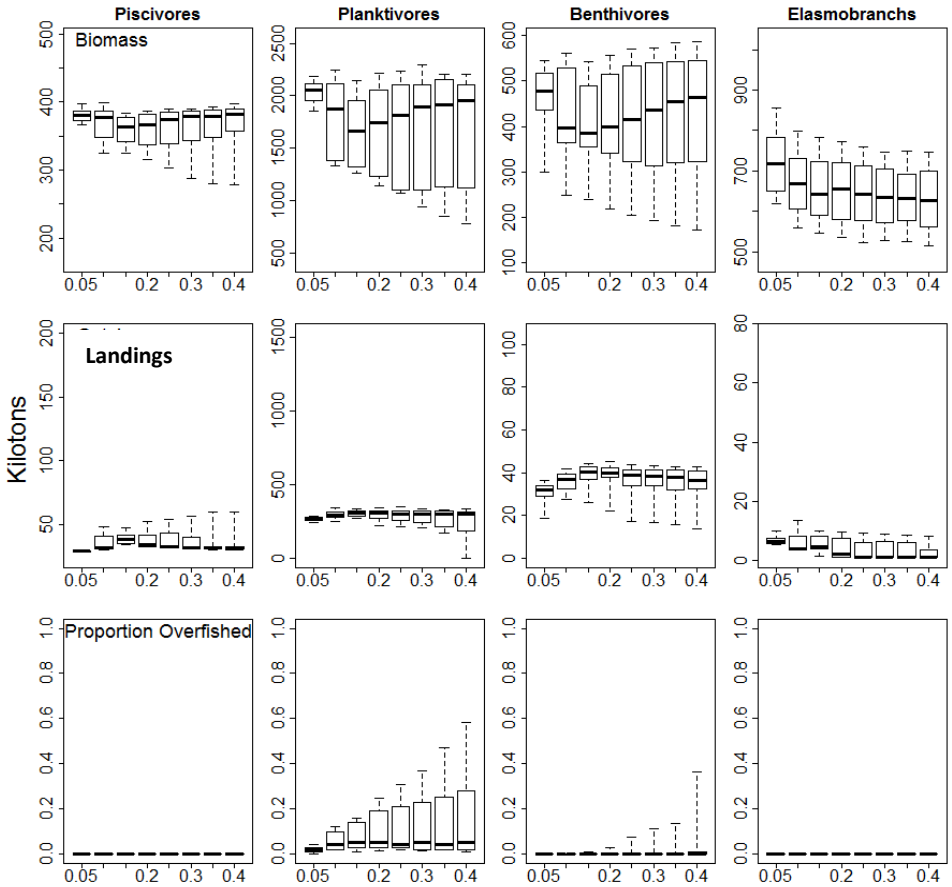

Figure 4.12. Biomass, landings, and proportion overfished as a function of exploitation rates ranging from 0.05-0.4 in increments of 0.05 (rows) for each of the four functional groups (columns) under the ramped rate (threshold) scenario implemented with ramped exploitation with ramped exploitation with enhanced protection for elasmobranches. The exploitation rate now refers to the nominal level; this level is then modulated in response to resource status.

Examination of the species-level biomass levels reveals that the updated modulation of the exploitation rates is capable of maintaining each at more stable levels (Figure 4.13). Similar results obtain for landings (Figure 4.14).

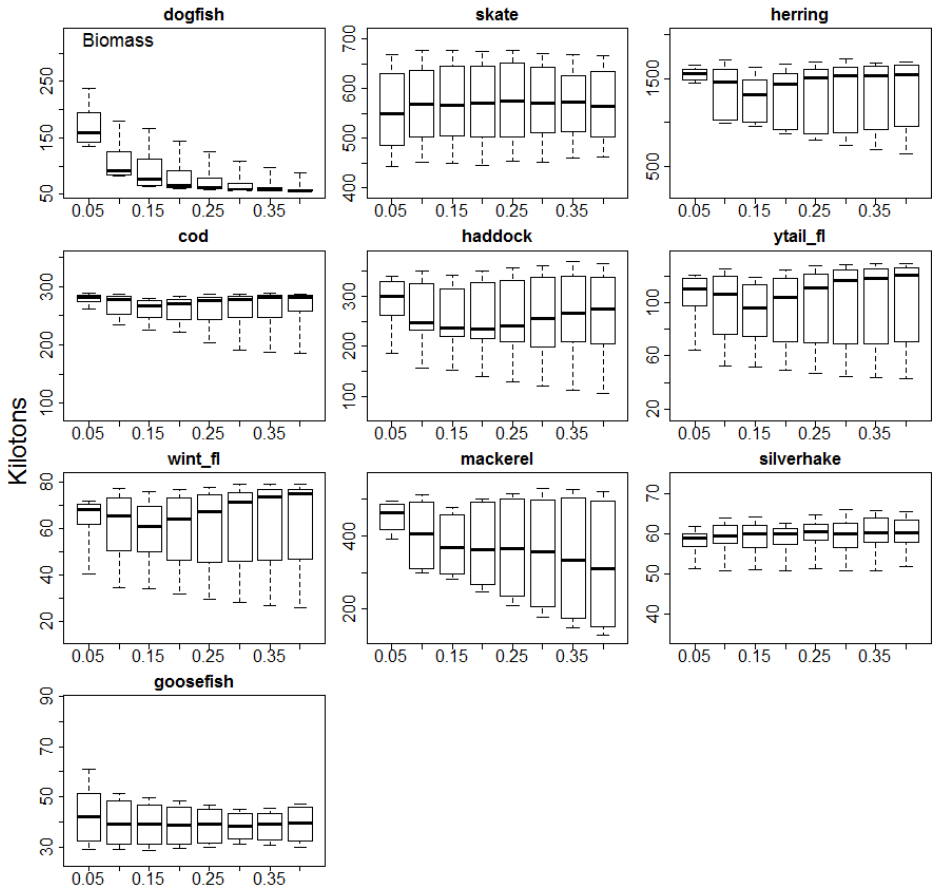

Figure 4.13. Biomass as a function of exploitation rates with ramped exploitation with enhanced protection for elasmobranches. The exploitation rate now refers to the target level; this level is modulated in response to resource status.

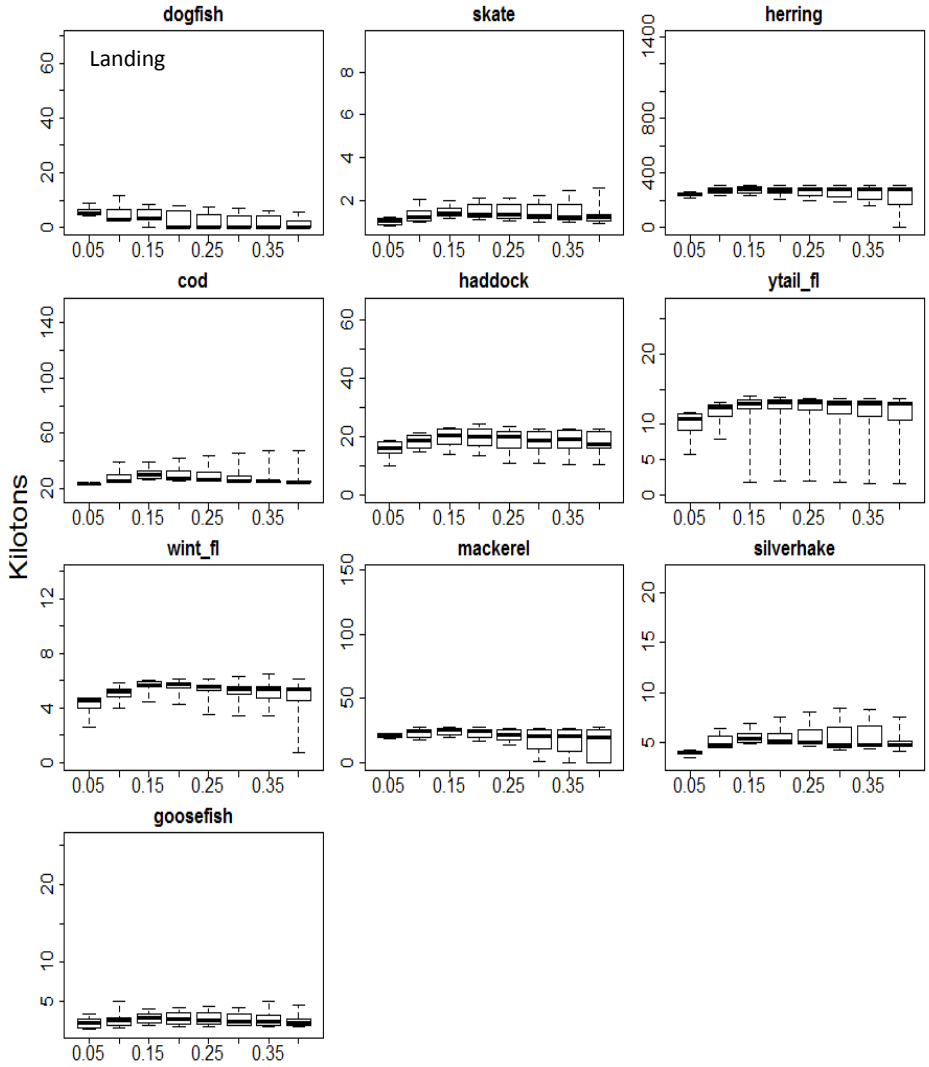

Figure 4.14. Landings as a function of exploitation rates under ramped exploitation with enhanced protection for elasmobranches. The exploitation rate now refers to the nominal level; this level is modulated in response to resource status.

Fleet Tradeoffs

Direct and indirect interactions among different fleets have the potential to substantially affect resource status and yield in fishery ecosystems. Fleet components that share targeted species collectively exert a cumulative impact on these resources. Depending on the gear characteristics used they can also exert differential impacts on non-target species and habitats. Accordingly, the relative magnitude and spatial allocation of fishing effort by different fleets holds important implications for ecosystem structure and function.

Below, we examine potential tradeoffs in biomass and yield between the demersal trawl fishery and the demersal fixed gear fleets. The trawl fishery has a substantially larger presence

on Georges Bank than the fixed gear component with important ramifications for the interpretation of the results provided below. We show results for changes in fishing effort ranging from 0 to 200% of the average effort levels in both fleets; we hold the pelagic trawl effort constant at its historical mean level.

Because of the marked disparity in effort and resulting yields attributable to these two fleet components, the fixed gear fishery exerts relatively little effect on the overall biomass of piscivores and benthivores (Figure 4.15). Indirect effects on planktivore biomass and yield are clearly evident (Figure 4.15). The decrease in biomass of piscivores with increases in demersal trawl and fixed gear effort results in a decrease in predation on planktivores and a corresponding increase in biomass and yield for this functional group. At intermediate to higher levels of historical fishing effort for the trawl and fixed gear components, more interesting tradeoff options begin to emerge in which higher levels of yield can be attained in different combinations of effort in these two fleets (Figure 4.15).

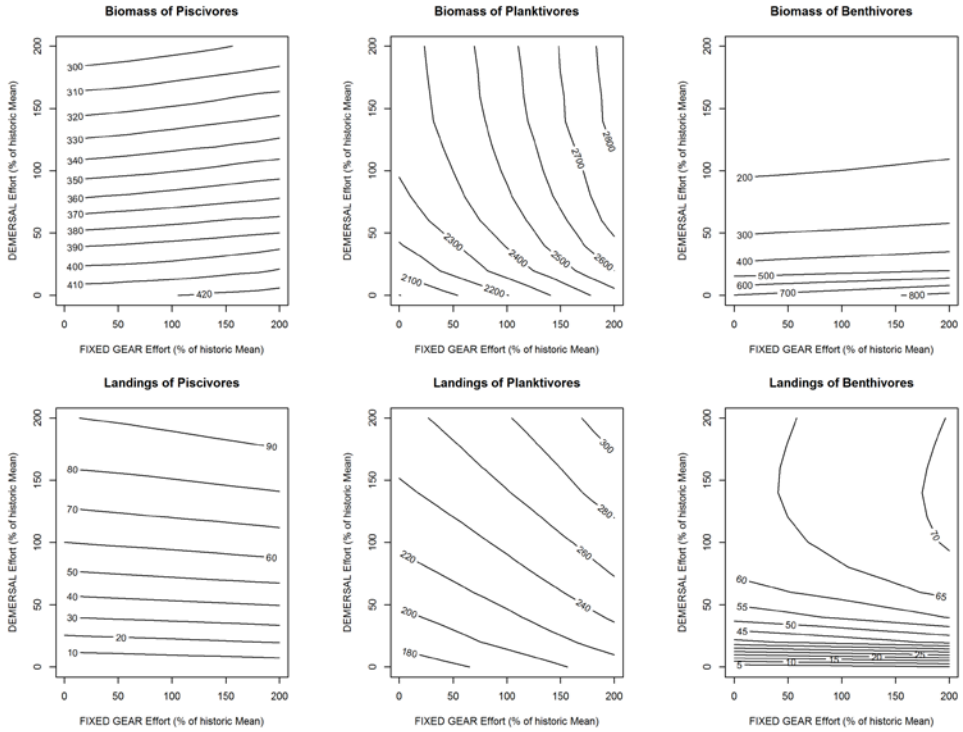

Figure 4.15. Biomass (kt) and yield (kt) isopleths for changes in historical effort levels in the demersal trawl and fixed gear fleets with pelagic trawl effort held at its historical mean. Effort levels are expressed as percentages of the historical mean for demersal trawl and fixed gear fisheries.

Assessment Model Performance

We examined the Modelling Efficiency of the simple multispecies production model and the multispecies delay-difference model when applied to Hydra model output with observation error added. For this exercise, the goal is not to develop proxy reference points based on simpler assessment models applied to more complex underlying generating models. Rather, we wish to assess the utility of broadly applicable but simple models that can integrate information from survey and catch series to estimate total biomass for each species. These estimates, if sufficiently robust can then be used to test whether an individual species drops below its designated floor. Based on information on survey variability in this region (NEFSC 1989), we employed observation error levels with coefficients of variation of 20-30%. We further considered autocorrelation in the observation process at three levels (ρ = 0, 0.3, and 0.6). In this exercise, we did not include systematic bias in the observations but note that this can be readily accommodated. In the analyses presented here, we fixed the shape parameter at γ=2 (quadratic). In prior analyses, we found that estimating three parameter recruitment models was problematic, with typically high covariances among parameter estimates. Sequentially fitting models with fixed levels of the shape parameter and selecting one based on the profile likelihood is more feasible. In future work, we plan to systematically vary γ and use the Modelling Efficiency metric to guide model selection.

Here, we will present one example (σ^2=0.2, ρ=0.3) for illustration. We found that the median MEF level fell within the range 0-1 for both the delay-difference (DD) and the simpler Lotka-Volterra type model with no stage structure, indicating better performance of these models than the null case (using the time series mean; see Figure 4.16). The model performance for silver hake and monkfish was inferior to that of the other 8 species. The delay-difference model, did not outperform the simpler Lotka-Volterra type model in these tests. Overall, our results suggest that simpler models can potentially be used to represent the dynamics of models with substantially greater underlying complexity. Because a substantial fraction of species managed by NEFMC currently are assessed using index-based methods involving only observations derived from standardized NEFSC research vessel surveys or a combination of survey and catch data, results suggest that the simple multispecies models considered here can offer a middle

ground in assessment model complexity that can accommodate a broad range of species managed by NEFMC.

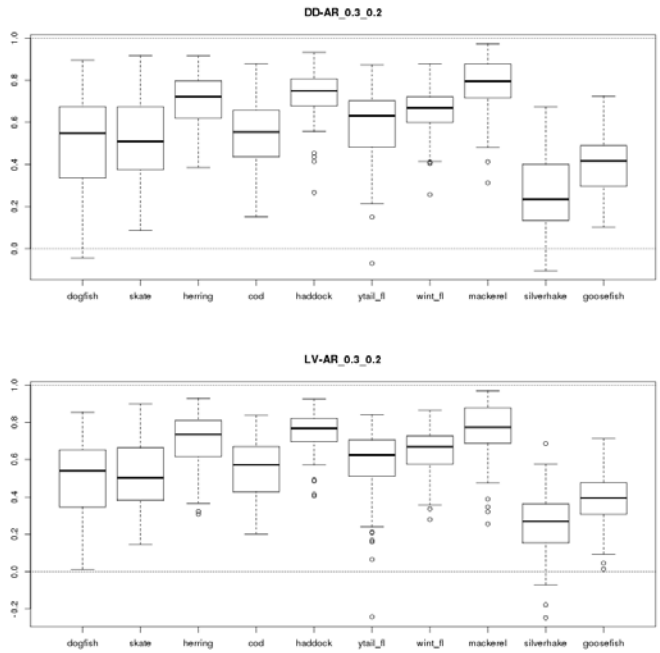

Figure 4.16. Modelling efficiency estimates for the multispecies delay-difference model (DD; upper panel) and the simpler Lotka-Volterra-type (L-V; lower panel) model with (σ^2=0.2, ρ=0.3). [The model efficiency metric can be expressed MEF=(1-RMSE^2)/s^2; see methods for further details).

Kraken

Portfolio Analysis

Simulated historical versus optimized revenue as a percentage of each simulation's mean value is presented in Figure 4.17 in order to facilitate comparison across species. Although the results presented here are patterned on observations on the 10 species system and the three selected functional groups considered in this document, in the following we will assign numerical codes to species and functional groups rather than identifying actual species and groups. It is particularly important to keep in mind that the revenue target is constant across the portfolio-optimized component of the simulation, which is an assumption which can and should be revisited when ultimately engaged in assessing management alternatives. The results of the simulations indicates that the optimal portfolio is chosen to direct catch away from species with either substantial historic volatility, high positive correlations with other species in the system, or

a mix of both. For example, in a balanced portfolio, optimal revenue of both Species 3 and 9 are substantially lower than historical levels. Conversely, species such as 1 and 6 are exploited more heavily by the model, given their substantially lower historical variability. Comparing revenue to catch there is general concurrence in regards to the direction of the shift across species. However, there are some distributional differences worth pointing out. For example, comparing revenue vs. catch for Species 8, the revenue variability of the optimized simulation results is substantially higher than the catch from the same time period. The opposite can be said for a comparison of the historical revenue versus catch for Species 8. This suggests that the portfolio is exploiting differences between biological and market correlations in minimizing the variance surrounding system-level revenue. Additionally, the optimized revenue for Species 8 indicates substantial increases in variability when compared to the historical revenue flow. This highlights an important consideration, in that although the optimal portfolio species mix minimizes the variance in the system at large, any single species could actually be associated with increased variability in revenue and catch streams. This is particularly true given that the model does not simulate the steady-state, but rather can be thought of as the approach path, which is of more interest to managers in a heavily perturbed system. A similar result can be seen in the biomass of Species 1, which exhibits a substantial increase in variability within the optimized segment of the simulation when compared to the historical segment.

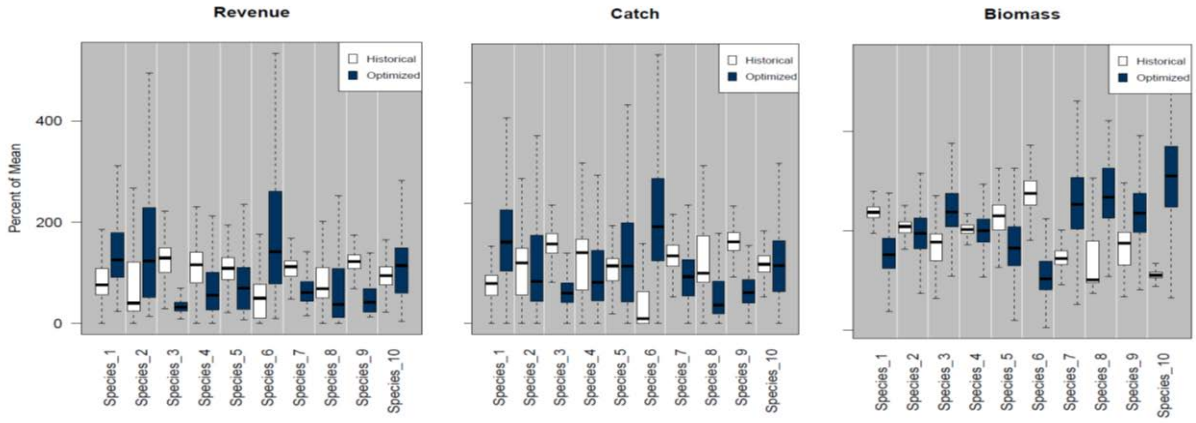

Figure 4.17 Historical revenue, catch, and biomass *vs* portfolio optimized values.

The number of times across simulations that either the guild ceilings or species floors bind are depicted in Figure 4.18. A comparison of the two figures indicates that the species floors bind much more frequently than the guild ceilings, which indicates that the optimum portfolio is more sensitive to the exploitable biomass within, rather than between, guilds.

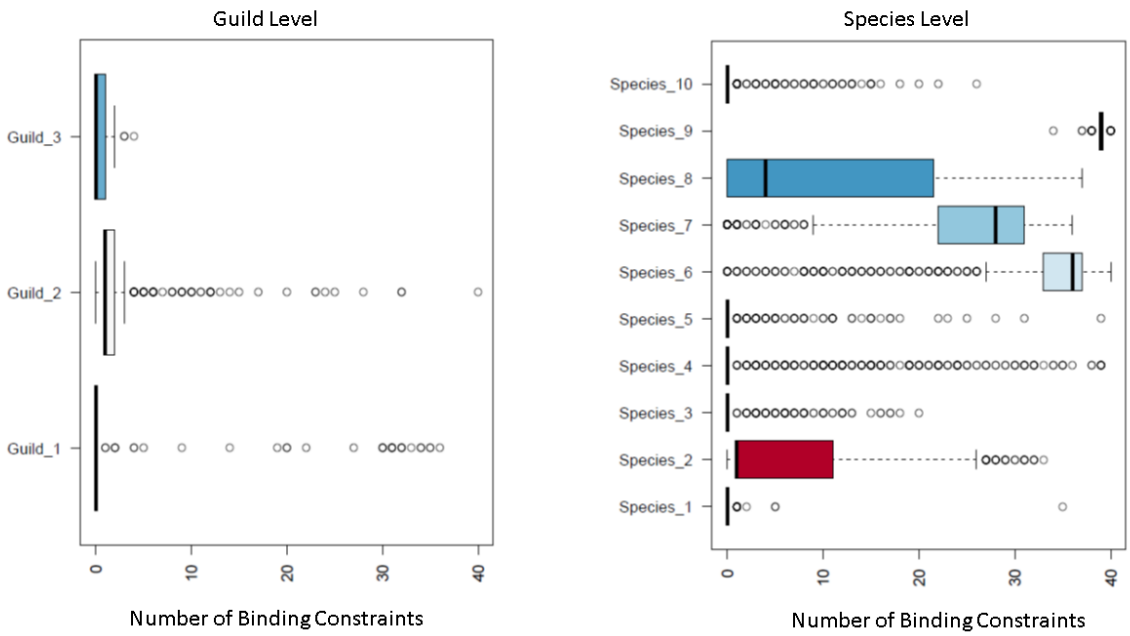

Figure 4.18. Number of binding Guild and Species-level ceiling constraints across all simulations.

Discussion

The challenge of developing effective management strategies for multispecies fisheries subject to both technical and biological interactions is well recognized and innovative approaches are being developed to confront the known difficulties in addressing these fundamental issues (e.g. Mackinson et al. (2009, 2018; Thorpe et al. 2015, 2016, 2017). The essential elements of the problem has long been recognized in New England. Shortly following the adoption of the Magnuson-Stevens Fishery Conservation and Management Act of 1976, the newly formed New England Fishery Management Council (NEFMC) established a Northeast Fishery Management Task to evaluate options for recovery and sustainable management of fisheries in the region. The Task Force clearly recognized the inherent difficulties in managing mixed-species fisheries in the region and proposed that:

> *"… management might address itself to the productivity and harvest potential of an entire ecosystem, since the ecosystem in the long run has greater stability than any of its components."*
>
> and
>
> *" … individual species, groups of species, or particular fisheries (defined by area or gear) would be regulated to control the relative balance of the species mix"* (Hennemuth et al. 1980) .

In our analysis, we returned to core elements of the Task Force recommendations as a basis for defining and implementing a prototype multispecies management strategy for Georges Bank. Our goal is intended to address the potential strengths and weaknesses of focusing management actions at higher levels of ecological organization. Our approach of defining ceilings (or total catch caps) to set upper constraints on removals from the system and floors (protective constraints on reductions in biomass at the functional group and individual species levels) has been developed in recognition of the inherent difficulties in effecting exact compositional control of the catch of individual stocks in mixed species fisheries.

Our results indicate that management strategies in which remedial reduction in exploitation rates is implemented only when an overfished level is reached at either the

individual species or functional group level, perform significantly worse for all metrics than ramp-down strategies except at low exploitation rates. With increasing exploitation rates, performance of the fixed (or threshold) strategy degrades rapidly even with strategies that provide enhanced protection for the most vulnerable species.

Application of strategies in which graduated remedial action is taken once defined trigger levels of biomass are reached result in much greater resilience to increases in nominal (target) exploitation rates. The highest levels of revenues, landings, and stability of landings were attained under the ramp-down strategy in which the protective floors were implemented at the functional group level rather than for individual species. The highest revenues occurred at an exploitation rate of 0.25 under this scenario. Not surprisingly, the ramp-down strategy with floors identified at the species level performs better for metrics related to conservation status than when protections are implemented only at the functional group level as nominal exploitation rates increased. The enhanced protection strategy for vulnerable species provided the greatest overall resilience to higher exploitation rates.

Collectively, these initial simulation results suggest that 'applying the brakes early' can sharply reduce the incidence of overfished status determinations while maintaining higher yields and revenues

We have complemented more traditional biologically-based management strategies in our objectives with a portfolio analysis which seeks to reduce risk in economic returns as measured by variance in revenue streams. The New England Fishery Management Council recently identified stability as a core component of its risk policy. In its Risk Policy Roadmap, stability is defined as "Evaluating the trade-offs of minimizing variability while achieving the greatest overall net benefits to the nation", and that "Metrics that monitor variability from year to year, e.g. in quotas, should be developed" (Risk Policy Working Group 2016). The overarching goal, then, is to assess the trade-offs between generating a high flow of benefits and the ability to ensure that flow of benefits can be generated in a stable and sustainable manner.

In economics, modern portfolio theory was developed to assess this exact trade-off (Markowitz 1952). Portfolio analysis measures the extent to which financial assets change relative to each other, with the idea that in a well-balanced portfolio a decrease in the value of

one asset will be off-set by an increase in another. The framework has been extended to assess trade-offs in fishery management (Edwards et al. 2004, Sanchirico et al. 2008), in that species and guilds can be viewed as generating a flow of benefits whose stability can be assessed in a similar manner to financial assets.

When coupled to a biological simulation, portfolio analysis can be used in two capacities. First, the coupled model can be used to identify the mix of harvested species which generates the lowest amount of deviation from a targeted revenue value. Second, the portfolio analysis can be used to assess trade-offs, and provides a manner to gauge strategy performance, with respect to the objective of system stability; facilitating both conservation and business planning.

The coupled Portfolio-Kraken model is a worked example of a flexible framework that can be employed to assess trade-offs in support of Ecosystem-based Fishery Management. Portfolio theory directly addresses the objective of stability as stated in the NEFMC Risk Policy. By coupling the portfolio analysis to a biological surplus production function, we present examples of outputs that can help inform managers with respect to not only the levels of risk inherent in management alternatives, but also where in the system that risk lies. By providing a theoretically sound measure of risk which can be developed across multiple biological models, portfolio theory can help standardize the assessment of economic risk in an ecosystem context; providing an informative output that can be utilized formally in Management Strategy Evaluation, or more generally in assessing trade-offs across alternatives.

References

Appolonio, S. and J.J. Dykstra. 2008. "An enormous, immensely complicated intervention": groundfish, the New England Fishery Management Council and the world fisheries crisis. E-Book Time LLC, Montgomery 246pp.

Barrowman, N. J. & Myers, R. A. (2000). Still more spawner-recruitment curves: the hockey stick and its generalizations. Can. J. Fish. Aquat. Sci. 57:665-676

Curti, K. Age-structured multispecies model of the Georges Bank fish community. Graduate School of Oceanography, University of Rhode Island, Narragansett R.I. PhD thesis

Bell, R.J., M.J. Fogarty, and J.S. Collie. Stability in marine fish communities. Mar. Ecol. Prog. Ser. In press.

Brown, B. E., J. A. Brennan, M. D. Grosslein, E. G. Heyerdahl, and R. C. Hennemuth. 1976. The effect of fishing on the marine finfish biomass in the Northwest Atlantic from the Gulf of Maine to Cape Hatteras. Int. Comm. Northwest Atl. Fish. Res. Bull. 12:49-68.

Brown J.H. 1995. Macroecology. Univ. Chicago Press, Chicago. 269 pp.

Butterworth, D.S. 2007. Why a management procedure approach? Some positives and negatives. ICES J. Mar. Sci. 64:613-617.

Butterworth, D.S., K. Cochrane, and J. DeOliveira. 1997. Management procedures: A better way to manage fisheries? Am. Fish. Soc. Symp. 20:83:90.

Cohen, E.B., M.D. Grosslein, and M.P. Sissenwine. 1982. Energy budget of Georges Bank. Can. Spec. Publ. Fish. Aquat. Sci. 59:95-107.

Chassot, E., S. Bonhommeau, N.K. Dulvy, F. Melin, R. Watson, D. Gascuel, and O. Le Pape. 2010. Global marine primary production constrains fisheries catches. Ecol. Lett. 13:495-505.

Collie, J.S. and A. K. DeLong. 1999. Multispecies interactions in the Georges Bank Fish Community. Ecosystem Approaches for Fisheries Management. Univ. Alaska Sea Grant, AK-SG-99-01, Fairbanks. pp. 187-210.

Collie, J.S. and H. Gislason. 2001. Biological reference points for fish stocks in a multispecies context. Can. J. Fish. Aquat. Sci. 58:2167-2176.

Edwards, S. F., J. S. Link, and B. P. Rountree. 2004. Portfolio management of wild fish stocks. *Ecological Economics* 49:317–29.

Fogarty, M.J. 2014. The art of ecosystem-based fishery management. Can. J. Fish. Aquat. Sci. 71:479-490.

Fogarty, M. J. and S. A. Murawski. 1998. Large-scale disturbance and the structure of marine systems: fishery impacts on Georges Bank. Ecol. Appl. 8:6-22.

Gaichas, S.K., R. Gamble, M. Fogarty, H. Benoit, T. Essington, C. Fu, M Koen-Alonso, J. Link. 2012. Assembly Rules for Aggregate-Species Production Models: Simulations in Support of Management Strategy Evaluation. Mar. Ecol. Prog. Ser. 459: 275–292.

Gaichas, S.K., Fogarty, M., DePiper, G., Fay, G., Gamble, R., Lucey, S., and Smith L. 2016. Combining stock, multispecies, and ecosystem level fishery objectives within an operational management procedure: simulations to start the conversation. ICES J. Mar. Sci. doi.10.1093/icesjms/fws119.

Gamble, R.J. and J.S. Link. 2009. Analyzing the tradeoffs among ecological and fishing effects on an example fish community: A multispecies (fisheries) production model. Ecol. Mod. 220:2570-2582.

Hennemuth, R.C., B.J. Rothschild, L.G. Anderson, and W.A. Lund, Jr. Overview document of the Northeast Fishery Management Task Force, Phase I. TM F/NEC-1: October 1980. NTIS Access. No. PB81-202343.

Howell, D. and B. Bogstad. 2010. A combined GADGET/FLR model for management strategy evaluations of the Barents Sea Fisheries. ICES J. Mar. Sci. 67:1998-2004.

Jin, D., G. DePiper, and P. Hoagland. 2016. Applying portfolio management to implement ecosystem-based fishery management (EBFM). North American Journal of Fisheries Management 36(3): 652-69.

Lucey, S. and M.J. Fogarty. 2013. Operational fisheries in New England: Linking current fishing patterns to proposed ecological production units Fish. Res. 141 3-12

Mackinson, S., B. Deas, D. Beveridge, and J. Casey. 2009. Mixed-species or ecosystem conundrum: Multispecies considerations inform thinking on long-term management of North Sea demersal stocks. Can. J. Fish. Aquat. Sci. 66:1107-1129.

Mackinson, S., M. Platts, C. Garcia, and C. Lynam. 2018. Evaluating the fishery and ecological consequences of the proposed North Sea multi-annual plan. PLOS ONE https://doi.org/10.1371/journal.pone.0190015.

Markowitz, H. 1952. Portfolio selection. *Journal of Finance* 7:77–91.

McHugh, J.L. 1959. Can we manage our coastal fisheries? Trans. Am. Fish. Soc. 88:.105-110.

McHugh, J.L. 1988. Can we manage our coastal fisheries - II? Mar. Fish. Rev. 50:41-45.

Perretti, C.T. M.J. Fogarty, K. Friedland, J. Hare, S. Lucey, R. McBride, T.J. Miller, R. Morse, L. O'Brien, J. Pereira, L. Smith, M. Wuenschel . 2017. Regime shifts in fish recruitment on the Northeast U.S. continental shelf. Mar. Ecol. Prog. Ser. 574:1-11.

Risk Policy Working Group. 2016. Report from the Risk Policy Working Group: Risk Policy Road Map. New England Fishery Management Council, Newburyport, MA.

Sanchirico, J. N., M. D. Smith, and D.W. Lipton. 2008. An empirical approach to ecosystem-based fishery management. *Ecological Economics* 64:586–96.

Silvey, S. D. (1975). Statistical Inference, Wiley

Stow, C.A., J. Jolliff, D.J. McGillicuddy, S.C. Doney, J.I. Allen., M.A.M Friedrichs, K.A. Rose, and P. Wallhead. 2008. Skill assessment for coupled biological/physical models of marine systems. J. Mar. Sys. 76:4-15.

Thorpe, R.B., W.J.F. Le Quesne, F. Luxford, J.S. Collie and S. Jennings. 2015. Evaluation and management implications of uncertainty in a multispecies size-structures model of population and community responses to fishing. Meth. Ecol. Evol. 6:49-58.

Thorpe, R.B., P.J. Dolder, S. Reeves, P. Robinson and S. Jennings. 2016. Assessing fishery and ecological consequences of alternate management options or multispecies fisheries. ICES J. Mar. Sci. 73:1503-1512.

Thorpe , R.B., S. Jennings, and P.J. Dolder. 2017. Risks and benefits of catching pretty good yield in multispecies fisheries. ICES J. Mar. Sci. doe:10.1093/icesjms/fsx062.

Tsou, T. & Collie, J.S. (2001). Estimating predation mortality in the Georged s Bank fish community. Can. J. Fish. Aquat. Sci. 58:908-922

Tyrell, M.C., Link, J.S., Moustahfid, H. & Overholtz, W.J. (2008). Evaluating the effect of predation mortality on forage species population dynamics in the Northeast US continental shelf ecosystem using multispecies virtual population analysis. ICES J. of Mar. Sci. 65:9:1689-1700

Appendix

Basic Model Structure

Parameter inputs to the model for the simulations presented in the main body of the paper are included below. The model is set up to simulate the interactions of 10 species with 5 length bins each and three fishing fleets over the course of 53 years in a single homogeneous area. We summarize parameter sources here and list parameters in Tables A1 (species and length specific parameters), A2 (recruitment parameters) (species-specific parameters), and A3 (predator prey linkages) below.

Length bin widths in cm are specified for each of the 10 species to reflect growth patterns and ontogenetic shifts in feeding across the 5 length bins (Table A1). The model calculates minimum and maximum lengths in each bin based on these bin widths, and converts bin length in cm to weight in g using the standard weight = *a* times length to the power *b*. Length-weight parameters (Table A2) for each species were taken from Hall et al. (2006).

Table A1. Species and length specific model parameters: Length bin width (cm), stomach weight (g), and initial numbers (N, millions of fish).

Species	**Length bin 1**	**Length bin 2**	**Length bin 3**	**Length bin 4**	**Length bin 5**
	Bin width	**Bin width**	**Bin width**	**Bin width**	**Bin width**
Spiny dogfish	20	20	20	20	30
Winter skate	20	20	20	20	40
Atlantic herring	5	5	5	5	20
Atlantic cod	20	20	20	40	50
Haddock	10	10	20	20	20
Yellowtail flounder	10	10	10	10	20
Winter flounder	10	10	10	10	10
Atlantic mackerel	10	10	10	10	10
Silver hake	10	10	10	10	30
Monkfish	20	20	20	30	40
	Initial No.	**Initial No.**	**Initial No.**	**Initial No.**	**Initial No.**
Spiny dogfish	59.666	57.908	48.845	41.853	47.742
Winter skate	6.421	8.806	9.752	10.703	30.972
Atlantic herring	536.966	1210.835	1448.127	1597.726	6037.405
Atlantic cod	3.392	4.357	4.273	9.508	11.500
Haddock	0.000	4.654	17.411	21.481	24.756
Yellowtail flounder	2.229	4.532	5.958	9.316	27.078
Winter flounder	2.389	3.733	4.067	4.765	19.680
Atlantic mackerel	172.549	208.301	187.980	181.121	141.193
Silver hake	12.785	20.898	23.408	31.279	25.278
Monkfish	2.924	4.418	3.749	2.600	2.226

Recruitment Module

Methods:

The functional form, $f(S_{t-1}, \underline{\theta})$, of the spawner-recruit relationships was chosen to take the form of a hockey stick model (Barrowman & Myers, 2000) and a generalized form of the hockey stick model. Specifically,

$$f(S_{t-1}, \underline{\theta}) = S_{t-1} \qquad \text{if } S_{t-1} \leq \delta$$

$$= S_{t-1} + \frac{\beta}{\alpha}(S_{t-1} - \delta) \qquad \text{if } S_{t-1} > \delta$$

where α is the slope at origin (recruits/biomass), an estimate of density dependent survival, δ is the change-point, the value of spawning stock in which the slope, α, changes. β is the change in slope at the change-point. When $\beta = -\alpha$ then the above equation simplifies to the hockey stick model and resembles a simple piecewise linear alternative to the Beverton Holt model. When $\beta < -\alpha$ the slope after the change point decreases resembling a simple piecewise linear alternative to the Ricker model.

Parameter estimation is achieved via the method of maximum likelihood (Silvey, 1975) in which the maximum likelihood estimators (MLEs), $\hat{\underline{\theta}}$ and $\hat{\underline{\sigma}}$ of $\underline{\theta}$, and $\underline{\sigma}$ are found by maximizing the log likelihood,

$$\log L(\underline{\theta}, \sigma; \underline{S}_{t-1}) = -n\log(\sigma) - \frac{1}{2\sigma^2}\sum_{t=2}^{n}(\log(R_t) - E[\log(R_t)])^2$$

which under this model simplifies to

$$\log L(\underline{\theta}, \sigma; \underline{S}_{t-1}) = -\frac{n}{2}\log\sum_{t=2}^{n}\left(\log(R_t) - \ln\left[\alpha f(S_{t-1}, \underline{\theta})\right]\right)^2$$

since

$$\hat{\sigma}^2 = \frac{1}{n}\sum_{t=2}^{n}\left(\log(R_t) - \ln\left[\alpha f(S_{t-1}, \underline{\theta})\right]\right)^2$$

We take advantage of the properties of the profile log likelihood to obtain the MLE of the change-point parameter, δ. This comprises fixing δ and numerically maximizing the log likelihood to obtain $\hat{\alpha}$. This is repeated over a range of values for δ. The MLE of $\delta, \hat{\delta}$, is the value of δ which maximizes the log likelihood.

Under the assumption of the hockey stick model then the estimation process is simplified since given δ, $\hat{\alpha}$ has a closed form solution,

$$\hat{\alpha} = \frac{1}{n} exp\left(\sum_{t-2}^{n} log\left(\frac{R_t}{f(S_{t-1})}\right)\right)$$

We therefore no longer need to numerically maximize the log-likelihood but instead simply evaluate it at δ and $\hat{\alpha}$.

Table A.2. Stock-recruitment parameter estimates, data sources, time periods covered, model type (HS-hockey stick; OC-overcompensatory), multiplier adjustment applied to obtain age-0 recruits.

Species	Parameter Estimates			Data Source	Time Period	Model	Multiplier
	α	β	δ				
Spiny dogfish	.000278	-.00031	166786	K. Sosebee, pers. comm	1969-2006	OC	1.161834
Winter skate	.000385	-.00059	176234	Curti, K. L. et al (2013)	1978-2008	OC	1.221403
Atlantic herring	.0428	-.428	92565	Tyrrell, M.C. et al (2008)	1982-2002	HS	1
Atlantic cod	.000497	-.0006	62037	Curti, K. L. et al (2013)	1978-2008	OC	1.616074
Haddock	.00497	-.00497	7521	Perretti	1961-2009	HS	3.320117
Yellowtail flounder	.0101	-.101	2560	Tsou, T.S., and Collie, J.S. (2001)	1978-1993	HS	1.221403
Winter flounder	.00515	-.00515	2642	Perretti	1983-2013	HS	1.221403
Atlantic mackerel	.00116	-.00116	195263	Tyrrell, M.C. et al (2008)	1982-2002	HS	1
Silver hake	.177	-.195	4617	Curti, K. L. et al (2013)	1978-2008	OC	3.320117
Monkfish	.00163	-.00188	5175	Curti, K. L. et al (2013)	1978-2008	OC	1.349859

Selecting spawner-recruit models:

We determine *a priori* which species would take the form of a hockey stick model and which species would take on the form of the generalized model (denoted in the table as HS or OC respectively). This decision is based on species life history traits. Segmented spawner-recruit models are then fit to the data. To account for uncertainty in the data and to tackle the issue of "missing" data for lower levels of spawning stock biomass we adopt a sampling regime to select variants of these fitted models using the initial fits as starting points. The sampling regime has a similar approach to that of Thorpe et al (2015) in that an operating model is used in the selection process and that empirical data is used to set bounds for model output to satisfy.

This "Darwinian" approach is summarized in four steps:

i. A set of spawner-recruit models are sampled (one per species)
ii. The operating model (Hydra) is run using the sampled models as input.

iii. The output is compared to empirical data (biomass and landings) to assess the appropriateness of the sampled spawner-recruit models
iv. The process is repeated many times resulting in a collection of viable models

The sampling stage is governed by a few simple rules depending on whether the initial fitted model is a hockey stick or a generalized model. For species fit using a hockey stick model we sample a new hockey stick model, the only change being the location of the change-point. The new change-point is sampled from the interval bounded on the lower end by ½ smallest observed spawning stock biomass value and on the upper end by the initial fitted change-point. i.e. the sampled model will result in being at least as steep at the origin as the fitted model. We can then find the corresponding value of α using the simulated value of the change-point.

For species fit under the generalized model we sample the change-point and calculate α in the same way as for the hockey stick model. We then constrain the slope post change-point to pass through the point of the initial fit at the largest observed spawning stock biomass. These simple rules give sufficient spawner-recruit variability without straying too far from the initial fits. These sampling rules are subject to change in the future to allow greater variability.

The operating model is now run, deterministically, using the sampled set of spawner-recruit models for a period of time representing 150 yrs. The first 100 years are without any fishing pressure to allow the system to reach equilibrium, or some kind of stability. The final 50 years represent historical fishing pressure.

The output of the model is then checked against three criteria. If all are satisfied then the set of spawner-recruit models are kept. These three criteria are:

1. After the period of no fishing, all species are required to have a mean biomass (mean of last 10 years) exceeding the minimum observed biomass from survey data
2. After the period of fishing all species are required to have a mean biomass (mean of the last 10 years) that lie between .5 x minimum observed and 2 x maximum observed biomass from survey data.
3. After the period of fishing, all species landings must fall between the minimum and maximum reported landings.

Growth and Condition Module

Growth parameters (Table A3; Figure A1) were estimated by fitting to length at age data from fishery independent surveys of Georges Bank for 8 species with observed data, and taken from Hall et al. (2006) for species lacking length at age data (spiny dogfish and winter skate).

Maturity parameters (Table A3) were mainly taken from O'Brien et al. (1993), aside from monkfish which were taken from Richards et al. (2008).

Length-weight parameters were taken from NEFSC (unpublished) quality-control files.

Table A3. Species-specific model parameters for length-weight relationships, maturity ogives, and growth.

Parameter	Spiny dogfish	Winter skate	Atlantic herring	Atlantic cod	Haddock	Yellowtail flounder	Winter flounder	Atlantic mackerel	Silver hake	Monkfish
Length-Wt										
a	0.003	0.004	0.01	0.009	0.01	0.008	0.011	0.007	0.007	0.02
b	3.122	3.317	2.99	3.052	3.068	3.129	3.138	3.319	3.05	2.897
Maturity										
nu	-5	-5	-34.4725	-5.31	-5.658	-11.6405	-9.2895	-16.7885	-13.166	-10.668
omega	0.1	0.1	1.36	0.133	0.1995	0.484	0.3685	0.6495	0.5825	0.2885
Growth										
psi	11.281	18.778	11.652	22.317	23.06	16.001	17.769	20.483	13.78	9.1808
kappa	0.6882	0.5957	0.4564	0.7349	0.5021	0.6189	0.5529	0.2633	0.6486	0.9556
Linf	99.99	114.1	29.051	113.59	73.8	44.71	56.296	43.256	41.224	-150.73
k	0.1	0.1441	0.4523	0.1975	0.376	0.4776	0.2916	0.206	0.4036	-0.0472

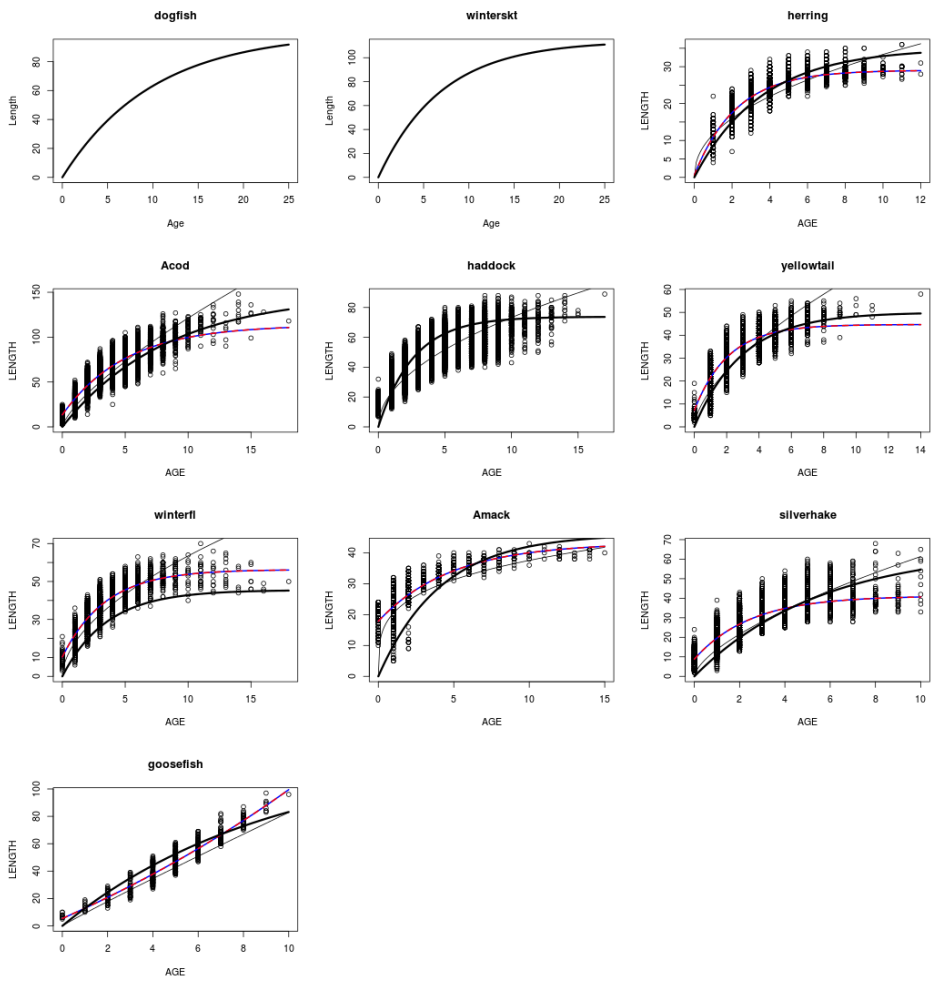

Figure A1. Growth functions fit to length at age data for each modeled species from Georges Bank. Literature values for von Bertalanffy growth were used for spiny dogfish and winter skates because no length at age data was available for Georges Bank (source: Gaichas et al. 2016)

Consumption Module

Size specific mean stomach weights were taken from Bowman and Michaels, (1984) and aggregated to the model size bins using weighted averages based on sample size in each published size bin (Table A1). While the model allows for annual variation in size-specific stomach weight, we held these values constant for the duration of the simulation.

Table A.4. Estimates of mean stomach content weight for Georges Bank fish species included in prototype analysis

	Stomach wt	**Stomach wt**	**Stomach wt**	**Stomach wt**	**Stomach wt**
Spiny dogfish	0.090189781	1.952671779	9.334322368	28.80493233	77.55885308
Winter skate	0.093423453	0.939220418	3.915192982	11.46903371	44.88111925
Atlantic herring	0.01	0.03	0.8	1.5	3
Atlantic cod	0.035	0.103736364	1.952671779	18.42060702	84.48736889
Haddock	0.031	0.096183673	0.939220418	3.915192982	12.07313904
Yellowtail flounder	0.016072464	0.086965517	0.237958824	0.442743017	1.583142857
Winter flounder	0.016072464	0.086965517	0.237958824	0.442743017	1.583142857
Atlantic mackerel	0.01	0.08	1.3	2	3
Silver hake	0.039893347	0.179748344	0.512104803	4.879748476	20.262
Monkfish	0.090189781	1.952671779	9.334322368	28.80493233	77.55885308

Predator-prey interactions were governed by a binary vulnerability matrix (Table A5) where the possibility of one species eating another was determined by review of food habits data (Link and Almeida, 2000; Smith and Link, 2010).

Table A5. Predator-prey interactions. Predators are listed in columns, with their potential prey indicated by 1 in rows. For example, spiny dogfish may eat all other species in the model aside from monkfish, while yellowtail flounder, winter flounder, Atlantic herring and Atlantic mackerel do not eat any other species in the model.

	Spiny dogfish	**Winter skate**	**Atlantic herring**	**Atlantic cod**	**Haddock**	**Yellowtail flounder**	**Winter flounder**	**Atlantic mackerel**	**Silver hake**	**Monkfish**
Spiny dogfish	1	0	0	0	0	0	0	0	0	1
Winter skate	1	0	0	0	0	0	0	0	0	0
Atlantic herring	1	1	0	1	1	0	0	0	1	1
Atlantic cod	1	1	0	1	1	0	0	0	0	1
Haddock	1	1	0	0	1	0	0	0	0	1
Yellowtail flounder	1	0	0	0	0	0	0	0	0	1
Winter flounder	1	0	0	0	0	0	0	0	0	1
Atlantic mackerel	1	1	0	1	0	0	0	0	1	1
Silver hake	1	1	0	1	1	0	0	0	1	1
Monkfish	0	0	0	0	0	0	0	0	0	1

The preferred predator/prey weight ratio on a logarithmic scale (Ψ_j in equation 13 above) was set at 0.5 for all species, and the variance in predator size preference (σ_j^2 in equation 13 above) was set at 2.0 for all species, as recommended in Rochet et al. (2011). The food intake parameters (equation 14) were set to $д_i$ = 0.002 for dogfish and skates and 0.004 for all other species, and $ж_i$ = 0.11 for all species following recommendations in NEFSC 2010, Appendix B (http://www.nefsc.noaa.gov/publications/crd/crd1003/pdfs/butterapp1.pdf). Other prey biomass (Ω in equation 15) was set to 30,000. The number used in Hall et al. 2006 was not reported, but was tuned until stable dynamics and "sensible" M2 levels were achieved; we similarly tuned this parameter to be the smallest number that stabilized dynamics of prey species (herring, mackerel, and silver hake) in the no fishing runs.

Fleet Module

Fishery selectivity parameters (Figure A2) were derived from De Alteris and Grogan, (1997). The parameters reported there were converted to ours as follows: DeAlteris and Grogan's alpha2 (curve steepness) is equal to our *d* in Equation 16. DeAlteris and Grogan's Selection Factor (SF) is the length at 50% selection (L50) divided by the average mesh or

hook size, and our *c* in Equation 16 is -alpha2*L50, so we used *c* = -*d* * SF * average mesh or hook size. We used average values for diamond mesh trawl (gear 1) and offshore trap (gear 2) because they existed for all species studied, which were Atlantic cod, haddock, yellowtail flounder and winter flounder. We further assumed that the trawl fleet would catch all species, that the longline fleet would catch Atlantic cod, haddock, dogfish, skates, and goosefish, and that the pelagic gear would catch Atlantic herring, mackerel, and haddock as shown in Figure S3.

Table A6. Selectivity, s, and catchability, q, parameters

	Demersal Trawl			Pelagic Trawl			Fixed Gear		
	Selectivity		q	Selectivity		q	Selectivity		q
	c	d		c	d		c	d	
Spiny dogfish	-12.90	.25	5.95e-8	-12.06	.22	5.50e-8	-12.06	.22	3.77e-6
Winter skate	-10	.25	3.31e-7	-10	.25	0	-10	.25	4.56e-8
Atlantic herring	-4	.25	4.64e-8	-4	.25	1.88e-5	-200	1	0
Atlantic cod	-12.90	.25	5.25e-7	-12.06	.22	0	-12.06	.22	2.54e-7
Haddock	-11.68	.25	1.34e-6	-10	.25	7.13e-7	-10	.25	1.67e-7
Yellowtail flounder	-15.44	.48	3.00e-6	-200	1	0	-200	1	0
Winter flounder	-13.89	.57	1.96e-6	-200	1	0	-200	1	0
Atlantic mackerel	-5	.25	1.34e-8	-5	.25	2.17e-5	-200	1	0
Silver hake	-8	.25	4.40e-6	-8	.25	1.52e-6	-8	.25	0
Monkfish	-12	.25	7.78e-7	-12	.25	0	-12	.25	5.14e-7

Table A7. Survival probabilities for discarded fish P(D) and p(Surv|D) across all size classes

	Bottom Trawl		Pelagic Trawl		Longline	
	P(D)	P(Surv|D)	P(D)	P(Surv|D)	P(D)	P(Surv|D)
Spiny dogfish	1	.7	0	1	.68*	.8
Winter skate	1	.9	0	1	.24	.95
Atlantic herring	0		0		0	
Atlantic cod	0		0		0	
Haddock	0		0		0	
Yellowtail flounder	0		0		0	
Winter flounder	0		0		0	
Atlantic mackerel	0		0		0	
Silver hake	0		0		0	
Monkfish	0		0		0	

Note: * for largest size class. All other size classed P(Discard) = 1

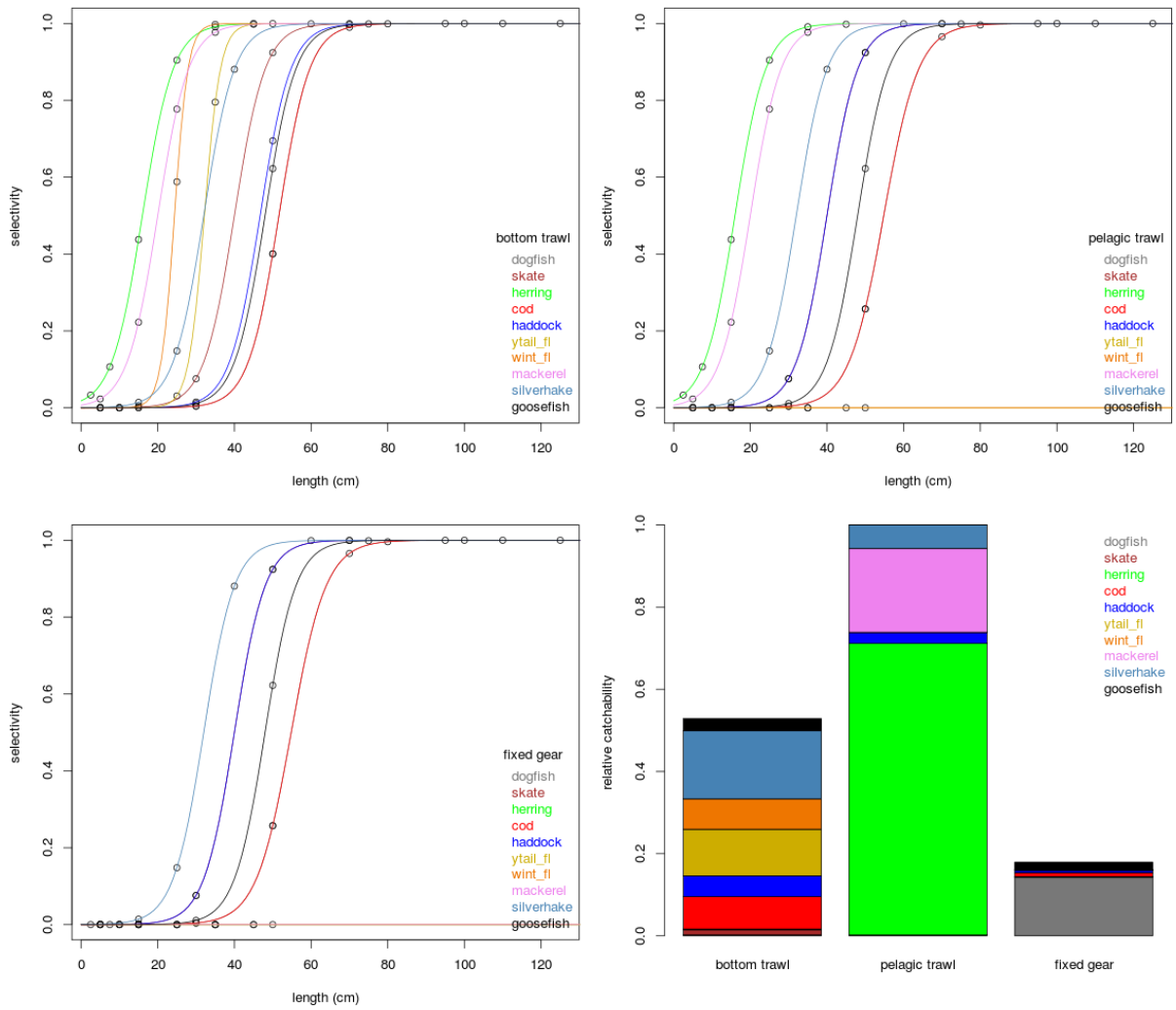

Figure A2. Size selectivity and relative catchability by fleet as implemented in the simulation model. These are intended to be illustrative and are only loosely based on fishery data aggregated over multiple gear types and vessel sizes (Gaichas et al. 2016).

Fishing Effort

Relative harvesting efficiency varies markedly among different vessel size classes and fishing gears. To account for these differences, nominal fishing effort was standardized using a general linear model approach (e.g. Mayo et al. 1992) based on the multiplicative model:

$$U_{ijk} = \alpha_i \beta_j (qB) exp(\varepsilon_{ijk})$$

where U_{ijk} is the *a* for the ith gear, jth tonnage class, and kth observation; α_i and β_j represent gear and tonnage class effects, *q* is the catchability coefficient, *B* represents mean population biomass and ε_{ijkl} is a normally distributed random variable with mean 0 and constant variance. Because the population biomass is not directly known, the term qB is replaced by the mean CPUE (μ) and

all coefficients are estimated relative to an arbitrarily defined standard Least squares estimates of the model coefficients were made under the constraints: $\Sigma \log_e \alpha_i = \Sigma \log_e \beta j = 0$ for the linearized model:

$$log_e U_{ijk} = log_e + log_e \alpha_i + log_e \beta_j + \varepsilon_{ijk}$$

Retransformation of the model coefficients to linear scale was made after correction for bias following Granger and Newbold, (1977). Trajectories of normalized effort levels for the three fleet sectors are shown in Figure A3.

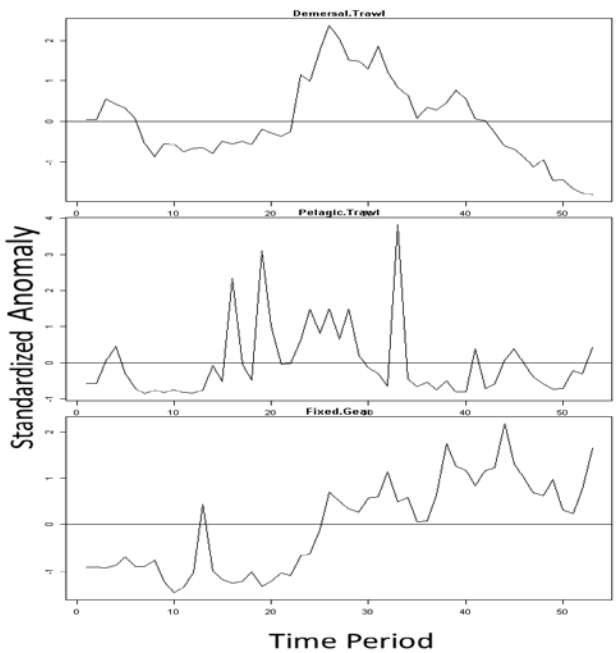

Figure A.3 Standardized anomalies of relative fishing effort of the demersal and pelagic trawl fleets and the fixed gear fishery on Georges Bank